SNS-300000000-TR0001-R00

Conceptual Design Report for the Spallation Neutron Source Power Upgrade MIE Project

A U.S. Department of Energy Multilaboratory Project

SPALLATION NEUTRON SOURCE

SNS

Argonne National Laboratory • Brookhaven National Laboratory • Thomas Jefferson National Accelerator Facility • Lawrence Berkeley National Laboratory • Los Alamos National Laboratory • Oak Ridge National Laboratory

SNS-300000000-TR0001-R00

Conceptual Design Report for the Spallation Neutron Source Power Upgrade MIE Project

April 2006

Prepared for the
U.S. Department of Energy
Office of Science

UT-BATTELLE, LLC
managing
Spallation Neutron Source activities at
Argonne National Laboratory
Brookhaven National Laboratory
Thomas Jefferson National Accelerator Facility
Lawrence Berkeley National Laboratory
Los Alamos National Laboratory
Oak Ridge National Laboratory

under contract DE-AC05-00OR22725
for the
U.S. DEPARTMENT OF ENERGY

Submitted by:

Tom Mann, Project Manager, SNS Power Upgrade Project

Stuart Henderson, Accelerator Physics Group Leader

Concurrences:

Norbert Holtkamp, Director, Accelerator Systems Division, SNS Project

---

Ian Anderson, Director, Experimental Facilities Division, SNS Project

---

Carl Strawbridge, Director, Project Site Support Office, SNS Project

---

Thom Mason, Associate Laboratory Director for the SNS Project

TABLE OF CONTENTS

LIST OF FIGURES

LIST OF TABLES

ACRONYMS

ac	Alternating Current
AFE	Analog Front End
ANL	Argonne National Laboratory
ANSI	American National Standards Institute, Inc.
AP	Accelerator Physics
ARR	Accelerator Readiness Review
ASC	Accelerator Safety Committee
BA	Budget Authority
BCP	Baseline Change Proposal
BESAC	Basic Energy Sciences Advisory Committee
BNL	Brookhaven National Laboratory
BPM	Beam Position Monitor
CCL	Coupled-Cavity Linac
CD	Critical Decision
CDE	Cavitation Damage Erosion
CDR	Conceptual Design Report
CF	Conventional Facilities
CHL	Central Helium Liquefier
CLO	Central Laboratory Office
COTS	Commercial-Off-the-Shelf
DCD	Design Criteria Document
D&D	Decontamination and Decommissioning
DESY	Deutsches Elektronen Synchrotron
DFE	Digital Front End
DOE	Department of Energy
DTL	Drift-Tube Linac
EAC	Estimate at Completion
EIA	Electronic Industries Association
EIS	Environmental Impact Statement
e-p	Electron-Proton
ES&H	Environment, Safety, and Health
ESH&Q	Environment, Safety, Health, and Quality
EVMS	Earned Value Management System
FCM	Field Control Module
FPGA	Field Programmable Gate Array
FSAD	Final Safety Assessment Document
FTE	Full-Time Equivalent (Person)
FY	Fiscal Year
GeV	Giga-electron Volts
HB	High-Beta
HEBT	High-Energy Beam Transport
HOG	Hot Off-Gas
HOM	Higher-Order Mode
HPRF	High-Power Radio Frequency
HPTS	High-Power Target Station
HTA	Horizontal Test Apparatus
HVAC	Heating, Ventilating, and Air-Conditioning
HVCM	High-Voltage Converter Modulator

Hz	Hertz
I&C	Instrumentation and Control
IGBT	Insulated Gate Bipolar Transistor
IOC	Slot-Zero Controller
IPT	Integrated Project Team
IRP	Inner Reflector Plug
JAERI	Japan Atomic Energy Research Institute
JSNS	Japan Spallation Neutron Source
LAL	Laboratoire de l'Accelerateur Lineaire
LANL	Los Alamos National Laboratory
LBNL	Lawrence Berkeley National Laboratory
LCC	Life Cycle Cost
LDRD	Laboratory Director's Research and Development Program
LEBT	Low-Energy Beam Transport System
LLRF	Low-Level Radio Frequency
LWTS	Long-Wavelength Target Station
MEBT	Medium-Energy Beam Transport
MeV	Million electron Volts
MIE	Major Item of Equipment
MHz	Mega Hertz
MIMTM	Magnet Impact Testing Machine
MO	Master Oscillator
MPS	Machine Protection System
MTBF	Mean Time Between Failures
MTTR	Mean Time To Repair
MW	Megawatt
NEPA	National Environmental Policy Act
NPDES	National Pollutant Discharge Elimination System
ORNL	Oak Ridge National Laboratory
ORO	Oak Ridge Office
PD	Project Director
PFN	Pulse Forming Networks
PI	Proportional-Integral
PLC	Programmable Logic Controller
PM	Project Manager
PPS	Personnel Protection System
PSR	Proton Storage Ring
PSSO	Project and Site Support Office Division
PUP	Power Upgrade Project
RAM	Reliability, Availability, and Maintainability
RCT	Radiation Control Technician
Rf/rf	Radio Frequency
RFO	Radio Frequency Output
RFQ	Radio Frequency Quadrupole
RFTF	Radio Frequency Test Facility
RID	Ring Injection Dump
RSB	Ring Service Building
RTBT	Ring-to-Target Beam Transport
SC	Office of Science
SCL	Superconducting Linac
SCR	Silicon Controlled Rectifier

SNS	Spallation Neutron Source
SOA	Safe Operating Area
SRF	Superconducting Radio Frequency
TEC	Total Estimated Cost
TJNAF	Thomas Jefferson National Accelerator Facility
TPC	Total Project Cost
TTF	Target Test Facility
WBS	Work Breakdown Structure
XFD	Experimental Facilities Division

1. EXECUTIVE SUMMARY

The Spallation Neutron Source (SNS), shown in Fig. 1.1, is a user facility designed for studies of the structure and dynamics of materials using thermal and cold neutrons. It employs a linear accelerator (linac) to produce a 1-ms-long negative-hydrogen ion (H^-) beam 60 times per second and accelerate it to 1 GeV, resulting in a total beam power of greater than 1 MW with a design of 1.4 MW. The H^- beam is converted to protons during injection through a carbon stripping foil and is then compressed to 700 ns in a 248-m-circumference accumulator ring. The SNS initial baseline accelerator delivers its proton beam power to a single mercury target, where neutrons are generated by the spallation process and used for neutron science with a suite of up to 24 instruments. The initial baseline design and some hardware allow for increased beam power following the recommendations of the Basic Energy Sciences Advisory Committee (BESAC) subpanel (Russell panel) that provided the input to the initial Level 0 baseline parameters for the SNS. This document summarizes an upgrade program that makes use of existing margins designed into the facility to increase the beam power to greater than 2 MW with a design goal of 3 MW. This plan builds upon recent progress in SNS development programs to improve superconducting cavity performance in the linac, to mitigate intensity thresholds in the accumulator ring, and to reduce cavitation damage in the mercury target. Because key elements of the upgrade rely on replicating existing designs, the upgrade is positioned for aggressive deployment, with construction starting in FY 2008 and finishing in FY 2012. The range of the Total Project Cost (TPC) of the SNS Power Upgrade MIE Project is between $150M and $173M**,** including contingency and escalation. This upgrade will lead to an immediate improvement in the performance of all installed scattering instruments at the SNS, and in the future will provide beam power that can also be extracted to a potential second target station, thereby widening the suite of SNS instruments and the scope of science that can be studied.

The SNS Power Upgrade MIE Project will roughly double the scientific capability of the Spallation Neutron Source at a cost that is approximately 10% of the initial facility cost.

Fig. 1.1. Photo of the Spallation Neutron Source site.

2. INTRODUCTION AND BACKGROUND

This Conceptual Design Report presents a preliminary design, scope, cost, schedule, and R&D plan for the Power Upgrade Project (PUP) for the SNS at Oak Ridge National Laboratory (ORNL). The scientific justification and need for a very-high-intensity pulsed neutron source in the United States have been firmly established by numerous studies by the scientific community since the 1970s. These include the 1984 National Research Council Study *Major Facilities for Materials Research and Related Disciplines* (the Seitz-Eastman Report) [1], which recommended the immediate start of the design of both a steady-state source and an accelerator-based pulsed spallation source. More recently, the 1993 Basic Energy Sciences Advisory Committee report *Neutron Sources for America's Future* (the Kohn Panel Report) [2] again included construction of a new pulsed spallation source among its highest priorities. This conclusion was even more strongly reaffirmed by the 1996 BESAC Report (the Russell Panel Report) [3], which recommended the construction of a spallation source to satisfy the basic requirements listed below in Table 2.1.

Table 2.1. Requirements for an accelerator-based neutron source

Initial beam power on target greater than 1 MW
Upgradeable to higher beam power, 4–5 MW
Protons with a beam energy of 1–3 GeV
Beam pulse length on target less than 1 ms
Beam repetition rate 10–50 Hz
Technology emphasis on high reliability

This need is being fulfilled by the construction of the SNS, which is nearing completion at ORNL. The SNS started as a line item construction project in FY 1999, cost $1411.7M, and was constructed at ORNL in collaboration with six Department of Energy (DOE) national laboratories [Argonne National Laboratory (ANL), Brookhaven National Laboratory (BNL), Los Alamos National Laboratory (LANL), Lawrence Berkeley National Laboratory (LBNL), ORNL, and Thomas Jefferson National Acceleratory Facility (TJNAF)]. When completed in June 2006, the initial SNS project will have a baseline power level of greater than 1 MW with a design goal of 1.4 MW. In accordance with the 1996 BESAC recommendation, the SNS is designed to be economically upgradeable in proton beam power, so as to maintain its position of scientific leadership. Recently the importance of neutron scattering and this SNS Power Upgrade Project was recognized by the Office of Science study *Facilities for the Future of Science, A Twenty Year Outlook*, November 2003 [4], in which the SNS Power Upgrade was ranked very high as a midterm priority.

Following the Russell Panel Report recommendations, many technical margins have been built into the SNS design and hardware to facilitate this Power Upgrade into the 2- to 4- MW range and ultimately to perhaps 5 MW. These margins are listed below in Table 2.2 and were incorporated into the baseline for the initial existing SNS Facility.

Based on these existing margins, a cost-effective SNS Power Upgrade Project is relatively straightforward, as is described in this report. The resulting increased beam power leads to improved performance for the entire SNS instrument suite and can support a potential second target station, widening the suite of instruments and the scope of science that can be studied. The power upgrade proposal has been reviewed and endorsed by the BES Advisory Committee and is included in the DOE Strategic Plan and the Office of Science 20-Year Facilities Plan. Critical Decision 0 (Mission Need) was approved November 23, 2004, by the director of the DOE Office of Science.

The technical objective of the SNS Power Upgrade is to design, build, install, test, and beam commission the equipment necessary to increase the SNS beam energy from the initial baseline of 1.0 GeV to 1.3 GeV and the beam power from the initial level-0 baseline of greater than 1 MW to greater than 2 MW using the existing target station. This report lists parameters for the upgraded facility increasing the design goal from 1.4 MW to 3.0 MW of beam power. The SNS Power Upgrade Project is specifically designed to increase the design goal beam power from 1.4 MW to 3.0 MW through the product of two factors, energy multiplied by intensity: the beam energy will be increased by 30% from 1.0 GeV to 1.3 GeV; and the time-averaged accelerator output beam intensity will be increased by 65% from 1.4 mA to 2.3 mA for 3.0 MW of beam power. There is very little technical, cost, or schedule risk in increasing the SNS accelerator beam energy by 30%. The technical risk lies in the intensity side of the equation; the three main areas of technical risk requiring R&D are in the ion source, carbon stripping foil, and Hg target.

The next chapter gives a brief scientific justification for this project, followed by the integrated physics design. Chapters 5, 6, and 7 give technical descriptions of the accelerator, target, and facilities upgrades, respectively. The report ends with an R&D plan, followed by a brief discussion of the preliminary project cost and schedule.

Table 2.2. Existing margins in the initial SNS Project for higher power operation

• The baseline SCL accelerates the beam from 186 MeV to 1.0 GeV, is 157-m long, and contains 23 cryomodules. The linac tunnel was built with another 71 m of length to accommodate nine additional cryomodules.
• The cryogenics plant has the additional cooling capacity needed for nine cryomodules. The transfer lines that feed these nine cryomodules are in place.
• Superconducting cavity input radio frequency (rf) power couplers have been tested to 750 kW, compared to 550 kW needed in the initial baseline, and are adequate for many of the cavities in the Power Upgrade.
• Piezoelectric tuners have been installed in all 81 baseline superconducting cavities in order to reduce the required rf power control margins, thereby allowing the existing rf plant to provide more beam power without major configuration changes.
• The superconducting cavity gradients, on average, have been tested to approximately 20% over the baseline specification.
• High Energy Beam Transport (HEBT)–Ring–Ring-to-Target Beam Transport (RTBT) tunnel geometry, and in particular the H^- bending dipole magnets, can support 1.3-GeV operation.
• The ring accelerator physics design is for 2.0 MW at 1.0 GeV.
• Most magnets, with the exception of two injection chicane magnets, support 1.3-GeV operation.
• Most magnet power supplies support 1.3-GeV operation.
• The HEBT design includes energy corrector and spreader rf cavities to minimize downstream ring beam loss.
• The beamline hardware devices for active transverse instability dampers are installed in the ring.
• Many target systems were constructed for 2 MW.
• The target biological shield was constructed for 4 MW.
• Electrical, water, and cooling infrastructure has some reserve capacity.

3. SCIENTIFIC JUSTIFICATION

Because the vast majority of neutron-scattering experiments are intensity limited, even modest improvements in source intensity can lead to scientific measurements that were previously out of reach. An increase in power by a factor of 2 or 3 will enable practical study of smaller samples and real-time studies at shorter time scales. It will also allow a modest increase in resolution on most instruments and will allow more experiments to take advantage of the highest resolution available on each instrument. Since many such experiments are at the scientific frontier, such a power increase will immediately make a significant increase in the scientific productivity of SNS. Another benefit will be an increased volume of research supported because of faster throughput of already feasible experiments. Further increases in scientific capabilities can be expected in the longer term, as instruments optimized to exploit these higher powers come on line. In addition, by providing beam power to support a second target station, a Long-Wavelength Target Station (LWTS), the Power Upgrade facilitates a significant expansion of capacity and substantial performance gains for long wavelength applications of neutron-scattering techniques. Although the LWTS can be implemented without the Power Upgrade, its power level, and hence its scientific performance, will be significantly curtailed if its operation were to come at the expense of the High Power Target Station (HPTS).

The SNS instrument designs being developed have been quantitatively benchmarked at the 1-MW performance level. In many instances with the new performance level offered by a megawatt-class spallation source, the instrumentation approaches count rates that will support single-pulse experiments. At 1 MW however, single-pulse measurements will still be limited to a subset of possible materials—that is, those with simple structures or favorable cross sections. By increasing the power level by a factor of 2, the range of materials that can be measured increases dramatically. Some examples of new areas of science that could be addressed include the following:

- **Engineering Materials**—The increase in power will make feasible dynamic experiments at the engineering diffractometer that can only be dreamt of today. Single-pulse diffraction will become possible for engineering materials such as steel, aluminum, and nickel-based superalloys. Because neutrons of different wavelengths are scattered by the sample at different times, continuous monitoring of the dynamics of a process would be possible. Examples of studies where information on this time scale is important include change of stress state during cyclic fatigue, development of recrystallization texture, decomposition kinetics in bulk metallic glass, and phase stability of metallic clusters. Another area that will benefit from the increase of target power is spatial mapping experiments. Spatial resolutions of 0.1 mm are required for studies of surface engineered materials and coatings; such measurements are difficult to achieve at a 1-MW flux.

- **Powder Diffraction**—Higher power will greatly increase the performance of the powder diffractometer in stroboscopic [crystal structure as a function of applied alternating stimulus, e.g., ferroelectrics under high-frequency alternating current (ac) voltages] and nuclear density distribution measurements (e.g., determination of hydrogen conduction pathways in fuel cell materials). Similarly, in a high-flux scenario, maximum entropy methods could be used to deconvolute the instrument and pulse shape functions from the measured diffraction data, possibly doubling the resolution of the powder diffractometer. This higher resolution is important in the study of subtle structural phase transitions and in separating Bragg peaks in complex, low-symmetry structures, which is a requirement for ab initio powder methods

when single crystals are not obtainable. Flux increases will also allow phase diagram determinations to be made extensively and rapidly.

- **Reflectometry**—Higher flux will also allow time-dependent reflectometry studies on thin films at high temporal resolution. Examples include diffusion experiments; parametric studies in which temperature, magnetic/electric fields, chemical environment, and/or pressure are changed; chemical kinetics; solid state reactions; phase transitions; and chemical reactions in general. In many cases, useful data sets could be produced on a pulse-by-pulse basis. We are close enough in flux at 1.4 MW to almost bridge the gap between reflectivity and Bragg diffraction along the specular diffraction rod. A factor of 2 increase in intensity will enable continuous measurement of layered structures from 3 to 10,000 Å in one scan on one instrument. This becomes important for in situ studies of the layer-by-layer growth of multilayers or the study of dynamic processes at surfaces and interfaces. Furthermore, an increase in intensity will break the threshold required for performing inelastic scattering experiments on thin films and surfaces. Such a capability, which does not exist at current neutron sources because of flux limitations, will open up a completely new domain of measurements with applications in membrane function, catalysis, and relaxation processes in magnetic films, for example.

- **Dynamics**—Inelastic experiments are generally flux limited. Two examples where current flux levels make experiments marginal at best are studies of protein dynamics and of thin layers of adsorbed polymers. To study the dynamics (side chain motions as well as global diffusion) of proteins in solutions that mimic biological environments, sample concentrations must be kept low because of protein clustering at higher concentrations, which makes the scattering particularly weak. A factor of 3 will extend the range of proteins that can be studied in this way. Another area of study that will benefit is the dynamics of thin films of adsorbed polymers (1 to several radii of gyration thick). Current study is limited to either intense sample preparation efforts (many iterations of coating individual silicon wafers) or study of relatively thick films. An additional factor of 3 in performance for the inelastic instruments will increase the viability of taking such measurements, because less sample material will be required.

- **Biomaterials**—Neutrons have a key role to play in the post-genomic era where the structure-function relationship of biological molecules has shifted more and more to the center stage. Even with the SNS (which represents a significant improvement over the current state of the art) or the High Flux Isotope Reactor, many neutron-scattering experiments with biological systems are not practical because of flux limitation. Most potential biological samples are available only in small amounts, behave well only in low concentrations, and have low contrast. Higher flux will enable a number of biological neutron-scattering experiments that are not possible at current flux levels. Moreover, the applicability of neutrons to structural problems where the role of hydrogen and loosely bound water is important is expected to expand considerably.

4. INTEGRATED PHYSICS DESIGN

The SNS initial baseline and SNS Power Upgrade design parameters are summarized in Table 4.1. In the SNS Power Upgrade, the beam power of the accelerator facility is doubled from the greater-than-1-MW capability of the baseline accelerator complex to greater than 2 MW. Rather than design for the minimum capability, we have chosen a 3.0-MW design goal capability, well in excess of this 2 MW, in order to provide engineering margin in the level-0 baseline goal and to provide the capacity for future upgrades such as the Long-Wavelength Target Station. Increasing the beam power to 3.0 MW is accomplished by increasing the peak H^- ion source current [measured at radio-frequency quadrapole (RFQ) output] from 38 to 59 mA and increasing the final linac beam energy from 1.0 to 1.3 GeV. Some modifications in the HEBT, ring, and RTBT are required to accommodate the higher beam energy and intensity.

Although there is margin in the linac rf systems for increasing the beam pulse length, we have chosen to maintain the SNS baseline 6% beam duty factor in the SNS Power Upgrade. A longer beam pulse, while feasible, is a less-cost-effective option that also complicates the operation of the ring, and therefore it is maintained as a possible backup option.

Table 4.1. SNS initial baseline and SNS Power Upgrade design parameters

	Initial Baseline	Upgrade
Beam kinetic energy, MeV	1000	1300
Design beam power, MW	1.4	3.0
Chopper beam-on duty factor, %	68	70
Linac beam macro pulse duty factor, %	6.0	6.0
Average macropulse H^- current, mA	26	42
Peak macropulse H^- current, mA	38	59
Linac average beam current, mA	1.6	2.5
SRF cryo-module number, med-beta	11	11
SRF cryo-module number, high-beta	12	12 + 8 (+1 reserve)
SRF cavity number	33+48	33+80 (+4 reserve)
Peak surface gradient (β=0.61 cavity), MV/m	27.5 (+/- 2.5)	27.5 (+/- 2.5)
Peak surface gradient (β=0.81 cavity), MV/m	35 (+2.5/-7.5)	31
Ring injection time, ms / turns	1.0 / 1060	1.0 / 1100
Ring rf frequency, MHz	1.058	1.098
Ring bunch intensity, 10^{14}	1.6	2.5
Ring space-charge tune spread, ΔQ_{SC}	0.15	0.15
Pulse length on target, ns	695	691

4.1 LINAC PHYSICS DESIGN

The choice of 1.3-GeV output energy is conservative, retaining an entire high-beta cryomodule in reserve to maximize operational flexibility and reliability and to facilitate rapid recovery from cavity faults, while at the same time allowing somewhat reduced gradient operation in the high-beta section relative to that in the baseline. Operation of all high-beta cavities at their design fields results in a beam energy of 1.4 GeV. The existing HEBT and ring

tunnel geometry allow a maximum beam energy between 1.3 and 1.4 GeV before beam loss from magnetic field H^- stripping would become intolerable.

The beam emittance criteria established in the initial baseline SNS linac design are maintained in the upgrade design goal. In particular, a design goal for the linac output transverse emittance of < 0.5 π mm-mrad (rms, normalized) is assumed. The acceptance of the linac proper is limited by the drift-tube linac (DTL) and coupled-cavity linac (CCL) bore radii of 12.5 mm and 15.0 mm respectively, which demand that the front-end output beam emittance be less than 0.35 π mm-mrad (rms, normalized). Although it may be straightforward to realize an increase in ion source current by increasing the outlet aperture of the source, the RFQ aperture limits the accelerated beam emittance. Whereas it may be possible to design a larger-aperture RFQ to accelerate a larger emittance beam, the limited DTL and CCL apertures remain an acceptance limitation in the linac. It was therefore decided to retain the existing RFQ and design an upgraded ion source and LEBT so that the front-end output beam emittance remains less than 0.35 π mm-mrad (rms, normalized).

The 1.3-GeV linac design has been carried out using the PARMILA code [5]. Figure 4.1 shows the energy gain for all cavities in the superconducting linac. The first 33 cavities are in the medium-beta section, and the remaining 84 are in the high-beta section. The nominal synchronous phase in the medium-beta section is -20.5°, while in the high-beta section it is -19.5°.

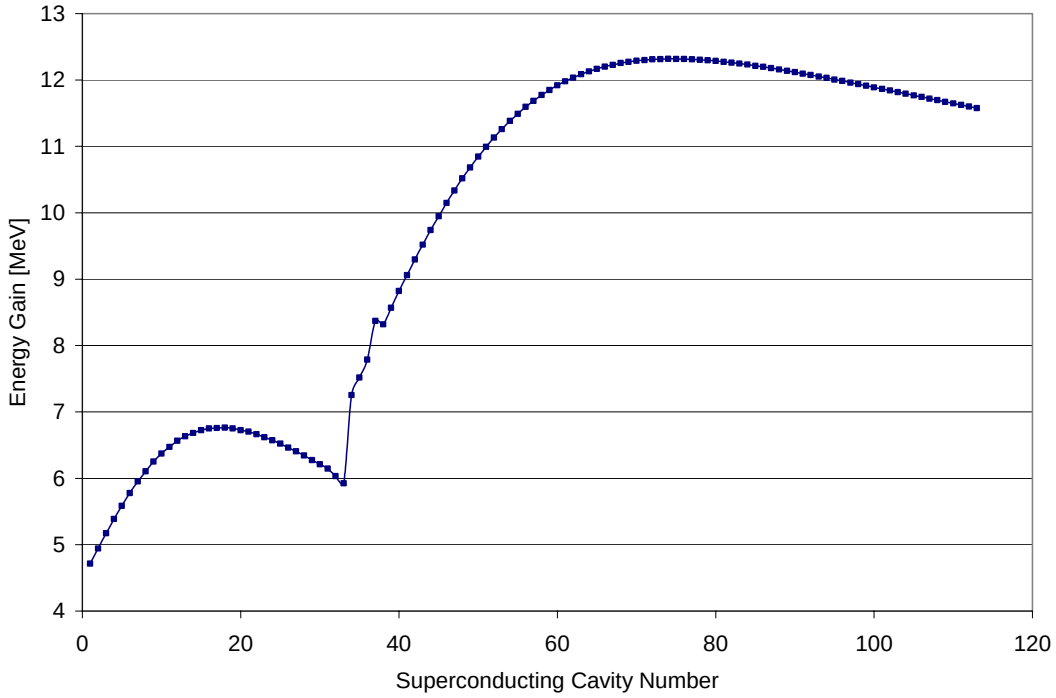

Fig. 4.1. Energy gain for each cavity in the SNS Power Upgrade superconducting linac. The first 33 cavities are in the medium-beta section and the remainder are in the high-beta section.

Similarly to the initial linac, the additional 36 high-beta cavities are powered individually by single klystrons. The total beam plus rf structure power per klystron at 3.0-MW operation is shown in Fig. 4.2. Overhead for control margin and waveguide losses are not included in the figure. The manufacturer's rated klystron output power is also shown. In the case of the 550-kW superconducting linac (SCL) klystrons, output powers as high as 900 kW have been obtained in tests. The highest beam power delivered to a single cavity in the upgrade is 517 kW. Further

discussion of the klystron output power capabilities and control margin are discussed in Sections 5.7, 5.8, and 5.9.

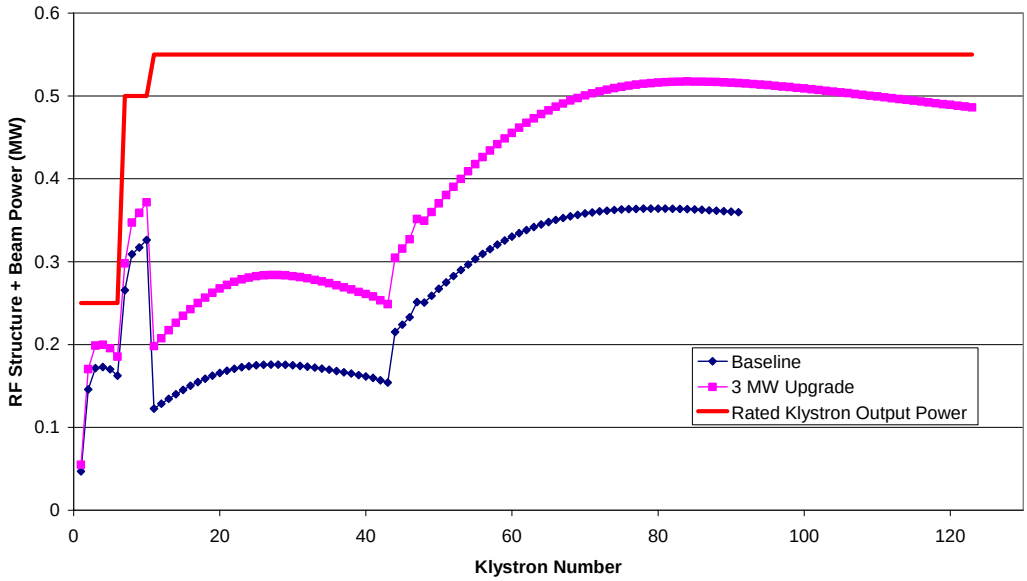

Fig. 4.2. Beam plus rf structure power per klystron in the linac for SNS baseline and Power Upgrade parameters. Klystron numbers correspond to normal-conducting (1–10), superconducting medium-beta section (11–43), and superconducting high-beta section (44–127). The normal conducting linac klystrons (1–10) have all powers divided by 10.

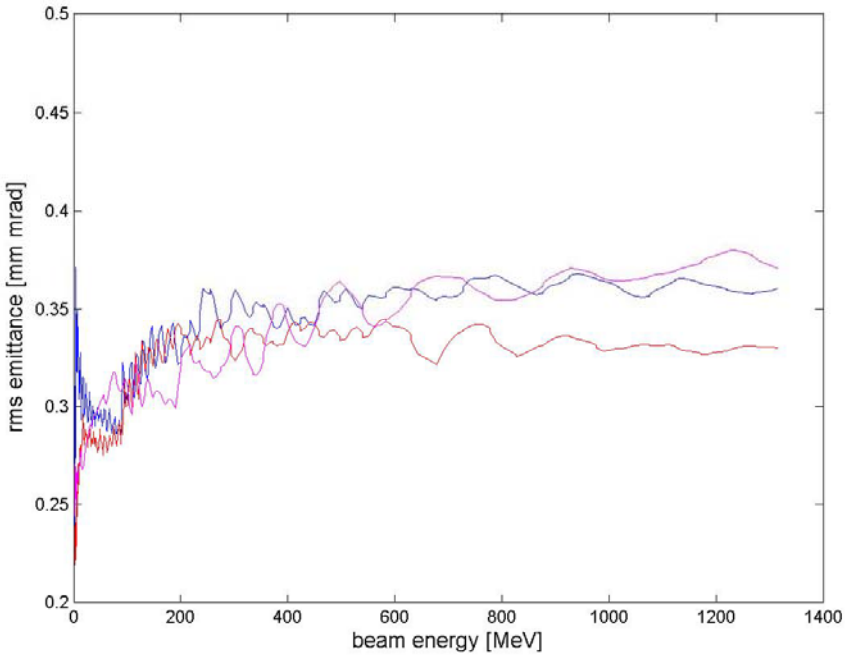

Fig. 4.3. Normalized rms beam emittance evolution in the linac for the ideal case without errors. The traces show horizontal (red), vertical (blue), and longitudinal (magenta) emittances. The input particle distribution is one obtained from measurements as discussed in the text.

Multiparticle simulations have been performed for the SNS Power Upgrade linac parameters using the PARMILA code. The predicted rms beam emittance evolution in the linac is shown in Fig. 4.3 for the ideal case without construction tolerances or setpoint errors. The initial beam distribution is that used in the SNS baseline design, which was obtained from ion source and Low-Energy Beam Transport System (LEBT) output emittance measurements obtained in initial tests at LBNL. Because the linac input distribution contains non-Gaussian tails as observed in actual measurements, this distribution provides a more realistic estimate for emittance evolution than that obtained using a simple 4-D waterbag input distribution.

Multiparticle simulations with anticipated construction tolerances and quadrupole and rf setpoint errors have also been performed with the PARMILA code. The anticipated errors, tabulated in Table 4.2, are identical to those used in the baseline SNS linac design. Figure 4.4 shows the predicted rms emittance evolution in the presence of errors for ten simulated linacs. As in the previous case, the simulation uses a particle input distribution that was obtained from ion source/LEBT emittance measurements. In all cases, the resulting output rms normalized transverse emittances remain below the design goal of 0.5 π mm-mrad.

Table 4.2. Linac construction tolerances and setpoint errors used in multiparticle PARMILA simulations

	Units	DTL	CCL	SRF
Quadrupoles				
static displacement (x&y)	± mm	0.125	0.125	0.125
dynamic displacement (x)	± mm	0.005	0.001	0.001
dynamic displacement (y)	± mm	0.001	0.0002	0.0002
pitch & yaw	± °	0.6	0.6	0.6
roll	± °	0.5	0.3	0.3
gradient	± %	measured	0.5	0.5
3rd order	on/off	on	on	on
harmonics	± %, °	measured	prototype	estimate
chromaticity	on/off	on	on	on
PMQ correction	on/off	on	-	-
Cavities & Cavity Fields				
static displacement (x&y)	± mm	0.125	0.3	2.0
static rf set point (1,2)				
amplitude	± %	1	1	(2)
phase	± °	1	1	(3)
Dynamic rf set point				
amplitude	± %	0.5	0.5	0.5
phase	± °	0.5	0.5	0.5
Beam Position Monitors				
uncertainty in electric axis	± mm rms	0.125	0.15	0.4
static displacement (x & y)	± mm	0.125	0.125	2.0

(1) Set point errors are correlated & depend on tuning procedure

(2) ß1 - ±10, ß2 – 21%. + 7% per Sundelin distribution

(3) Correlated with amplitude to preserve K_l

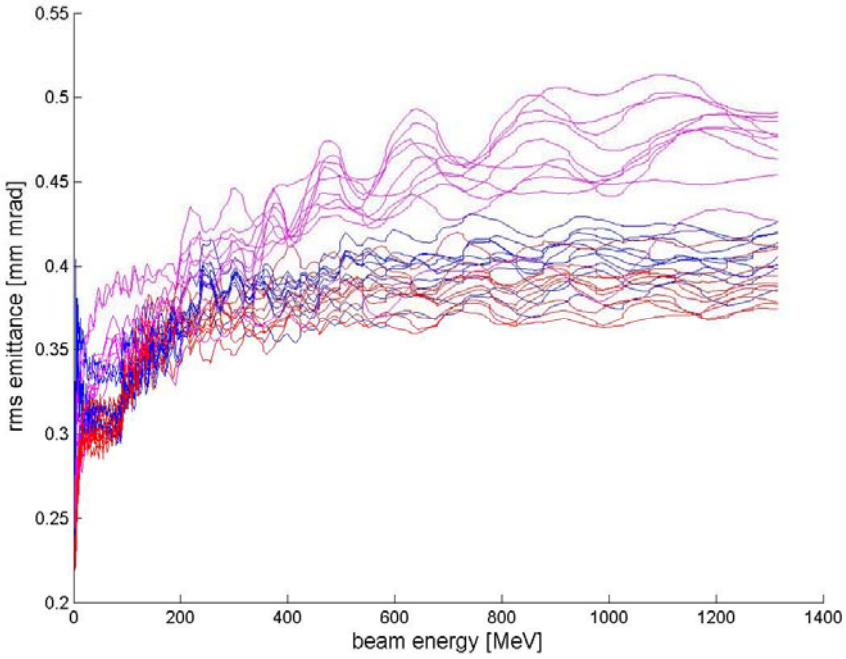

Fig. 4.4. Normalized rms beam emittance evolution in the linac for ten different random seeds, including anticipated construction tolerances and quadrupole and rf setpoint errors. The traces show horizontal (red), vertical (blue), and longitudinal (magenta) emittances. The input particle distribution is one obtained from measurements as discussed in the text.

4.2 RING PHYSICS DESIGN

The HEBT, ring, and RTBT were all designed and constructed in the initial SNS Project for 1.3-GeV beam energy, allowing a doubling of the beam power. The existing site has been designed to include the space for a second target station in order to fully utilize the beam power made available by the SNS Power Upgrade.

The maximum achievable intensity in the accumulator ring will be limited ultimately by collective effects. Very detailed and thorough studies of collective effects have been performed for the baseline SNS ring [6]. These studies include full treatment of space-charge forces in three dimensions; estimates of instability thresholds from the measured and estimated ring impedance; and estimates of electron-cloud production and electron-proton (e-p) instability effects [6,7,8]. The primary computational tool for these studies, as well as those for the baseline SNS accumulator ring, is the ORBIT code [9], which has been favorably benchmarked to a broad range of experimental data that probe both the space-charge and impedance models in the code [10]. Ring parameters for the SNS Power Upgrade are listed in Table 4.3.

We expect the ring losses in the SNS baseline to be dominated by space-charge-induced halo growth. To consider the space-charge limit, one can assume that the space-charge tuneshift (ΔQ_{SC}) is the relevant parameter and then scale directly from baseline parameters. Assuming that the accumulated beam is painted to the same physical dimensions, and that the bunching factor is independent of energy, then the space-charge tuneshift is proportional to the factor $N/\beta^2\gamma^3$, where N is the intensity and β and γ are the relativistic factors. Figure 4.5 shows two curves of constant $N/\beta^2\gamma^3$, the lower of which scales from the baseline SNS parameters (and corresponds to ΔQ_{SC} = 0.15), whereas the upper curve scales from existing beam dynamics simulations showing acceptable losses at 2 MW and corresponds to ΔQ_{SC} = 0.20. Therefore, the 3.0-MW upgrade goal

Table 4.3. SNS Power Upgrade Ring parameters for the 1.3-GeV lattice

Beam energy	1.3 GeV
Tunes (horizontal, vertical)	6.23, 6.20
Natural Chromaticity (horizontal, vertical)	-7.9, -6.9
Phase slip factor	-0.139
Collimator acceptance	300 π mm mrad
Minimum ring transverse acceptance	480 π mm mrad
Ring rf voltage (h=1, h=2)	40, 20 kV
Phase-space painting	X and Y
Uncontrolled beam loss goal	$1x10^{-4}$

can be viewed as a straightforward extension of the initial baseline ring, at least as regards space-charge effects.

These qualitative arguments are verified through ORBIT simulations of the SNS ring at the 3.0-MW Power Upgrade parameters. In these simulations, the full ring accumulation is modeled, including interactions of the beam in the stripping foil, full three-dimensional space-charge effects, full treatment of the ring rf and beam collimation systems, as well as transverse and longitudinal impedance effects. Figure 4.6 shows the tune footprint at the end of accumulation for both the natural chromaticity and zero chromaticity cases. Although the incoherent tune distributions cross slightly the integer resonance, the coherent tunes remain above the integer stopband, as studied in detail in [11]. Figure 4.7 shows the final painted beam emittance distributions at large amplitude to assess ring losses near the collimator acceptance. Collimation is accomplished in a two-stage collimation system consisting of an adjustable scraper and a pair of fixed collimators. The adjustable scraper operates in the range 200-300 π mm-mrad, while the

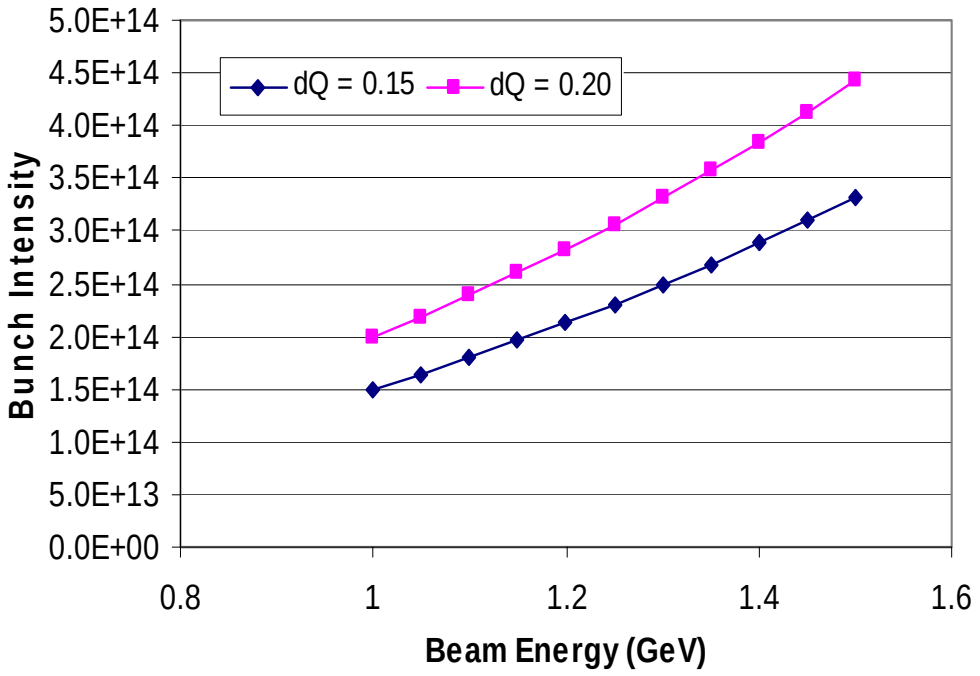

Fig. 4.5. Ring space-charge tuneshift scaling with energy. The intensity in the ring ($2.5x10^{14}$ at 1.3 GeV) has the same space-charge tuneshift as that in the initial baseline ring ($1.5x10^{14}$ at 1.0 GeV).

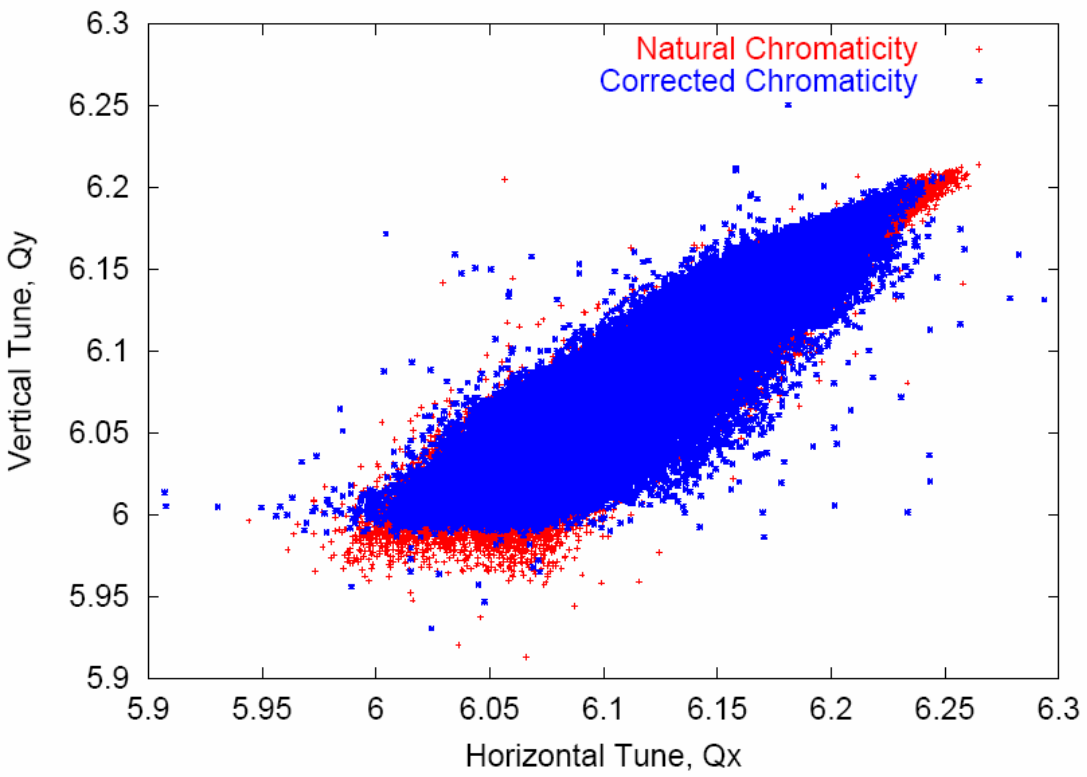

Fig. 4.6. Tune footprints at the end of accumulation for SNS Power Upgrade parameters. Distributions for both natural and zero chromaticity are shown.

fixed collimators have acceptances of approximately 300 π mm-mrad in both planes. The design goal for uncontrolled fractional beam loss in the ring is $1x10^{-4}$. From Fig. 4.7, we see that the beam loss goal of $1x10^{-4}$ is reached at approximately 220 π mm-mrad, which is well within the collimator acceptance and in the range of operation of the adjustable scrapers.

Collective instabilities are a possible limitation to ring beam intensity. Beam dynamics simulations have been performed with the ORBIT code with the Power Upgrade parameters to explore beam stability. The ring impedance is dominated by the extraction kickers. In order to extract a 1.3-GeV beam, the number of kicker modules must be increased from 14 to 16. We have taken the measured extraction kicker impedance, scaled appropriately to account for the additional kicker modules and performed ORBIT simulations to explore the instability thresholds. Figure 4.8 shows results of ORBIT simulations for 3.0 MW, including both 3D space-charge and the extraction kicker impedance with the chromaticity set to zero. The amplitude of the largest harmonic, n=14, is shown as a function of time during the 1-ms accumulation cycle. These simulations show that the ring intensity is below the instability threshold. We find an instability threshold at twice the extraction kicker impedance for zero chromaticity. At the natural chromaticity, the threshold is about three times the extraction kicker impedance.

The electron-proton (e-p) instability threshold is predicted to lie above the 3.0-MW SNS Power Upgrade design goal intensity [12]. Given the rather large uncertainties inherent in predicting the various features of this instability, we plan to install a wideband feedback system for damping a potential SNS e-p instability. This feedback damper will have a bandwidth and beam power in the order of 400 MHz and 1 kW. Recent successful experimental tests at the LANL Proton Storage Ring show that such instabilities in a long-bunch proton machine can be damped, as discussed in Section 8.3.

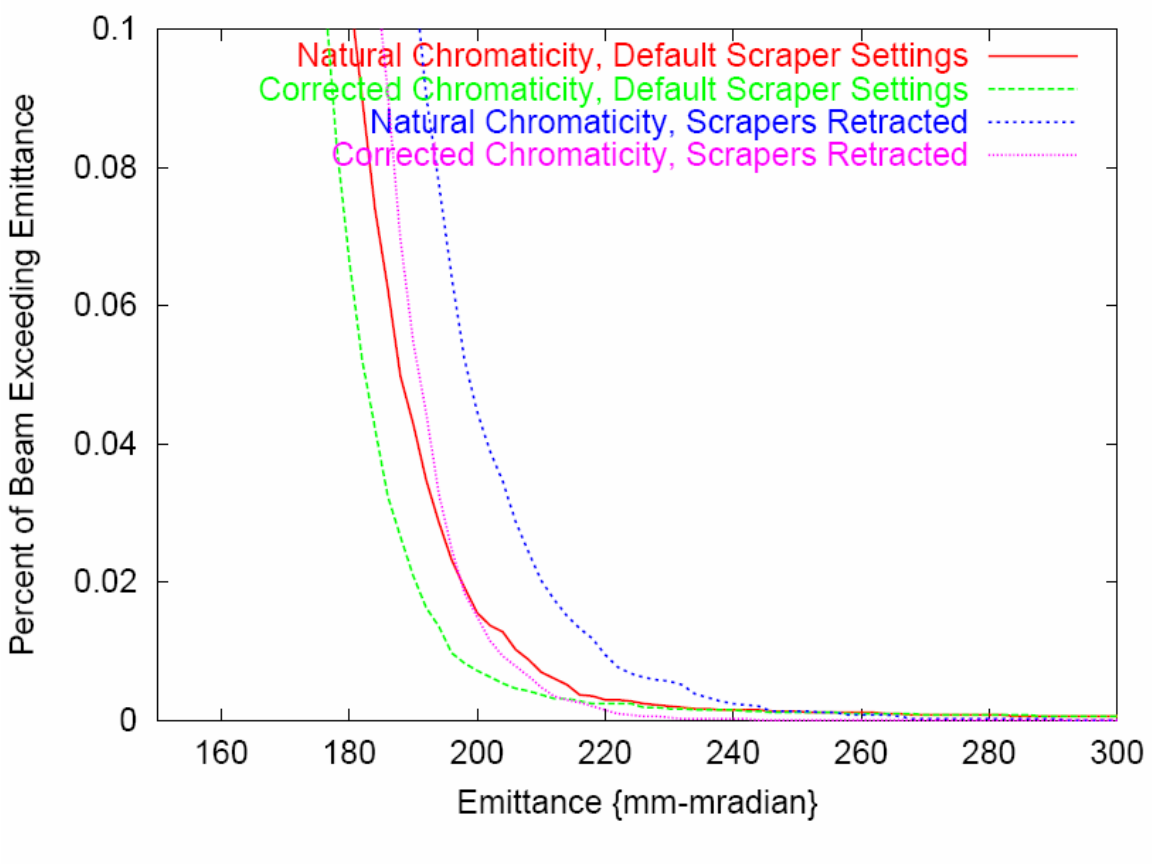

Fig. 4.7. Emittance distributions near the edge of the beam. Full scale is 0.1%. The fixed collimator acceptance is approximately 300 π mm-mrad.

Preliminary studies are under way to explore the benefits of a ring barrier rf system in order to improve the bunching factor. Two benefits arise from an improved bunching factor. First, the space-charge tuneshift is nearly uniform along the length of the bunch and has a smaller peak value, unlike with the existing baseline rf system, for which particles at the center of the bunch have depressed tunes approaching the integer value, as shown in Fig. 4.6. Secondly, the sharply falling longitudinal beam profile is advantageous from the standpoint of the "e-p instability," in that the trailing-edge multipacting mechanism is partially disrupted, as discussed in Section 8.1.

4.3 TARGET PHYSICS DESIGN

The Power Upgrade Project will increase the SNS beam power from greater than 1.0 MW to greater than 2.0 MW with a design goal increase from 1.4 MW to 3.0 MW. The beam energy increase from 1.0 GeV to 1.3 GeV is not a significant factor in the target design. In addition to increasing the beam power on the initial existing target station, the Power Upgrade will enable a second target station, a long-wavelength target station. With the exception of the stainless steel target container itself—containing the Hg and the inner neutron reflector plug—the remainder of the SNS target systems, including the mercury pump, mercury-to-water heat exchanger, moderator, supercritical hydrogen refrigerator for the moderators, shielding, and utility systems, is designed to operate at the upgrade power level of 2 MW or greater. The LWTS would require about 1 MW of beam power.

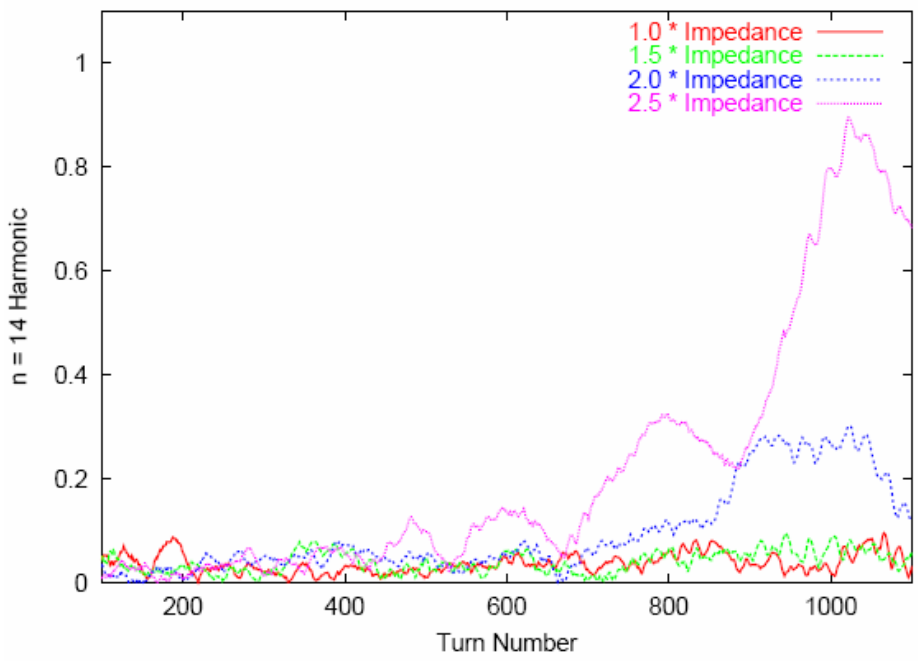

Fig. 4.8. Simulation of the n=14 harmonic amplitude during ring beam accumulation for the extraction kicker impedance artificially inflated by the factors given in the legend.

The mechanism that may limit beam power to the mercury target container is cavitation damage caused by the intense pressure pulse induced in the mercury during each beam pulse. Two primary pathways are being pursued to overcome this potential limitation: mitigating the pressure pulse by injection of a fine dispersion of small gas bubbles in the mercury, thereby reducing the driving force for initiating cavitation, and establishing gas layers between the mercury and target vessel to protect it against the damaging effects of cavitation collapse. Alternate materials and surface treatments to the target vessel are believed to have limited potential to further extend its power capacity and lifetime; therefore they are not major elements of the target R&D effort. They will be researched to a limited extent, nonetheless. Note that the original target is surface treated with the Kolsterising® process.

In addition, the proton beam window, inner reflector plug, moderators, some target utilities, and instrumentation and controls will require upgrades.

4.4 SUMMARY OF INTEGRATED PHYSICS DESIGN

Most of the SNS Power Upgrade is a straightforward extension of the existing SNS baseline, as regards beam dynamics. A number of detailed studies, both experimental and theoretical, have been carried out to validate the Power Upgrade configuration and design parameters. These studies have made use of the existing simulation tools that have been utilized for design of the baseline SNS, and which have been tested and benchmarked to a variety of experiments. Areas requiring further R&D are physics optimization, ion source and LEBT, SCL input rf power couplers, injection stripping foil, and Hg spallation target.

5. ACCELERATOR SYSTEMS HARDWARE UPGRADES

5.1 ION SOURCE AND LEBT UPGRADE (WBS 3.3.1)

The beam current required from the ion source and LEBT depend strongly on the beam emittance, because the RFQ transmission decreases rapidly with increasing emittance and increasing beam current. Figure 5.1 shows that a 59-mA medium-energy beam transport (MEBT) peak current requires an RFQ input current between 67 and 95 mA for a normalized rms emittance between 0.20 and 0.35 π·mm·mrad. Clearly, a low-emittance source has significant benefits.

These current requirements are a significant increase over the baseline requirement of 41 mA with a 0.2π·mm·mrad emittance, which is also shown in the figure. This baseline requirement is almost met by the emittances measured at the output of the SNS LEBT. The electron dumping field likely causes the horizontal emittance to exceed the vertical emittance by ~20%. LBNL measured the emittances at 33 mA in 2001 before the RFQ was mounted, while we measure the emittances on the test stand at the output of a duplicate LEBT. The measurements agree, except that we find the emittance to increase significantly with increasing beam current [13]. These measurements suggest that the requirements for the SNS Power Upgrade cannot be met by simply increasing the output current of the baseline ion source and LEBT.

The Power Upgrade requirement will be met by combining a low-emittance, high-current ion source with an LEBT that causes minimal emittance growth, both of which have been demonstrated.

The Japan Atomic Energy Research Institute (JAERI) developed a filament-driven multicusp H- source that delivered up to 72 mA with a 5% duty cycle [14]. Its emittance was measured at

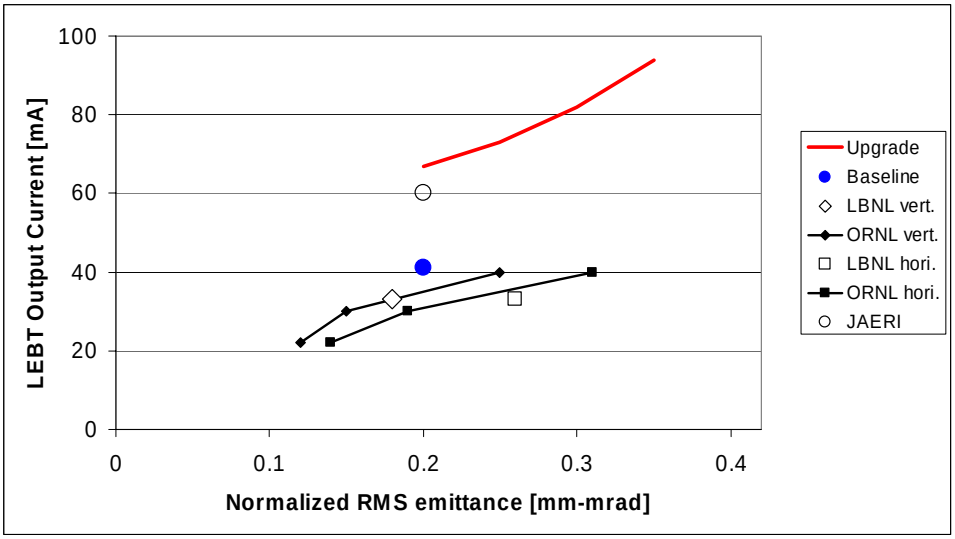

Fig. 5.1. LEBT beam current requirements vs. emittance.

the source output with 60 mA, where the normalized rms-emittance was 0.2 π·mm·mrad [15], as shown in Fig. 5.1. Even if its emittance increases linearly with beam current, the JAERI source meets the Power Upgrade requirement for the RFQ input current.

Magnetic LEBTs have been shown to inflict minimal emittance growth, especially after the beam is neutralized through collisions with the background gas [16, 17]. In addition, magnetic LEBTs are very robust and thus provide the high availability required for a user facility.

The lifetime of the JAERI ion source is limited to ~100 h [14], significantly less than our 3-week baseline requirement. This drawback is mitigated by our proposed two-source Y LEBT shown in Fig. 5.2. The two-source magnetic Y LEBT has two identical ion source beam lines that are merged with a double-focusing switching magnet into the RFQ injection line. While one ion source is delivering beam, the other source beam line is vacuum-isolated with a gate valve. This allows for the replacement of the isolated ion source with a newly conditioned spare. After the spare is vacuum-conditioned, the ion source will be conditioned and tested to full requirements using the diagnostics installed in both ion-source beam lines. After passing the acceptance tests, the source will idle until the performance of the operational source drops below the acceptance limit.

The proposed system is identical for both ion source beam lines, which reduces the changeover to inverting the polarity of the switching dipole magnet. After brief fine-tuning, we expect to restore full power beam operation in less than an hour.

A bending angle of 60° has been selected to minimize the LEBT length and associated collisional beam losses.

The beam line symmetry requires the beam to exit the switching magnet normal to the magnetic pole face. The beam exits the magnet with matched x and y Twiss parameters and therefore can be focused into the RFQ with a compact solenoid.

The entrance angles into the magnetic dipole field are used to achieve some double focusing, although some x-y asymmetry always remains with switching magnets. This unavoidable asymmetry is compensated with a magnetic quadrupole doublet in each ion source beam line.

A first-order beam transport calculation [18] of a fully neutralized H^- beam through the proposed LEBT is shown in Fig. 5.3. It shows the 0.2- and 0.4-kG/cm gradients in the 5-cm-long quadrupole doublets to focus the beam horizontally while defocusing it vertically. The focusing by the 1.5-kG dipole magnet and its 47° entrance angle lets the beam exit with fully matched vertical and horizontal emittances. A 20-cm-long, 3.4-kG solenoid injects the beam into the RFQ with the required Twiss parameters.

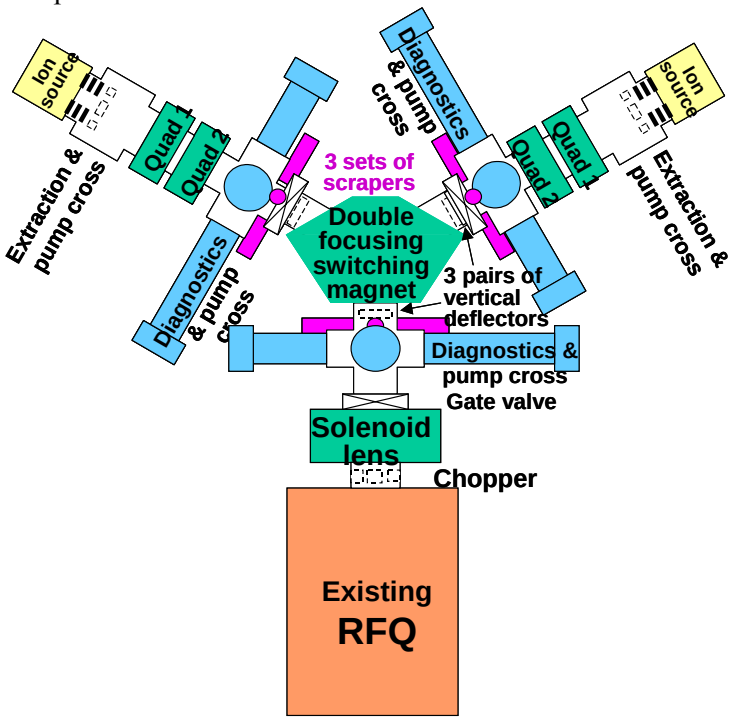

Fig. 5.2. Proposed two-source magnetic Y LEBT.

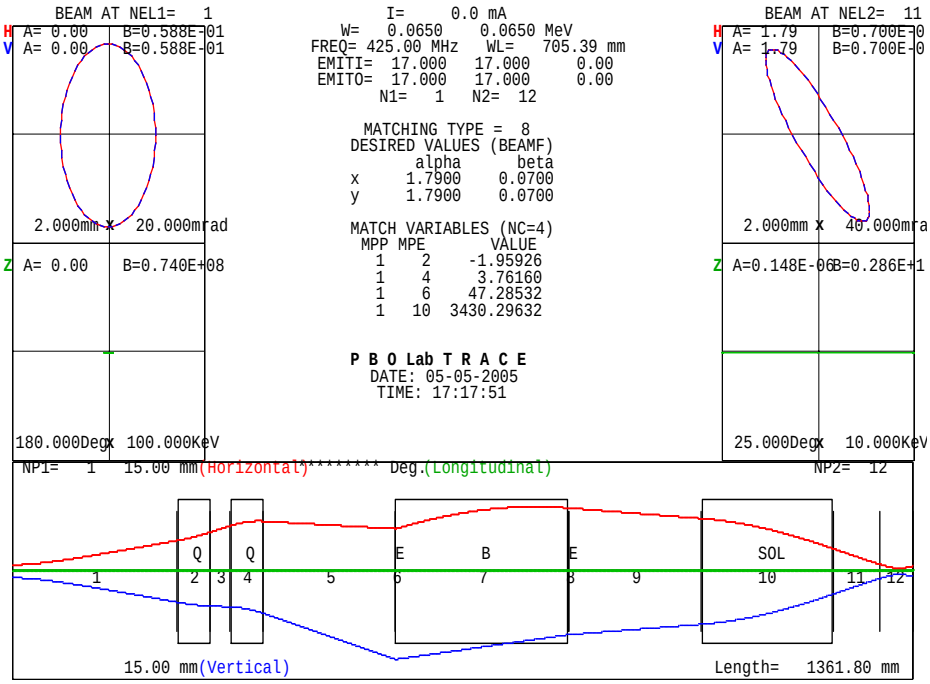

Fig. 5.3. Calculated transport of a neutralized H^- beam through the proposed Y LEBT.

The LEBT chopper is located just in front of the RFQ. The rapidly changing electric fields inside the RFQ and inside the chopper prevent a significant accumulation of positive ions and a neutralization of the beam. The entrance aperture to the chopper will be positively charged to confine and accumulate the positive ions inside the beam upstream of the chopper. Full neutralization is achieved before the end of the 0.2 ms that are currently blanked by the chopper.

The chopper electrodes have dimensions similar to the baseline chopper and therefore can operate with the baseline electronic system. However, the chopper requirements are significantly relaxed because the chopper electrodes will be operated near ground potential. For example, this allows the use of conventional off-the-shelf unipolar high-voltage switches, which avoids all problems encountered with the custom-built bipolar switches that are required for the baseline chopper. Accordingly, we propose to rebuild the chopper electronics to improve reliability and availability.

Positive ions generated in the ion source extraction field enter the source. A triode extraction system with a positive center electrode confines the ions generated in the downstream beam and allows for its neutralization.

The ~1.4-m-long LEBT trajectories require increased pumping to keep the collisional losses at the ~10% level. This is accomplished by differentially pumping the ion source outlet and doubling the pumping speed downstream of the extraction aperture. Pumps installed in the gaps between the dipole and the focusing magnets help to further lower the pressure along the trajectory. However, even with the increased pumping, the 50–100 sccm H_2 escaping from the ion source generates an H_2 background in which the H^- will neutralize in less than the first 200 μs that are blanked by the baseline chopper.

Beam current toroids in each of the three beam lines allow monitoring of the performance of the ion source and LEBT. Diagnostic stations are combined with pumping stations in the gaps between the dipole and the focusing magnets. Water-cooled, suppressed Faraday cups serve as full power beam stops and tuning monitors. Water-cooled Allison scanners allow for accurate emittance measurements of the 65-kV H^- beam at full intensity and full duty cycle. Emittance

measurements are planned as a part of the acceptance test for each newly installed source because the ion source emittance could help to control the losses of the accelerated beam. Biasable, four-jaw beam scrapers near the entrances and exit of the dipole magnet allow for collimating the beam. Allison scanners in the RFQ injection line support physics studies and troubleshooting.

5.2 RFQ AND MEBT (WBS 3.3.1)

To support the Power Upgrade design goal, the Front End will provide 2.5-mA average output beam current, which is a 60% increase over the initial baseline and corresponds to a peak RFQ beam current of 59 mA. In addition, there is a small increase in chopper beam-on duty factor from 68% to 70%. The RFQ output energy of 2.5 MeV remains unchanged. The present RFQ was designed for 56-mA nominal peak current; therefore it can be used for 59-mA peak current without modification. This 60% beam current increase will require additional rf power for the RFQ, as shown in Table 5.1, which is well within the capabilities of the existing rf system for the RFQ.

The existing initial-baseline MEBT was designed for 56-mA nominal peak current and therefore can be used for 59 mA without modification. Possible beam halo increases from increased space charge forces can be mitigated employing the same hardware installed for 1.4-MW operation—specifically, horizontal scrapers and axially symmetric beam optics in the second half of the MEBT.

5.3 DTL AND CCL (WBS 3.3.1)

The existing initial-baseline Drift Tube Linac and Coupled-Cavity Linac structures were also designed for 56-mA nominal peak current and therefore can be used for the 59-mA peak current without modification. The strength of the permanent magnet quadrupoles in the drift tubes of the DTL cannot be adjusted to optimize beam focusing, and consequently, the transverse acceptance of the DTL will decrease with increasing beam current. The Front End output emittance should be limited to less than 0.35 π mm-mrad for lossless transmission through the DTL and CCL.

Table 5.1. Rf power requirements in kW for the Front End, DTL, and CCL. The last column includes 10% control margin and waveguide losses.

	Structure kW	Beam kW Baseline (26mA)	Beam kW PUP (42mA)	Total kW PUP (42mA)	Total kW, inc. margin
RFQ	630	63	102	732	805
MEBT1	11	0	0	11	12
MEBT2	7	0	0	7	8
MEBT3	8	0	0	8	9
MEBT4	16	0	0	16	18
DTL1	339	131	211	550	605
DTL2	1058	399	645	1703	1873
DTL3	1277	439	709	1986	2185
DTL4	1292	436	704	1996	2196
DTL5	1284	415	671	1955	2151
DTL6	1254	372	601	1855	2040
CCL1	2126	529	854	2980	3278
CCL2	2466	623	1007	3473	3820
CCL3	2494	678	1095	3589	3948
CCL4	2523	739	1193	3716	4088

The beam current increase will require additional rf power for the six DTL tanks and four CCL rf modules as listed in Table 5.1, where the powers are in kW. The initial baseline average rf pulse current is 26 mA ,while the Power Upgrade requires 42 mA. The existing DTL klystrons have 2.5-MW rated output power, while those in the CCL have 5-MW rated output power. As shown in Table 5.1, the required power increases are within the existing available capabilities of the rf systems. However, High Voltage Converter Modulator ME-1, which powers the RFQ, DTL-1, and DTL-2 klystrons, requires minor upgrades to satisfy the increased average power demand.

5.4 SUPERCONDUCTING LINAC (WBS 3.3.2)

The energy increase required to meet the upgrade power goal will be achieved by installing nine additional high-beta (β=0.81) cryomodules. These slots are presently filled with warm drift beam pipes. The nine warm sections exist and are part of the existing beam transport line. Figure 5.4 shows a schematic of one high-beta cryomodule.

The additional 36 high-beta cavities will have a nominal gradient of 15.6 MV/m, more than sufficient to reach 1.3 GeV, and in fact providing additional operational flexibility. The final energy will exceed the nominal 1.3 GeV and will allow for operation with some cavities off, some cavities used for energy feedback, and some cavities used as online spares in case of component failure. The entire cryogenic infrastructure, central helium liquefier (CHL), and transfer lines, are in place already and will allow installation and cooling of the nine additional cryomodules.

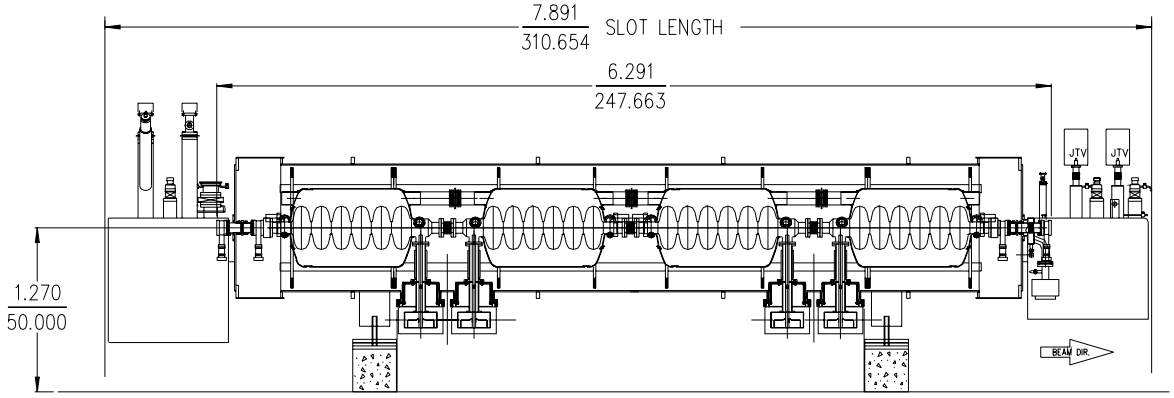

Fig. 5.4. High-beta cryomodule schematic. The dimensions of the upgrade cryomodules are constrained by the locations of the existing cryogenic line connections and warm sections.

Tuners for the upgrade will be of the same design as the original cryomodules. Lorentz force detuning may not be a problem for high-beta cavities, whereas it has been observed in the medium-beta cavities at gradients higher than the design values. Because of the difficulty of retrofitting, piezoelectric tuners (shown in Fig. 5.5) have been and will be installed in all cavities to deal with potential resonances near harmonics of the 60-Hz repetition frequency. However, only 33 piezo drivers and controllers, enough for all the medium-beta cavities, will be acquired. This equipment will only be installed on cavities, either medium- or high-beta, that show unstable behavior at higher repetition rates.

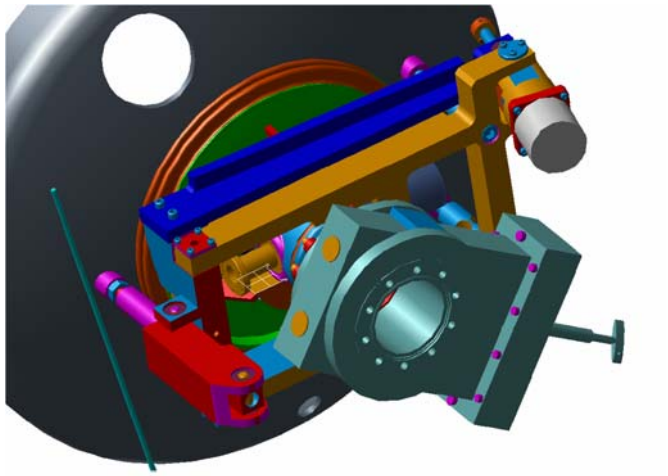

Fig. 5.5. Mechanical and piezoelectric tuners for the SNS cavities. The design of the tuners will be maintained for the upgrade cavities.

Twenty-four high-beta niobium cavities already exist at SNS and can be used for the upgrade cryomodules, possibly with some modifications. The additional cavities needed to complete the set of new cryomodules will be acquired as part of the cryomodule procurement package.

The testing and operation of the initial baseline superconducting cavities and their support systems during commissioning have given us clear insight into features that will improve reliability and operability of the upgrade cavities, cryomodules, and their auxiliary components. The areas where improvements will be necessary are:

- **Higher-Order Mode (HOM) filters tuning diaphragm reinforcement.** The thin HOM filter diaphragm, as shown in Figs. 5.6 and 5.7, is susceptible to deformations due to the heat treatment of the end groups performed to increase the thermal conductivity. End caps will have to be developed to prevent deformations that can lead to the notch filter's detuning with consequent large power flow through the HOM filters' feedthrough.

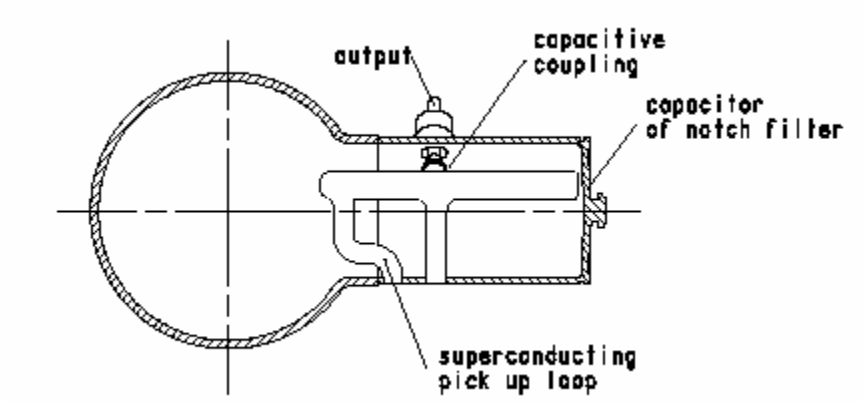

Fig. 5.6. Internal structure of the SNS HOM filter. The notch filter rejection frequency is tuned by moving the end diaphragm.

- **HOM filter feedthroughs.** The HOM feedthroughs used in the original SNS cavities are inadequate to handle large average and peak power excursions, which have been observed during the testing of the cryomodules. Jefferson Lab has already developed an improved feedthrough that will be used in the upgrade cryomodules.

- **Mitigation of field emission effects.** Field emission-induced quench is the final reason for gradient limitations in the cavities tested so far. Assuming that the radiation does not produce considerable damage to components inside the cryomodule, the field emitted electrons' heating on the end groups could be brought under control by some minor modifications to the cooling system. By adding some pressurized helium lines to the coupler cooling circuit, it is possible to stabilize the end group temperatures, thus achieving more stable operation at high gradients.

- **Fundamental power coupler.** As the beam current is increased, the beam loading term on the rf system increases proportionally. Even at the design gradients, the average power transferred through the couplers, shown in Fig. 5.8, may reach or exceed the maximum average power value of the present design. Whereas the couplers themselves can likely sustain higher average power than the design values, their center conductor temperature would increase beyond the limits, contributing a much higher radiative load to the heat budget of the end groups. This effect can be mitigated by improving the cooling of the couplers' center conductor and/or improving the cooling of the couplers' end group. Due to the additional beam loading term to the average power, it is likely that the existing initial baseline cryomodules may have to be operated at lower gradients than those envisioned for the first phase of operation, thus putting a heavier burden on the upgrade cavities and power couplers. More details are given in Section 8.5.

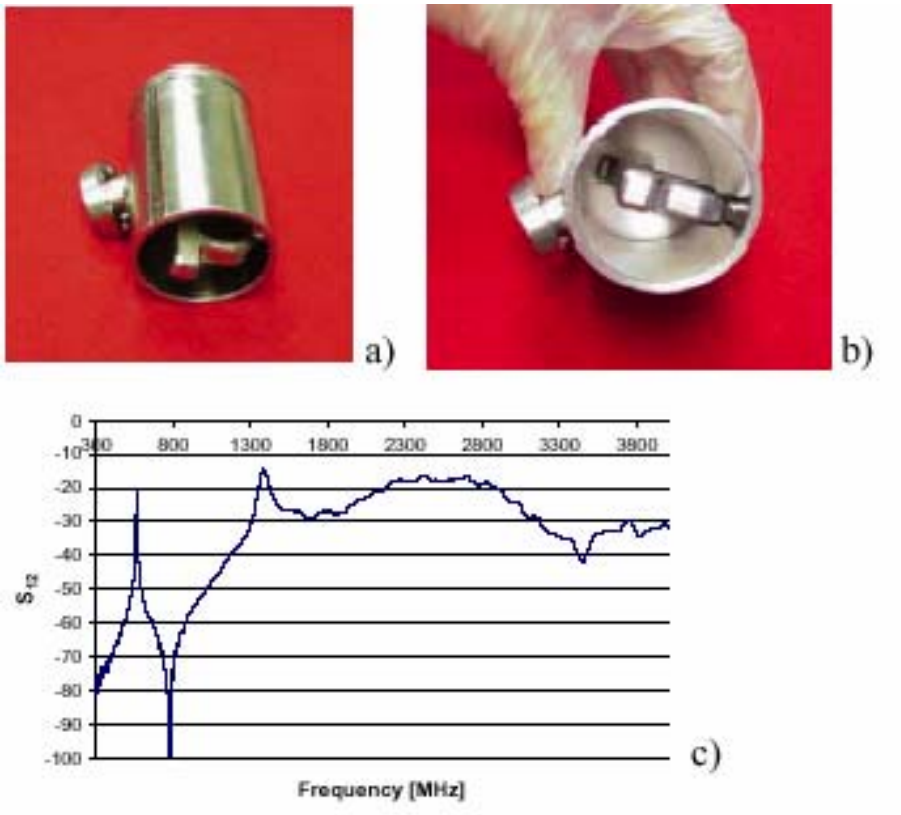

Fig. 5.7. HOM filter construction and its rf transfer function.

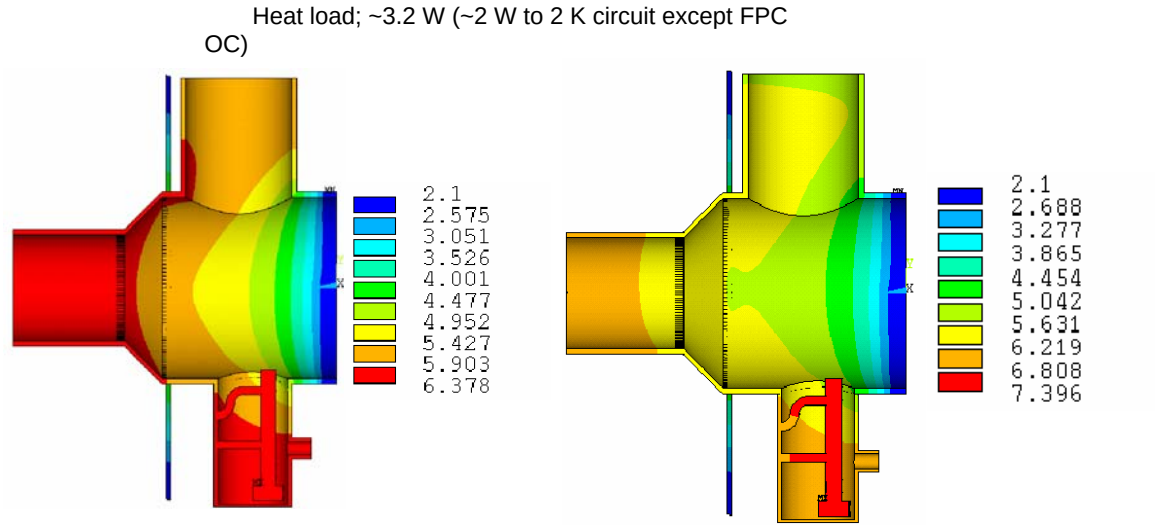

Fig. 5.8. Temperature distribution of the cavity's fundamental power coupler end group without and with rf. Heating from the coupler's center conductor affects the temperature distribution in the end groups. Field emission heating (observed experimentally but not included in these calculations) can significantly limit the cavity gradients.

A necessary vehicle to verify the design improvements and to implement a production philosophy based on the testing of cavities with all the real components and under real pulse power conditions is a horizontal cryostat, similar to that developed at Orsay for Cryholab, as shown in Fig. 5.9. This cryostat will allow performance coupler conditioning together with cavity testing and will eliminate several steps in the production sequence.

Fig. 5.9. The horizontal test cryostat at Laboratoire de l'Accelerateur Lineaire (LAL) at Orsay. This fast-cycling cryostat, together with peripheral components used in the final assembly, can support testing of cavities under realistic operating conditions.

5.5 SUPERCONDUCTING RADIO FREQUENCY (SRF) FACILITY (WBS 3.3.3)

Presently the SNS has no cavity and cryomodule SRF facilities. Nevertheless, the requirements for the Power Upgrade do not warrant developing full-production cavity and cryomodule capabilities at the SNS. The SRF facilities for the Power Upgrade should be simple, easily maintainable, and inexpensive, so that attention and resources can be dedicated to the quality of the end product and not to maintaining complicated SRF facility systems. Towards this end, the Michigan State University SRF facilities were studied, and a similar approach was determined to be acceptable for a maintenance and limited production support facility at the SNS. The SNS facility is based on the requirements to maintain, repair, and test Upgrade and existing cryomodules. Another important capability is coupler conditioning to support production. The transfer of the couplers to the conditioning cart must be done in a Class 100 cleanroom environment.

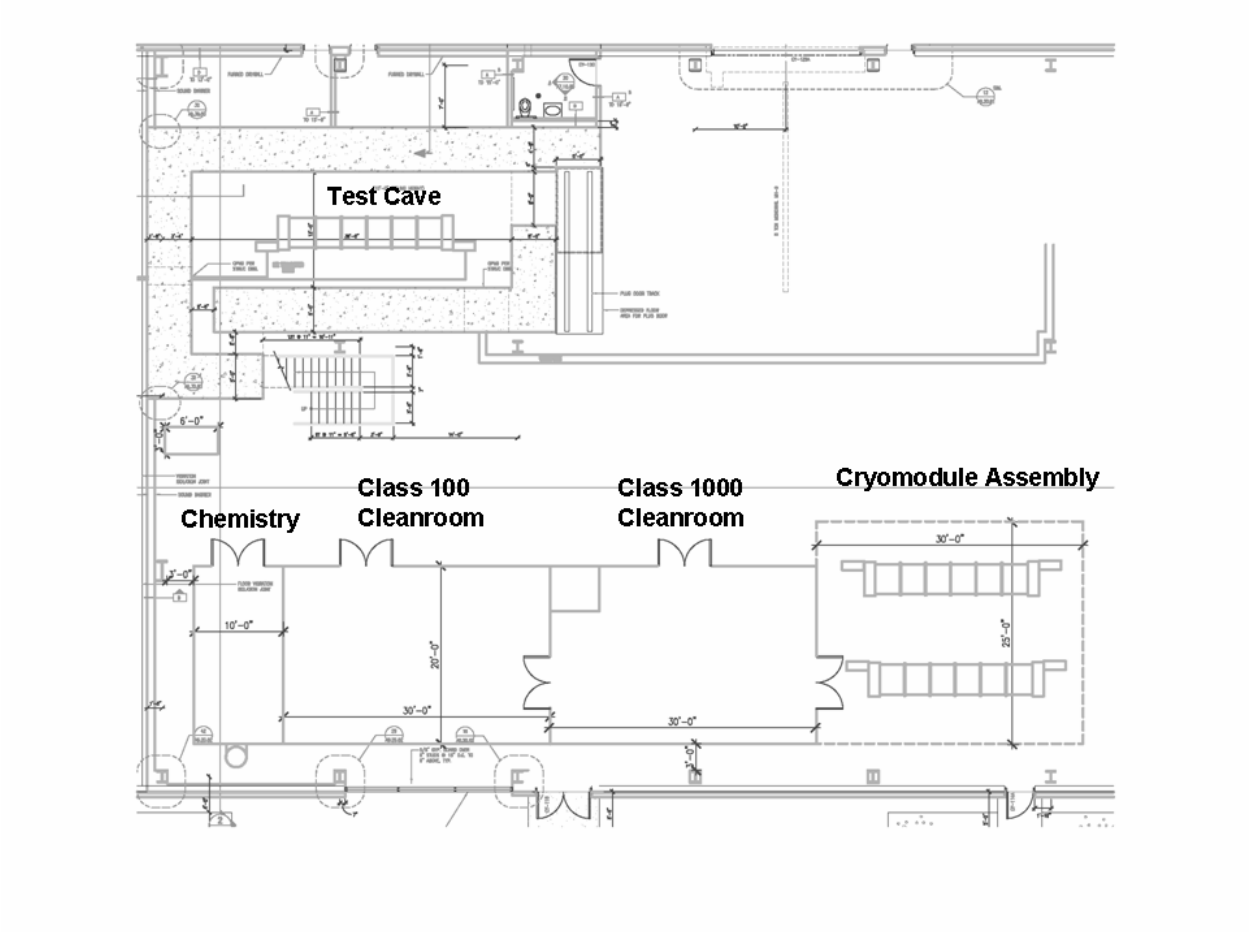

Fig. 5.10. Layout of the SNS SRF Facility in the existing RFTF building.

The layout of the facility is shown in Fig. 5.10. The following systems will be added to the SRF area in the existing RFTF building:

- Ultra-pure water system with 300-gal capacity to improve the existing facility high purity water skid. It is sized to support etching and rinsing one cavity during a single 8-h day. The system will be improved by the addition of extra filtration and reverse osmosis purification capability.

- Cleanroom equipment to support high-pressure rinsing, coupler conditioning cart installation, and string assembly in the Class 100 area, and general parts cleaning and cavity handling for vertical testing in the Class 10,000 area.
- Chemistry room (12 ft by 20 ft) with an acid scrubber system that will support manual etching and handle quantities of acids appropriate for the SNS needs.
- Cryomodule assembly area (25 ft by 30 ft with plastic curtains) that can accommodate assembly of a single cryomodule (on an installation rail) as well as the simultaneous repair of another cryomodule.
- An above-ground horizontal test cryostat for use in the test cave. This test cryostat will test SNS high-beta helium vessels and fundamental power couplers at full pulsed power. It is modeled after the CHECHIA at the Deutsches Elektronen Synchrotron (DESY) and the Cryholab at Orsay.
- A sub-atmospheric helium pump for temporary operation until the test refrigerator is operational. This helium system can be implemented in stages. Initial operation will be effected with liquid helium from outside vendors and two storage dewars, pumped via a commercially available Roots blower. Once it becomes operational, the test refrigerator will be used for cavity and cryomodule testing. The proposed facility includes a manual high-pressure rinse cabinet and string assembly and cryomodule tooling.

5.5.1 SRF Facility Cryogenic System (WBS 3.3.3)

The SRF Facility will require a cryogenics system to support component testing and R&D in the facility described above. The minimum load design specifications for this facility are 200 W at 2.1 K and an additional 200 W shield load between 38 K and 54 K. To reduce serious SNS downtime and financial risks, this cryogenics system will also be designed to be capable of maintaining the linac at 4 K during CHL maintenance or major breakdowns. The subsystems needed to achieve this are a 4 K Cold Box, Distribution Box, Transfer Lines, Refrigeration Recovery, Kinney Pump, Helium Dewar, and the Warm Compressor System already in place. The block diagram of the SRF Facility cryogenics system and its connection to the existing cryogenic system are shown in Fig. 5.11.

5.6 CRYOGENIC SYSTEMS (WBS 3.3.3.3)

The Central Helium Liquifier houses equipment that liquefies and circulates helium through the SCL. It contains equipment to allow smooth and efficient operation of the cryogenic systems. In addition, there are gas and liquid storage areas, and areas for tank and tube trucks to enter and make deliveries. Underground cryogenic transfer lines transport supercritical helium to and from the CHL to the cryomodules in the SCL linac tunnel. Figure 5.11 shows a block diagram of this cryogenic system.

This system consists of eight major subsystems: gas storage, compressor system, main 4 K cold box, 2.1 K cold box, purification system, 7000-L LHe dewar, Linac distribution system, and the cryomodules. The gas storage system has eight 30,000-gal tanks that can store helium at approximately 250 psig. Helium gas flows from these tanks to and from the compressor system and to and from the purification system. The compressor system (located in the compressor room of the CHL Building) consists of three dual-stage compressors, with two in constant operation and the third as a standby. The compressed helium flows to the main cold box (cold box room on the east side of the CHL Building), where it is pre-cooled with liquid nitrogen. It is further cooled to 4.5 K within the cold box through a series of turbo expanders and countercurrent flow heat exchangers. This main 4 K cold box supplies the 7000-L LHe dewar and the linac tunnel distribution system. The LHe dewar was designed to support the commissioning of the

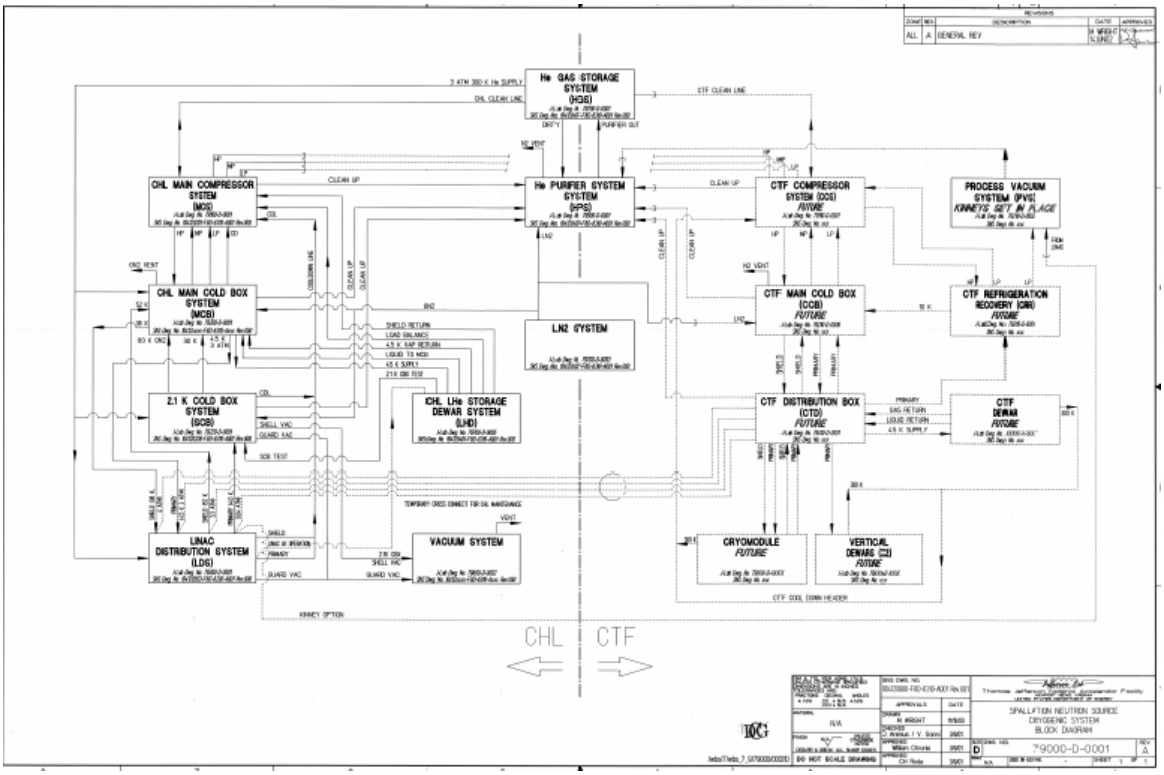

Fig. 5.11. Block diagram of the SRF Facility cryogenics system and its connection to the existing cryogenic system.

refrigeration system prior to the commissioning of the transfer lines and of the cryomodules. During normal operation, the 7000-L LHe dewar is used to manage the refrigeration system capacity. The tunnel distribution system is composed of approximately 950 ft of both supply and return transfer line. These lines connect the refrigeration system to the cryomodules. Helium is liquefied across a Joule-Thompson valve in the cryomodule. The 2.1 K cold box pumps on the liquid inventories in all the cryomodules, thereby lowering the temperature of the liquid to 2.1 K. This 2.1 K liquid (superfluid) provides cooling to the superconducting cavities. Table 5.2 lists major cryogenic system load parameters for 32 cryomodules required for the Power Upgrade (23 initial cryomodules and 9 Power Upgrade cryomodules). The existing initial baseline cryogenic plant is adequate for these nine additional cryomodules. In addition, the transfer lines for the additional cryomodules were installed as part of the initial baseline construction.

Table 5.2. Refrigeration Parameters for 32 Cryomodules

	Primary	Secondary	Shield
Temperature	**2.1 K**	**4.5 K**	**35–55 K**
Pressure	**0.041 bar**	**3 bar**	**4.0-3.0 bar**
Static Load	**863 W**	**5 g/s**	**6070 W**
Dynamic Load	**764 W**	**2 g/s**	**0**
Capacity	**2400 W**	**15 g/s**	**8500 W**

5.7 HVCM SYSTEM (WBS 3.3.1.2 AND 3.3.2.4)

The High Voltage Converter Modulators (HVCMs) provide cathode power to the klystrons to generate the necessary rf power levels. They are based on insulated gate bipolar transistor (IGBT) technology and operate at peak power levels near 10 MW. The upgrade will require increases in the power levels at which the seven room-temperature linac HVCM systems presently operate. While the four CCL HVCM systems will still be well within the Safe Operating Area (SOA) for the increased beam intensity, the three DTL HVCM systems will be forced to operate at or above the SOA. In particular, the HVCM for the RFQ and DTL tanks #1 and #2 will need to operate at 1.0 MW of average power to support the triad of klystrons at the maximum voltage level required of the three, which will generate excessive switching losses on the IGBT H-bridge networks. ICAP-4 simulations indicate that operation at up to +/-1300 V dc will be required, and that IGBT commutation currents will be approximately 1500 A. Previous experiments on the SCL HVCM system yielded IGBT failures at commutation currents in excess of 1000 A. Therefore, the upgrade plan includes implementing a parallel IGBT scheme in each H-bridge to reduce commutation currents to 50% of those predicted by simulations, upgrading the transformer/silicon controlled rectified (SCR) controller to produce higher voltages, increasing the voltage rating on the energy storage capacitor bank, and redesigning the output choke to handle the higher currents. However, alternative solutions are being studied that change the primary resonance conditions and may allow us to operate at or below the upper limit of IGBT commutation currents with the existing single IGBT topology.

For the SCL HVCMs, higher beam currents dictate rf power levels approaching 700 kW, which dictates a modulator output voltage in excess of 80 kV. A series of ICAP-4 simulations were performed to determine the HVCM limitations associated with operating at this level, with the results shown in Fig. 5.12. Operation with 12 SCL klystrons for each HVCM was chosen because the combination can meet the output voltage requirements with a minor upgrade to the ac systems and will take advantage of the parallel IGBT scheme development. Also, the 12-pack configuration allows for more operating margin and better reliability than a 9-pack scenario. This approach represents the minimum cost approach when consideration is given to the entire rf system, although there is some minor risk associated with the parallel IGBT development effort. However, as is the case for the RFQ/DTL modulator, an alternative resonance scheme will also be investigated with the possibility of reducing the dc operating voltage and eliminating the need for a parallel IGBT topology.

The 36 additional klystrons for the Power Upgrade Project will then require three additional HVCMs. Specifications and costing for these additional three HVCM systems were straightforward and were based on the original system costs with the necessary upgrades and enhancements.

5.8 SCL HIGH-POWER RADIO FREQUENCY (HPRF) SYSTEM (WBS 3.3.2.3)

Based on the analysis of the HVCM capacities in section 5.7, 12 klystrons per modulator will be used similarly to the existing medium beta rf architecture shown in Fig. 5.13, but with the modulators upgraded to handle the higher rf power requirements. Figure 5.14 shows the initial baseline rf power requirements (corresponding to 26 mA pulse beam current), the requirements in the Power Upgrade (corresponding to 42 mA pulse beam current), and HVCM capacities for modified and unmodified units. The power requirements shown in the figure include 12% control margin and 3% waveguide loss. It is important to note that if one klystron in a group is operated at a higher voltage, all klystrons in that group are subject to the same voltage and consequent power consumption. Table 5.3 summarizes the rf equipment needed for the Power Upgrade.

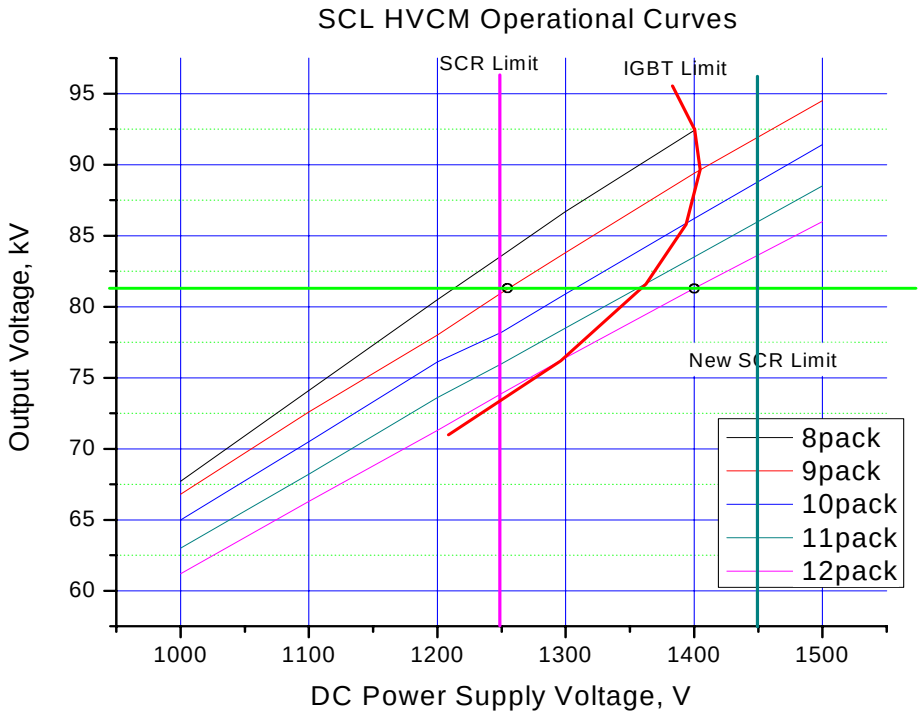

Fig. 5.12. HVCM output voltage vs. dc power supply voltage for various klystron configurations. Also shown are the 81-kV output voltage requirement (green), the present SCR voltage limit (magenta), the revised SCR limit obtained through upgrades described in the text (aqua), and the IGBT limit for a single device. The parallel IGBT scheme further raises that limit.

Power Upgrade Rf System Description: Two transmitters, each controlling six klystrons, will receive their high voltage from a single HVCM. Klystron control includes filament, magnets, ion pumps, cooling water flow, and solid state amplifier and numerous interlocks, all monitored by a programmable logic controller (PLC). From the klystron, the rf power is transmitted through a waveguide system to the cavity field input coupler on the cryomodule. The waveguide system consists of vacuum windows, waveguide straights, bends and flexible sections, directional couplers, a circulator, and circulator load. The last two components serve to protect the klystron from reflected power. One low-level radio frequency (LLRF) system (section 5.9) per cavity will control the rf phase and amplitude and provide equipment protection from arcs and other faults.

Transmitter: The control racks will continue with the same functionality but with some additional monitoring points to help perform fault diagnosis remotely. One PLC-based main rack will control three power supply racks. Each power supply rack will house filament, magnet, and ion pump power supplies for two klystrons. All power supplies of a type will be interchangeable and minimally modified from available commercial-off-the-shelf (COTS) product lines. Any of the six klystrons may be taken off line without affecting operation of the remaining systems. Minor changes have to be made to the HV oil tanks to facilitate isolating a klystron. The water manifolds may be distributed to enhance access to waveguide components and improve calorimetry.

Klystrons: The existing klystrons are suitable for higher power operation up to 750 kW with only an increase in water cooling flow. Water connections will be minimized and standardized at the klystron top to enhance klystron replacement and vibration isolation.

Waveguide Runs: The present waveguide runs overlap each other and are difficult to service. The Power Upgrade runs will be simplified with minimal overlap. The circulators and circulator loads will be accessible and will continue to be rated to take full power reflections. An inexpensive Rexolite window and drain between each circulator and load will protect the klystron and its respective cavity from a catastrophic water load failure. A simple waveguide shorting plunger will permit repaired klystron/components to be tested off-line during normal operation.

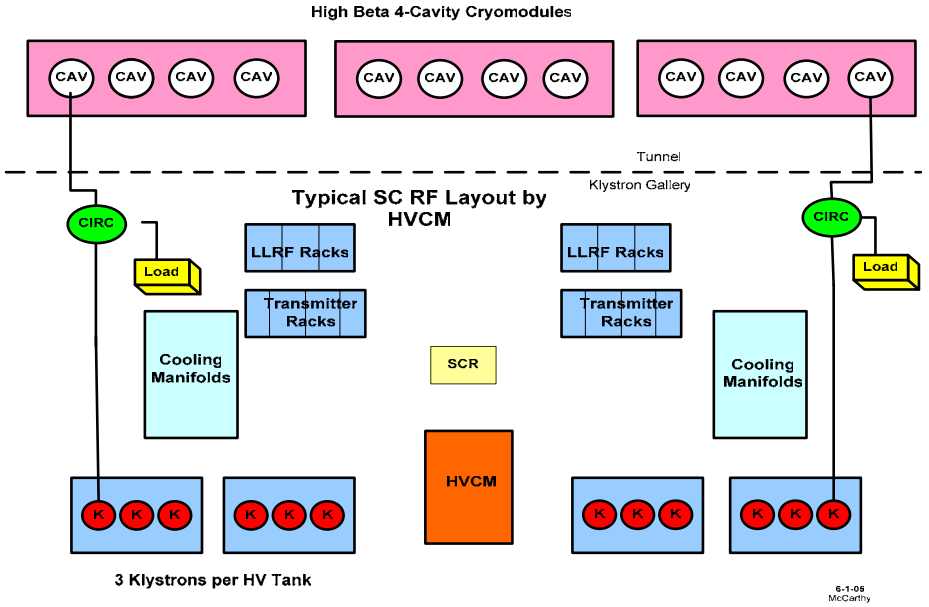

Fig. 5.13. Layout and photo of existing 12-klystron-per-modulator architecture that will be used.

operations. The rf architecture has one klystron per cavity; if any element in the cavity rf system fails, it can be isolated and operations may continue. If the Power Upgrade cavity fields are assumed to perform as well as existing cavities, then good potential exists for making up for lost

cavities. Using modified HVCMs, an average of 100 kW is available per klystron to increase the gradient in selected cavities. Four to seven cavities with sufficient gradient margin could compensate for an off-line cavity. Approximately 6 (of 84) high-beta (HB) cavities could be off-line without significantly sacrificing beam energy. The mean time between failures (MTBF) is affected by the quality of and the stress on the components. Improving the mean time to repair (MTTR) is a continuing effort. It will require tracking failures and performance degradation trends, better built-in test circuits, providing for rapid isolation of failed systems, and positioning components to enhance ease of replacement. An rf systems database has been started for tracking and trend analysis. We will incorporate the lessons from installation and operation of the existing system into many small design enhancements to improve availability.

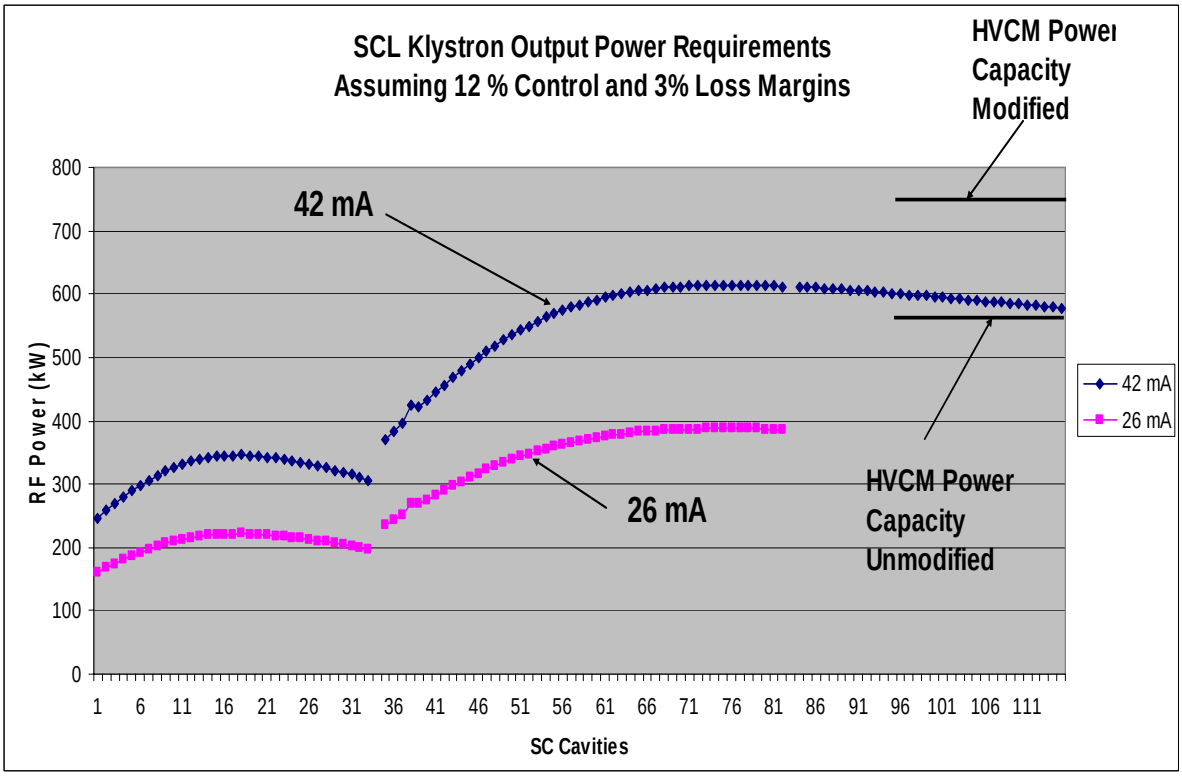

Fig. 5.14. Required rf power per klystron in the initial baseline and the Power Upgrade. Also shown are the HVCM capacities for modified and unmodified units. Modified HVCMs provide sufficient cathode voltage for the required rf power.

Table 5.3. Rf-related equipment increase for the SNS Power Upgrade

Major equipment	Initial SNS baseline	Power Upgrade	Increase for PUP
Cryomodules	23	32	9
SCRF klystrons	81	117	36
SCRF transmitters	14	20	6
SCRF HVCMs	7	10	3
SC LLRF systems	81	117	36

5.9 LOW-LEVEL LINAC RF CONTROL SYSTEM (WBS 3.3.2.3)

The low-level rf systems control the linac rf systems, and most importantly, the phase and amplitude of rf from each klystron. The initial baseline stability requirements for this control are 1.0 degree in phase and 1.0% in amplitude. The LLRF systems on the 96 existing rf systems more than meet this specification, with 0.5 degrees in phase and 0.5% in amplitude operating with a digital feed forward system. Because of this success, the 36 additional LLRF systems will be essentially identical to the system already deployed. A block diagram for these systems is shown in Fig. 5.15.

The LLRF system is a digital control system that fundamentally realizes a Proportional-Integral (PI) feedback controller. The heart of the system is the field control module (FCM),

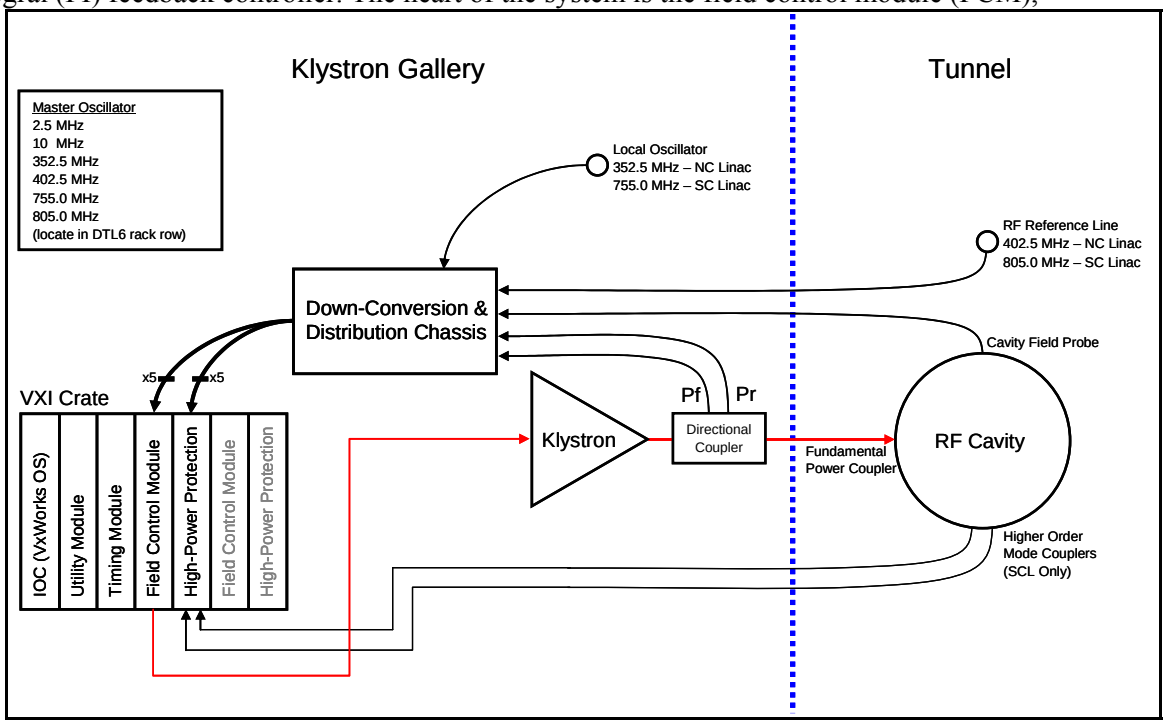

Fig. 5.15. Block diagram of the SNS linac low-level rf control system.

which digitizes four channels of 50 MHz analog inputs, digitally processes the data stream, and produces an rf output signal at either 402.5 or 805 MHz, depending on the location in the linac. The FCM is a VXIbus module and is comprised of a motherboard and three daughterboards: analog front end (AFE), digital front end (DFE) and rf output (RFO). The DFE consists primarily of four A/D converters and a single Virtex II field programmable gate array (FPGA). Communication with the outside world is via the slot-zero input-output controller (IOC) running the VxWorks operating system. The LLRF Finite State Machine is implemented as an Experimental Physics and Industrial Control System sequencer running on the IOC. The LLRF control system also provides high-power rf protection via the High-Power Protection Module, which provides for fast shutdown of the rf drive in case of rf overpower, arcs in the rf distribution system, poor vacuum, and "soft" interlocks such as cryo, coupler cooling, and HPRF permit. Down conversion of reference and cavity signals is performed in a temperature-regulated chassis. The master oscillator (MO) provides low-noise, phase-coherent reference signals that are distributed throughout the klystron gallery and tunnel.

The configuration of two LLRF control systems per rack will be used for the Power Upgrade. This implies splitting systems across two high-voltage converter modulators, which is already done in the baseline linac.

Piezoelectric tuners have been installed on all existing 81 SCL cavities and cooled to low temperature because of the difficulty of retro-fitting this hardware; however, the drivers and controls for these tuners were not part of the initial baseline project. Thirty-three drivers and controllers, enough for the medium-beta linac, will be constructed in the Power Upgrade. The LLRF control system will provide a drive signal to the piezoelectric tuner high-voltage amplifier. In principle, an arbitrary waveform generator is needed, although the interface details are unknown at this time because a particular amplifier has not yet been specified. This generator will be a COTS product if possible.

The production and procurement will follow closely the successful model that was established during the construction of the initial baseline SNS linac. Due to time constraints, all electrical components needed for the production of the FCMs and the high-power protection modules were purchased by SNS and provided in kits to the vendor who performed the assembly of the printed circuit boards. Responsibility for these procurements will likely be turned over to the vendor in the future.

5.10 HEBT (WBS 3.3.4)

The High Energy Beam Transport that transports the H^- beam from the SCL to the ring is 170 m long and contains a 90° achromatic bend to measure the beam energy and provide momentum collimation. The HEBT was designed and built to accommodate beam operations up to 1.3 GeV. The magnets, power supplies, water, vacuum, diagnostics, cabling, collimator systems, and linac beam dump are all capable of accommodating 1.3 GeV beam without modification.

The fractional loss per meter due to magnetic field stripping of the H^- beam can be expressed as

$$\frac{df}{ds} = \frac{B}{A_1} \cdot e^{\frac{-A_2}{\beta\gamma cB}},$$

where B is the magnetic field, β and c are relativistic factors, and A_1 and A_2 are constants. To maintain the fractional stripping losses of a 2.5 mA beam below 1 nA/m, the magnetic fields must be kept below 2.5 kG. The magnetic fields in the eight achromat dipoles at 1.3 GeV are 2.45 kG, so 1.3 GeV is the maximum practical beam energy in the HEBT.

The original design of the HEBT included 805 MHz rf cavities for control of beam injection into the longitudinal phase space of the ring. One cavity, the energy corrector cavity, will correct beam energy fluctuations with the standard time-of-flight technique and the other cavity, the energy spreader cavity, then paints this narrow energy distribution into the ring rf longitudinal bucket, thus giving sharp energy boundaries. Subsequent model-based simulations determined that these cavities were not required for 1.4-MW operation at 1.0 GeV, and fabrication and installation were de-baselined in the initial project. These rf systems probably will be necessary for low-beam-loss 3.0-MW operation at 1.3 GeV. The existing HEBT has been designed for these cavities; their preliminary design is similar to the CCL cavities, and detailed drawings exist. The fabrication and installation of these systems will be completed in the Power Upgrade. Detailed model calculations will be necessary to optimize and determine the exact requirements for these systems.

5.11 RING (WBS 3.3.4)

The accumulator ring has a circumference of 248 m with four straight sections. The straight section length was increased early in the initial project to allow space for the longer H^- injection magnets required for 1.3-GeV operations. Although much of the ring was designed and built to accommodate 1.3-GeV operations, there are several systems that will be modified. These are the injection chicane magnets, the injection kicker system, the injection section vacuum chambers, the extraction kickers, the collimator/scraper system, and the ring rf system. Some additional beam diagnostics will also be required. The injection chicane magnets, the injection kicker system, and the injection section vacuum chambers compose almost all the components within the injection straight section of the ring, so this section must be nearly completely redesigned for 1.3-GeV injection.

5.11.1 Injection Chicane Magnets (WBS 3.3.4.1)

The function of the injection chicane magnets is to merge the incoming H^- beam with the circulating H^+ beam. The magnets now installed are optimized for 1.0-GeV injection. As the beam energy is increased, the maximum allowable magnetic field must be decreased to avoid H^- field stripping. The chicane magnets must consequently be longer to achieve the same bend angle with the reduced magnetic field and the increased beam energy. The magnetic field shapes of chicane #2 and #3 must also be re-optimized to channel the stripped electrons away from the stripper foil toward the water-cooled electron catcher. These two new chicane magnets will also likely require new power supplies. The existing power supplies are rated for 4000 A at 18 V, and while the requirements for the new chicane magnets are not known at this time, it is unlikely that they will be adequate to power the new magnets.

5.11.2 Injection Kicker System (WBS 3.3.4.1)

The purpose of the injection kicker system is to paint the injected beam into the ring aperture. The maximum kick angle must be sufficient to move the circulating beam to within a few millimeters of the injected beam (the precise value will be determined by an injection optimization study). Two of the presently installed injection kicker power supplies (for the short vertical kickers) cannot deliver the current required for the 1.3-GeV beam. These supplies are rated for 1,400 A, but to achieve the full 46-mm deflection required to deflect the circulating beam to match the elevation of the injected beam will require ~1730 A. An upgrade to 1500 A is straightforward, and depending on the results of the injection study, this may be sufficient. If not, completely new supplies will be required. The other injection kicker supplies (long and short horizontal and long vertical) are already suitable for beam injection at 1.3 GeV.

5.11.3 Injection Section Vacuum Chambers (WBS 3.3.4.1)

The two new chicane magnets will require new vacuum chambers, and a new stripper foil mechanism (or two), with associated vacuum chamber and electron catcher, also will be required. The foil mechanism will allow measurement of the currents generated in the foils, and the associated electronics must be designed and installed. The electron catcher will also be monitored, possibly using a video camera. Since the activation levels in this region of the ring will be high due to the large angle nuclear and Coulomb scattering in the foil, the vacuum flanges will also be redesigned for remote and quick disconnects.

5.11.4 Extraction Kickers (WBS 3.3.4.1)

The 14 extraction kicker modules presently installed in the ring do not provide sufficient deflection for a 1.3-GeV beam. This was anticipated during the ring design, and space was reserved to add two additional kicker modules. This portion of the upgrade will therefore be straightforward. The two kicker vacuum tanks will be modified to each accommodate one additional kicker module, and the two new kicker magnets, pulse forming networks (PFNs), charging supplies, and controls will be duplicates of the existing units.

5.11.5 Collimators/Scrapers (WBS 3.3.4.1)

The presently installed collimator/scraper system was optimized for 1.0-GeV operation. The collimators will probably already meet the 1.3-GeV requirements, but the scraper blades may not provide sufficient deflection for a 1.3-GeV beam. A detailed design study is required to determine if any modifications are necessary. If new scraper blades are required, the entire scraper mechanism will have to be changed out, because the existing one will be highly activated and impractical to modify. The scraper design team will also consider electrically isolating the scraper blades and monitoring the currents due to beam interactions, since this will improve beam availability and reliability.

5.11.6 Ring Rf (WBS 3.3.4.2)

Beam loading due to the higher beam intensities in the ring will likely interfere with the performance of the ring rf system. The original design used three charging supplies, but this was reduced to two to minimize the cost. The third supply (in each of the four units) will be required for the upgrade beam intensity. Dynamic tuning supplies may also be required, as well as relocating the driver amplifiers to the beam tunnel. It is uncertain if these latter two modifications are necessary for the upgrade. The rf system performance will be characterized and analyzed as the present ring is commissioned, and the outcome of these studies will determine the extent of the required modifications.

5.11.7 Ring Diagnostics (WBS 3.3.4.5)

With the higher beam intensity in the ring there is an increased chance of beam instabilities that could limit the maximum intensity. Estimates of beam instability due to structure impedances show that it is unlikely we will encounter this type of instability, but the threshold for the electron-proton instability cannot be accurately estimated at this time. To ensure that this and other beam instabilities do not limit the performance of the ring, an active damping system will be installed. The beam line components for this system have already been installed, but the electronics need to be designed and installed. The power and bandwidth of this system are expected to be approximately 1 kW and 400 MHz. Personnel from SNS have also been working with colleagues from the LANL Proton Storage Ring (PSR) to test a prototype e-p active damping system at the PSR. Initial results look very encouraging, and we are confident that a similar system installed at the SNS ring will effectively damp this instability.

Other e-p mitigation systems include a clearing electrode in the vicinity of the primary stripper foil, which is presently installed but requires a high voltage power supply, and solenoid windings around the beam pipes in the collimator straight section, which also are presently installed but require power supplies.

Beam halo consists of a relatively small number of particles far from the core of the beam. Because of the relatively small number it is difficult to measure, but because the overall SNS beam intensity is so high, the halo contains enough particles that it can make a sizeable

contribution to the maximum allowable beam loss budget. For example, as stated in the Integrated Physics Design portion of this report, it is expected that the beam losses in the ring will be dominated by space-charge-induced halo growth. The HEBT and ring already contain beam scraper and collimator systems to help manage the beam halo. These systems will be augmented with beam diagnostic halo measurement systems to develop a better understanding of the extent of the halo, how it is formed, and how it depends on beam parameters.

5.11.8 Ring Injection Dump (WBS 3.3.4.6)

The existing Ring Injection Dump (RID) has been designed and built to dissipate 150 kW of beam power, which corresponds to 10% of the linac output beam power. The Power Upgrade will result in an increase in beam power to the RID that may reach 300 kW for the same stripping inefficiency and foil miss fraction that were assumed in the initial baseline design. Thermal analysis results indicate that the dump will be marginal at levels approaching 200 kW due to high temperatures in the surrounding concrete. Modifying the existing dump to dissipate 300 kW is a difficult task because of the design geometry. The concrete surrounding the dump is heated due to scattered particles from the dump material itself. As a result, options for upgrading the dump have been explored.

There are two beam physics requirements that will be modified in the Power Upgrade. First, the existing RID is designed to accommodate a beam displacement up to 5 cm from the nominal center of the dump. In the upgrade, this requirement will be reduced to 1 cm, which will be achieved by the installation of additional beam diagnostics and a low-field corrector in the injection dump line. This offset reduction will allow greater beam power handling capability for the same thermal stress limitations. Secondly, the existing RID design calls for 150-kW peak and average power handling capability; in the upgrade, the peak capability will be 300 kW, while the average capability will be 230 kW, corresponding to 7% of the linac output beam power. This difference takes into account the expected foil inefficiency degradation that is observed at similar facilities that make use of stripping foils for charge-exchange injection.

Further work is ongoing in several areas, including: extension of thermal analyses to greater than 200-kW beam power, studying new dump materials to reduce the scattered power into the surrounding concrete shielding, exploration of higher water cooling flow rates, and exploration of flowing lower temperature cooling water. Depending on the scope of required upgrades, the RID remains a risk for the Power Upgrade, and a final determination can only be made after experience is gained from high power operation at presently foreseen power levels. Therefore, the high-range cost estimate includes $5M for additional upgrades to the injection dump subsystems.

5.12 RTBT (WBS 3.3.4)

The Ring-to-Target Beam Transport is 151 m long and transports the beam from the ring to the target. Most of the systems in the RTBT are already capable of accommodating the 1.3-GeV beam without modification. There are, however, some exceptions.

5.12.1 Dipole Magnet DH13 (WBS 3.3.4.1)

The DH13 dipole magnet is directly in the line of sight for the gamma ray back-shine from the target. At the higher beam intensities, the radiation levels at this magnet may be too high, and the magnet will be changed out to a rad-hard design. The vacuum chambers in this region will also be redesigned for remote and quick disconnects. Other beam line hardware in this area will also need to be hardened, possibly by adding mineral insulated patch cables.

5.12.2 Closed-Loop Water Cooling System (WBS 3.3.4.1)

The water cooling loops for the RTBT magnets presently circulate water up to the equipment buildings. Water that is activated during normal operations therefore causes elevated radiation levels in these buildings. The upgraded beam power may cause the radiation levels to be high enough that it will be desirable to install tertiary cooling loops on the magnets that receive the most radiation. The most likely magnets to require the extra cooling loops are the rad-hard quadrupoles Q27 through Q30, and the dipole magnet DH13.

5.12.3 RTBT Diagnostics (WBS 3.3.4.5)

The beam profile and position on the target is an important issue for the upgrade. The present diagnostics are marginal for 1.4-MW operations, since the closest profile monitor to the target is 9.5 m upstream, and the beam profile on the target can therefore be only indirectly measured. This will likely prove to be inadequate for higher beam powers. The upgraded target should have a profile monitor within approximately 1 m of the target.

5.13 INTEGRATED CONTROL SYSTEM (WBS 3.3.5)

The Integrated Control System for the Power Upgrade will include controls for all of the new or upgraded accelerator, target, and conventional subsystems described elsewhere in this report. In addition, the Power Upgrade includes an extension to the Personnel Protection System (PPS). In general, these subsystems will be the same as or similar to the existing subsystems already in use for the SNS. The conceptual control system design is therefore for "more of the same," with the few exceptions noted below.

The control system can be thought of in two categories: the "global" subsystems—network, timing and PPS and machine protection (MPS)—that are common to all parts of the upgrade, and the distributed, subsystem-specific IOCs with their associated PLCs and fieldbuses, IO modules, and controllers. These two categories are discussed below:

5.13.1 Global Subsystems (WBS 3.3.5)

- ***Network:*** To accommodate added equipment for the SCL extension, the backbone network will be extended to Communication Room #6 in the Klystron Gallery, where new switches will be placed to extend and distribute the network to more "edge" switches placed in appropriate rack rows housing new accelerator equipment. This infrastructure extension will include the necessary fiber and fan-outs to support extensions to the timing and MPS systems.

- ***Machine Protection:*** The MPS design for the Power Upgrade is based on the continued validity of the assumption for the SNS that "the machine can take one full pulse with no damage." The present approach of using only one set of Beam Loss Monitors for both beam diagnostics and machine protection is also assumed. Eight additional MPS chassis will be required to support new inputs from the SCL extension.

- ***Timing:*** The Power Upgrade includes approximately 34 new VME/VXI-based IOCs. All of these will include a "Utility Module" for the timing system "Real-Time Data Link," and many (those for low-level rf, high-power rf, and some front end, approximately 27 in all) will require event receivers.

- ***Control Room, Servers, and Application Software:*** No change to the SNS Central Control Room is anticipated for the Power Upgrade. Some added storage capacity may be required for increased archiving capability. The existing SNS suite of application software will serve for the Power Upgrade.

- ***PPS:*** All new rf transmitters and modulators will be added as PPS inputs; however the PPS approach will remain unchanged. It is likely that additional chipmunks will be required for the Klystron Gallery.

5.13.2 Distributed Subsystems (WBS 3.3.5)

- ***Ion Source:*** Significant changes are proposed for the Ion Source and LEBT design. Although the basic controls approach using a PLC and field bus will be the same as for the SNS, the dual-source approach combined with added functional modularity will require more IOCs, and the many design specifics required to meet the increased current capability will require some new "one-off" controller and driver designs. The new approach will also require a considerable R&D effort and development of test stand controls.

- ***DTL and CCL:*** Only the addition of a few IO points and one PLC is anticipated for the warm linac control system.

- ***SCL:*** Most of the additions to the control system will be to support the nine new cryomodules and their associated subsystems. The major subsystems will be treated separately.

- ***Cryogenic systems:*** Controls for the nine new cryomodules will use the same design as for the existing SCL. Three IOCs and three PLCs are required.

- ***RF Systems:*** Controls for the 36 new cavities and 4 new converter-modulators will use the same hardware and software design as for the existing SCL. Eighteen new LLRF IOCs (two cavities/system as in the existing linac) and three high-power HPRF IOCs are required. The HPRF PLCs will be supplied by the HPRF equipment vendors and are not in the control system scope. Piezo tuner controls will be added to 33 SCL cavities. The controller hardware for these is in the rf system scope; some additional IOC software will be developed for the approximately 1000 new channels.

- ***Vacuum:*** The vacuum system for the SCL extension will not use the same design as the rest of the SCL; it will be a PLC-based system following as closely as possible the vacuum system design for the warm linac, HEBT, and ring. Two PLCs and one IOC are required.

- ***Power Supplies:*** Controls for all necessary beam line magnets and power supplies will already be in place; this is not a part of the Power Upgrade scope.

- ***HEBT-Ring-RTBT:*** The principle addition is controls for the HEBT energy corrector and spreader cavity systems. Controls for these rf subsystems will require two LLRF IOCs and two HPRF IOCs. One IOC and 2 PLCs will be required for the vacuum system and another IOC with two PLCs for the resonant cavity control system. Design in all cases will be similar, but not identical, to corresponding systems in the existing CCL.

- ***Target:*** The target upgrade for higher power includes a helium bubble injection system and an improved reflector plug. One IOC and about 50 IO points will be added to the existing control system.

- ***Facilities:*** The facilities control system will be extended to include the 1.0- to 1.3-GeV klystron gallery space, as well as the SRF laboratory. One IOC and one or two PLCs will be needed.

6. TARGET SYSTEMS UPGRADES (WBS 3.4)

6.1 MERCURY TARGET UPGRADE (WBS 3.4.1.1)

The SNS target assembly includes the target module, transport carriage and drive system, mercury process equipment, and related instrumentation. Upgrading the target assembly to accept higher power requires redesign, fabrication, and installation of an improved target module as well as the addition of utility systems in the Target Service Bay.

It is anticipated that higher power targets will require a gas injection system to either inject bubbles into the mercury stream or create gas layers to provide protection of the innermost container wall of the target module against cavitation damage. Since gas injection may not adequately protect the small passages used in the present design to cool the target module window with mercury, the module will be redesigned to provide a separate water cooling stream to cool the target walls of these passages.

In anticipation of the need to incorporate upgrade capabilities, gas injection lines and water cooling lines were added to the SNS mercury loop piping and target carriage assembly. However, providing the remainder of the gas injection and water cooling systems for the upgraded target module requires design, fabrication, and installation of new equipment in the service bay. Initial SNS operations will result in residual radiation levels and contamination in the service bay that will limit or preclude personnel entry for installation of these new systems; therefore, these utility upgrades will have to be installed using remote handling techniques. Because of this, extensive mock-up and out-of-cell equipment fit-up testing will be conducted. Also, it is assumed that a temporary enclosure will be constructed over the service bay's removable roof beams for transporting the subsystems and components into the service bay. Finally, additional shielding must be provided surrounding some of these new items to protect them from radiation levels in the service bay.

6.2 INNER REFLECTOR PLUG AND MODERATOR UPGRADE (WBS 3.4.1.2)

The Power Upgrade of the Inner Reflector Plug (IRP) and moderators will be accomplished through redesign of the lower IRP. The lower IRP contains the moderators and beryllium reflector and stainless steel shielding closest to the target. Lessons learned in the manufacture of the first IRP will be applied to the redesign of the lower IRP. The goal is to improve manufacturing processes so that closely held tolerances necessary for thermal performance can be met. In addition, the helium blanket surrounding the cryogenic moderators and the cryogenic transfer lines will be removed. This will allow for direct water cooling of the moderator outer vacuum vessel.

The cooling of the moderator outer vacuum vessel in the first IRP was the limiting factor in its thermal performance. The vacuum vessel in the first IRP was cooled only by conduction through helium gas to the outer helium vessel boundary. Removing the helium blanket and directly cooling the vacuum vessel with water should greatly improve the thermal performance of the lower IRP. Significant thermal hydraulic and thermal stress analysis will be required to provide the optimum design for lifetime and power handling.

The lower IRP has been designed as a single water-cooled vessel to contain both the beryllium and stainless steel shielding. A complex water cooling scheme was designed to provide cooling for these two very different materials. For the Power Upgrade, the lower IRP design will focus on separating the beryllium cooling from the stainless steel cooling. This will be accomplished by separating the lower IRP into two vessels. The inner vessel will house the beryllium and moderators, and the outer vessel will house the stainless steel shielding. Over time,

as the SNS evolves, changes to the moderators will require changes to the inner vessel only, and the outer vessel will remain unchanged.

The raceways in the current all-aluminum lower IRP created difficulties in the fabrication. By dividing the lower IRP into two vessels, access for water cooling pipes and passageways can be moved to the outer vessel that could possibly be a stainless steel vessel. The inner vessel most likely will remain as an aluminum vessel, but it will be cylindrical without raceways. This will move the difficult welding away from the aluminum vessel and into the stainless steel vessel where welding is easier.

Finally, there were many other difficult fabrication steps in producing the current IRP. All beam tubes were manufactured using carbon electrode electric discharge machining. This was time consuming and difficult. The new design will attempt to eliminate this process. The cooling channels in the plates between the moderators and the target were machined into both halves of a "split" plate. To minimize bypass flow, the plates were screwed together, and the heads of the screws were electron beam welded. This was also a time-intensive and expensive process. The new design will attempt to eliminate this process.

6.3 PROTON BEAM WINDOW (WBS 3.4.1.3)

An all-aluminum proton beam window will be pursued for the Power Upgrade Project. An aluminum window will produce less back and forward scattering from beam interaction. This should reduce the shielding requirements for the upstream and downstream sides of the window. Although shielding will be required, it will be housed in an aluminum structure to avoid any material transitions to the aluminum window. The thermal response of the aluminum structure and the thermocouples used for the halo monitor should provide a faster response for beam positioning. It may be possible to design other beam profile diagnostic devices if space becomes available.

A key advantage to an aluminum window is the reduced radiation damage from the beam. The window lifetime should be much greater, resulting in longer periods between replacements.

6.4 TARGET SUBSYSTEMS (WBS 3.4.2)

6.4.1 Target Utilities (WBS 3.4.2.1)

The Target Utility Subsystem will be upgraded to handle the higher hot off-gas (HOG) system throughput associated with the addition of the gas injection system used to mitigate the effects of higher pulsed heat loads in the mercury target. Gold absorbers will be added to remove mercury from the HOG stream, and a gas compression and storage tank system will be provided to give the required radioactive decay time before release.

6.4.2 Evaluation of Power Handling Limits (WBS 3.4.2.2)

The design criteria used for most of the SNS Target Systems components were developed for operation at 2 MW with a 60-Hz beam at 1 GeV. Generally, the designs were conservative and have some margin for higher power operation. The purpose of this evaluation is to use early SNS operational experience and analysis studies to quantify the margins for each system, determine which are most limiting, and identify reasonable upgrade paths.

The evaluation will include nuclear analysis studies at higher energy and power for the bulk shielding, shutters, shine shield, and pan. The bulk shielding surrounding the target, moderators,

and reflector was originally designed for 4 MW and not reduced, so it is likely to work at higher powers, although some localized areas in the high bay may exceed current guidelines.

Heat removal systems will be evaluated, including all the water utility loops and the mercury heat exchanger. This evaluation will consider the following items:

- Options for increased flow with new impellors for the water pumps will be examined.
- Options for increasing the mercury heat exchanger performance will be examined.
- The accident condition of dumping the mercury into the collection tank will be analyzed for high power, since the peak transient temperature of the concrete is expected to be limiting.
- The front of the target carriage is not cooled, and an evaluation of the temperatures there will be made.
- The effect of higher mercury loop temperatures on piping stresses will be analyzed.
- The margin for secondary water cooling loops will be evaluated.
- The margin for the cryogenic moderator systems will be estimated, and the possibility of increasing refrigeration capacity will be identified.
- The effects of increased heating on core vessel and internal components and support cylinders will be evaluated for temperature and thermal stress limits and deflections. High temperatures in the core vessel support cylinder could adversely affect the alignment of the neutron guide systems.
- Supporting systems will be evaluated, including ventilation and waste handling.

Results of these studies may identify a few areas where upgrades of existing systems could raise the power handling capability of the entire Target Systems. Costs for these speculative upgrades are not included in the project baseline budget but presumably could be funded from contingency if judged to be worthwhile.

6.4.3 Instrumentation & Controls (WBS 3.3.5)

Additional instrumentation and controls equipment and software will be required to support the new water cooling systems and gas injection system that will be installed in the Target Service Bay. Modifications to the existing systems for the inner reflector plug, moderator, and proton beam window are also anticipated. The costs for all target-related instrumentation and controls are included in WBS 3.3.5.

7. FACILITIES MODIFICATIONS (WBS 3.5.1)

7.1 KLYSTRON GALLERY

The 1.0- to 1.3-GeV portion of the klystron gallery consists of a building shell outfitted with 480/277-V electrical distribution for heating, ventilating, and air-conditioning (HVAC) loads and lighting and 208/120v utility outlets. As part of the Power Upgrade, the electrical distribution and mechanical systems required to support the accelerator, rf, vacuum, controls, and other associated subsystems will be completed.

The primary electrical distribution for the Power Upgrade Klystron Gallery will start with the addition of four 13.8-kV, 1500-kVA substations. One substation is to support the "house" loads; the other three will supply power to the three HVCMs being added to convert power for the 36 additional klystrons.

Detailed designs, including those for the deionized water distribution, HVAC, process water, sanitary water, tower water, power distribution, electrical duct bank, telecommunications and data communications, grounding system, and motor connections, will be prepared in FY 2008–09. This a straightforward task based on existing designs; the minor improvements planned will be drawn from current operating experience.

7.2 SRF LABORATORY

As part of the upgrade scope, the existing SRF Laboratory Building (shown in Fig. 7.1) will house SRF laboratories to support cavity tuning, rf testing, and R&D activities. Included in the facilities upgrade scope are the facility electrical and mechanical systems necessary to support cavity R&D and cryomodule maintenance activities, plus the integration of the auxiliary liquid helium refrigerator and cryogenic distribution lines into the rf test facility (RFTF)/central helium liquifier (CHL) building.

An auxiliary cold box will be installed to support cavity and cryomodule testing in the SRF facility. This cold-box installation requires construction of a pit in the warm compressor room in the CHL building. The pit dimensions are approximately 18 ft by 18 ft with a depth of 25 ft.

7.3 ELECTRICAL POWER DISTRIBUTION (WBS 3.5.1.3)

The addition of 36 klystrons, three HVCMs, an auxiliary 4.2 K refrigerator, and operation of the HEBT-Ring-RTBT magnets at higher current significantly increase the SNS site electrical load. The 161-kV switchyard fed by the TVA grid is adequate for the Power Upgrade, as it was constructed with two 70-MVA transformers to reduce the voltage to 13.8 kV. The switchyard was built so that the entire SNS load with upgrades could be powered by one of the 70-MVA transformers, allowing full operation if one transformer is unavailable. Total operating load measurements are not available; however, as listed in Table 7.1, the Power Upgrade increases the estimated total site electrical load from about 43 MW to about 54 MW, which remains well within the capability of one 70-MVA transformer. Modifications and new electrical distribution equipment installations are required. Areas that require electrical distribution modifications are the:

- Klystron Gallery build-out accelerator electrical load distribution
- SRF facility equipment installation

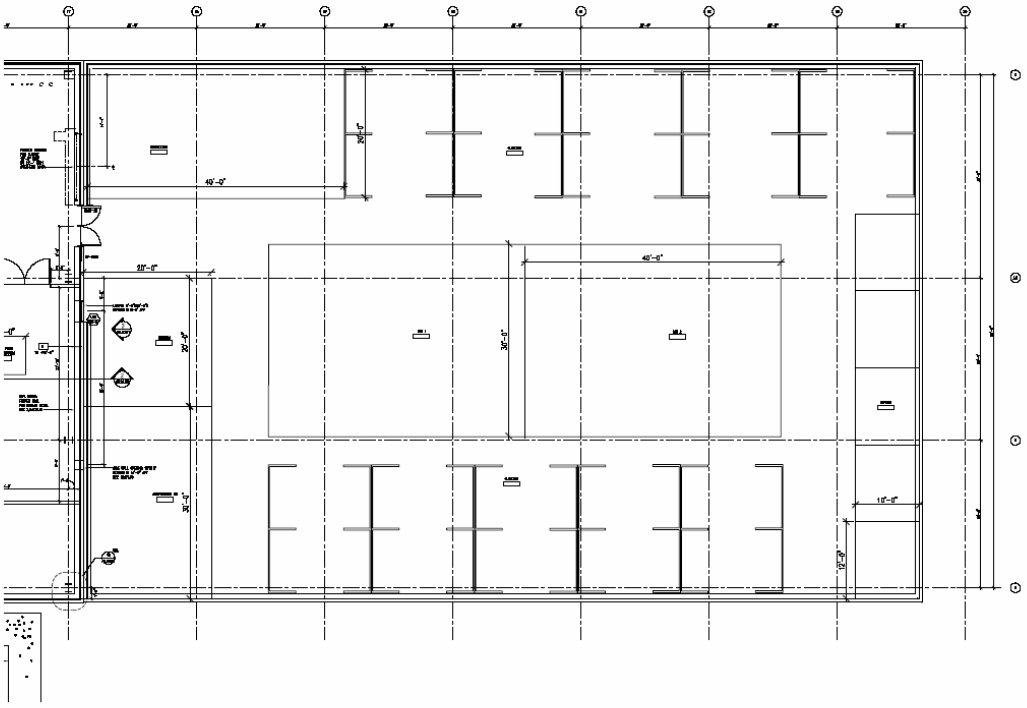

Fig. 7.1. Floor plan of the existing SRF Laboratory Building extension to the CHL/RFTF.

- Electrical transformer area on the south side of the Ring Service Building (RSB) and the addition of one 13.8-kV, 1500-kVA substation.

The Klystron Gallery electrical distribution load increases from 17.1 MW to 23.3 MW. To support this increase, four new 1500-kVA transformers will be installed on a new pad just south of the gallery structural build-out. Three of these new transformers support the three new HVCMs on a one-to-one basis. A new interrupter switch is required with each new transformer to provide isolation capability from the electrical distribution from the switchyard. Existing transformers /unit substations supplying the warm linac operate at higher power in the Power Upgrade configuration.

The fourth new 1500-kVA transformer supplies power to the other technical supporting systems—i.e., vacuum, controls, diagnostics, cooling loops, etc. An approximately 160-ft excavation in the east-west Klystron Way road will be required to bring 600-A service from an existing electrical manhole just south of the HEBT service access door. Underground access is available from that manhole to the main switchyard through existing chases under the road just west of the Central Utilities Building. This new feeder will tie into one of two existing, spare 600-A, 13.8-kV three-pole breakers in the main switchyard. Electrical distribution internal to the Klystron Gallery build-out is in the Accelerator Systems Division Electrical Group scope of work.

Ring electrical distribution upgrade to support the Power Upgrade requires the installation of one new 1500-kVA transformer (SS5) on a new pad extension on the south side of the RSB. This is an extensive addition requiring excavation for access to the basement of the RSB, penetrating the basement wall for new distribution, cabling, pouring a new pad, transformer installation, and commissioning. A further complication in this RSB modification is that scheduling requires that

much of the facility modification work proceed while the ring is in operation. A redesign of the building internal distribution is required to redistribute the existing ring loads/power supplies from their current configuration being fed by four transformers to the new configuration being fed by five transformers.

The underground distribution from the site switchyard is sized to supply the Power Upgrade load to the RSB. No new excavation is required to the Ring Service Building. The interrupter switch for the new SS5 transformer will be connected in parallel to the switches for SS4 and SS5/SS6. This connection is through an existing 5-in. conduit installed and capped from the SS5/SS6 interrupter. SS5/SS6 unit substations power the main ring power supply.

The SRF Facility and associated Auxiliary Liquid Helium Refrigerator were initially designed into the CHL-RFTF building. Electrical distribution to the CHL-RFTF building is adequate for this additional compressor, cold box, and Kinney vacuum pump installation. The estimated electrical load for the SRF cryogenic equipment is less than a megawatt. Internal building electrical distribution for the cryomodule test cave, cavity test dewars, cavity preparation labs, and clean room facilities is required.

7.4 WATER COOLING

The SNS utility cooling water systems feeding the four cooling towers are divided into two major subsystems, with two towers for the "tower water system" and two towers for the "condenser water" system. These two subsystems are configured to support the water cooling requirements of the accelerator systems, secondary side of target utilities, and all building services and HVAC, including the Central Laboratory Office (CLO) and Center for Nanophase Materials Science. These water systems are shown in Fig. 7.2, and the capacities and loads without and with the additional cooling equipment for the Power Upgrade are listed in Table 7.1.

Table 7.1. Existing utility capacities and loads and loads with the Power Upgrade

	Existing capacity	Existing loads	Loads w/ PUP
Electrical substations	2 x 70 MVA	43 MVA	54 MVA
Tower water	28.8 MW	20.5 MW	26.5 MW
Condenser water	19.1 MW	17.8 MW	19.4 MW
Chillers	16.9 MW	14.2 MW	15.5 MW

Some preliminary and partial measurements of cooling water capacities and loads have been completed; however, 1.4-MW beam-on-target measurements on a hot day have not been made, so the present capacity and load estimates are a combination of measured and estimated results. There are three circuits to consider:

- The tower water circuit cools most of the accelerator equipment through deionized water heat exchangers. The 100% tower cooling design capacity for this circuit is 28.8 MW. The existing load is estimated at 20.5 MW, and the Power Upgrade will give an additional 6.0-MW load for a total load of 26.5 MW. The two cooling towers for this circuit are probably adequate.
- The condenser water circuit mostly dissipates the heat from the chiller water circuits from the site air-conditioning systems. The 100% tower cooling design capacity for this circuit is 19.1 MW. The existing load is estimated at 17.8 MW, and the Power Upgrade will give an additional 1.6-MW load for a total load of 19.4 MW. The two cooling towers for this circuit may not be adequate.

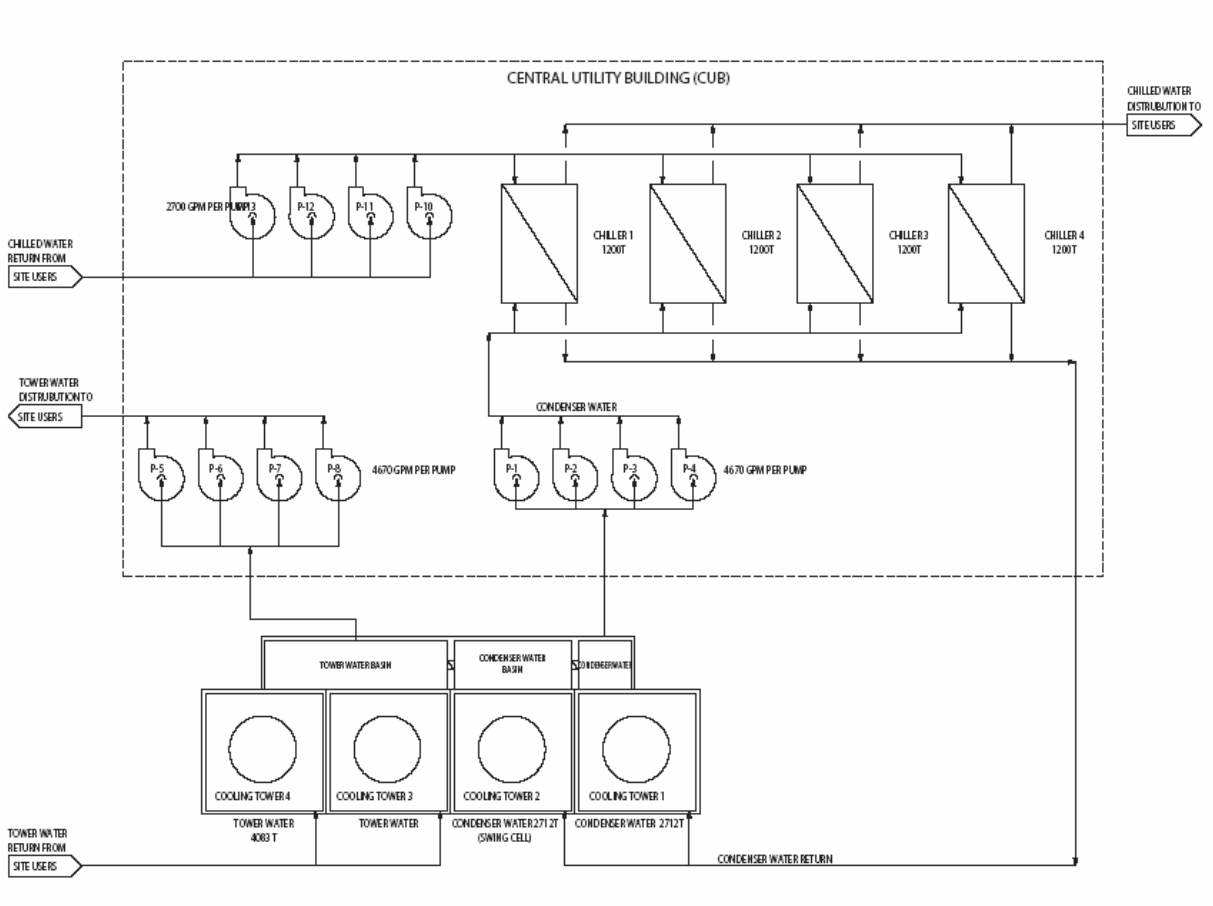

Fig. 7.2. Schematic of the SNS water cooling systems.

- The four big chillers for the air-conditioning systems have a total capacity of 16.9 MW. The Power Upgrade increases the chiller load from 14.2 MW to 15.5 MW; consequently the chillers seem adequate, but their cooling towers may not be adequate.

The numbers listed in Table 7.1 are preliminary and by no means final until full operational measurements are made. In addition, the cooling capacities are design numbers with no operational margins. The Power Upgrade total estimated cost (TEC) contains no scope for cooling system upgrades; however, the high estimate of the cost range contains the resources for one additional cooling tower.

7.5 RADIATION SHIELDING

SNS radiation shielding was evaluated in detail for accelerator operation at 1.0 and 1.3 GeV, up to 2 MW of beam power. Radiation levels were calculated for areas outside the accelerator enclosure. Calculations for the 1-GeV, 2-MW case are documented in the SNS Final Safety Assessment Document (FSAD) [19]. The difference between the 1.0-GeV and 1.3-GeV cases, assuming the same beam loss rate per unit length (e.g., 1 W/m to allow hands-on maintenance), is less than the calculational uncertainty. Radiation levels outside the accelerator enclosure scale linearly with this loss rate, which must be lower than 1 W/m to continue to allow hands-on maintenance, and no difference is expected for operation at 3 MW.

7.6 BEAM DUMPS

SNS beam dump operation was also evaluated at 1.0 GeV and 1.3 GeV, and there is no significant effect of the increased energy on the operation of either the passive or active dumps. The heat-handling capability of the dump structures is the same at either energy. Increased scattering length contributes only marginally. The existing linac and extraction beam dumps are sized for 7.5 kW of beam power and can only be used for tuning very low duty factor beams, which will continue with the Power Upgrade.

The Power Upgrade will result in an increase in beam power to the Ring Injection Dump, which is designed to dissipate 150 kW. As described in section 5.11.8, the RID in the Power Upgrade must handle 300-kW instantaneous beam power. Upgrades to the dump, improved diagnostics as well as modifications to the beam physics requirements, are being studied with the goal of increasing the power handling capability of the RID to Power Upgrade requirements.

8. RESEARCH AND DEVELOPMENT PLAN

8.1 PHYSICS OPTIMIZATION

Further beam dynamics studies are necessary to fully optimize the operating parameters at 3 MW. These studies will focus on optimization of operating conditions to limit beam loss in the accelerator complex, understanding fundamental mechanisms for halo growth in the linac and ring, and investigating new techniques for reducing halo growth and beam loss.

8.1.1 Optimization of Operating Conditions To Limit Beam Loss

The injection region in the ring needs to be upgraded and optimized for 1.3-GeV operation. Careful design of the magnetic field layout is required in order to properly dump the unstripped and partially stripped beams to minimize beam loss in the injection region. The injection painting conditions and collimator scraper settings require careful optimization to control beam loss in the ring at higher intensity. The energy corrector and momentum painting systems require optimization for 1.3-GeV operating conditions.

8.1.2 Understanding Fundamental Mechanisms for Halo Growth

Progress has been made in recent years in developing fully parallel 3D space-charge simulations for proton and ion linacs. These capabilities on local computer clusters will be utilized to investigate halo growth mechanisms and mitigation in the linac, making use of emittance and halo growth data obtained during SNS linac commissioning and early operation.

Ongoing beam dynamics studies aimed at understanding halo growth and beam loss mechanisms in the ring will continue. The ORBIT code has recently been modified to incorporate an electron-cloud module and self-consistent, coupled electron-proton motion [20]. This new capability will be exploited to assess in greater detail the beam stability at higher ring intensity. Mitigation mechanisms, including active feedback and shaping of the longitudinal beam profile, will be explored. Benchmarks with available data from the PSR, and eventually the SNS ring, will be performed.

Studies are under way to assess the benefits of a barrier bucket rf system for the ring in order to improve the bunching factor. A higher bunching factor will provide more uniform space-charge force and therefore tuneshift along the bunch, minimizing losses arising from the coherent half-integer resonance. In addition, the sharply decreasing longitudinal beam profile may partially disrupt the trailing-edge multipacting mechanism, thereby increasing the e-p instability threshold. The ORBIT simulation code has been modified to treat barrier rf systems, and preliminary comparisons between conventional and barrier rf systems are under way.

8.1.3 Investigating New Techniques for Reducing Halo Growth and Beam Loss

Other R&D efforts will be focused on new techniques for reducing halo growth and beam loss. Included among these is an investigation of self-consistent beam distributions and practical methods to obtain them in the ring with realistic injection painting. Recent work at ORNL has shown that self-consistent distributions, that is, beam distributions with linear space-charge force and therefore no halo growth, can be generated in practical conditions [21].

8.2 CHARGE-EXCHANGE INJECTION R&D

8.2.1 Stripping Foil (WBS 3.1.6)

Multi-turn charge-exchange injection into the ring is accomplished by stripping the injected H^- beam to H^+ with a 300 $\mu g/cm^2$ carbon stripper foil. Model calculations show peak temperatures of 2000 K to 2200 K for the stripper foil in the baseline ring design. Carbon foil lifetimes have been observed to decrease sharply for temperatures that exceed approximately 2500 K [22], so the temperatures are acceptable in the baseline design. For the Power Upgrade, the beam intensity will be 60% higher and the stripper foil must be about 8% thicker to achieve the same stripping efficiency at the higher beam energy. These factors will push the foil temperatures above 2500 K, so a modification to the stripping foil is necessary. Two possible modifications are to develop a foil that can withstand the higher beam intensities, and to use existing foil technology but have two separate thin foils (the foil temperature scales with the foil thickness). Both of these options will be explored and developed for the Power Upgrade. The final solution will be selected based on the results of the development efforts.

The investigation of microcrystalline and nanocrystalline self-supporting diamond stripping foils is a subject of active ongoing SNS research. A group from ORNL and the University of Tennessee has successfully produced corrugated diamond foils of appropriate thickness and geometry that are supported on one or two edges [23]. Lifetime tests of these foils have been performed at BNL on a beam that provides similar power deposition to that in the initial baseline SNS ring. These tests show superior performance relative to standard carbon foils and have shown lifetimes that satisfy the 100-h requirements necessary for operation at initial baseline parameters. Ongoing tests of a diamond foil installed for production running of the LANL PSR show good results. Continued development of diamond foil technology will be required to produce foils capable of withstanding the higher power densities in the Power Upgrade.

8.2.2 Laser-Stripping Injection (WBS 3.1.6)

Three important limitations arise from the use of stripping foils in the charge-exchange injection process. The first is the finite foil lifetime, which has already been discussed. Secondly, each proton injected into the ring passes through the foil six to ten times, depending on the injection setup. These multiple foil traversals can lead to uncontrolled beam loss due to large angle coulomb scattering or nuclear interaction in the foil. Thirdly, foil inefficiency leads to further uncontrolled beam loss and wasted beam power going into the injection beam dump. Because of these limitations, an effort has been under way at ORNL to develop a laser-based method for charge-exchange injection.

Efforts to date have focused on a “proof-of-principle” laser stripping experiment that is currently supported through funding by the ORNL Laboratory Director’s Research and Development (LDRD) Program. The double-stripping technique under study, developed by an ORNL team, uses a three-step method employing a narrowband laser [24]. In the first step, the beam traverses a strong magnetic field in which the H^- ions are stripped to H^0 ($H^- \rightarrow H^0 + e^-$) by the Lorentz-stripping mechanism. In the second step the H^0 beam is excited to the $n=3$ state by colliding a laser beam with the neutral hydrogen beam at an angle chosen to provide the necessary transition frequency in the hydrogen atom’s rest-frame. In the final step, the excited hydrogen is readily stripped ($H^{0*} \rightarrow p + e^-$) in a second high-field magnet. Since the H- beam has an inherent energy spread, the transition frequency is Doppler broadened to a width that would otherwise leave the upper state virtually unpopulated. In our approach, we overcome this difficulty by intersecting the H^0 beam with a *diverging laser beam*, as shown in Fig. 8.1. In this

way the angle of incidence of the laser light, and therefore the laser frequency in the atom's rest frame, changes along the hydrogen beam path in the laser-particle beam overlap region. This introduces an effective frequency "sweep" as the hydrogen beam traverses the laser interaction region that can be made large enough that all atoms cross the resonant frequency and are excited to the upper state with greater than 95% efficiency.

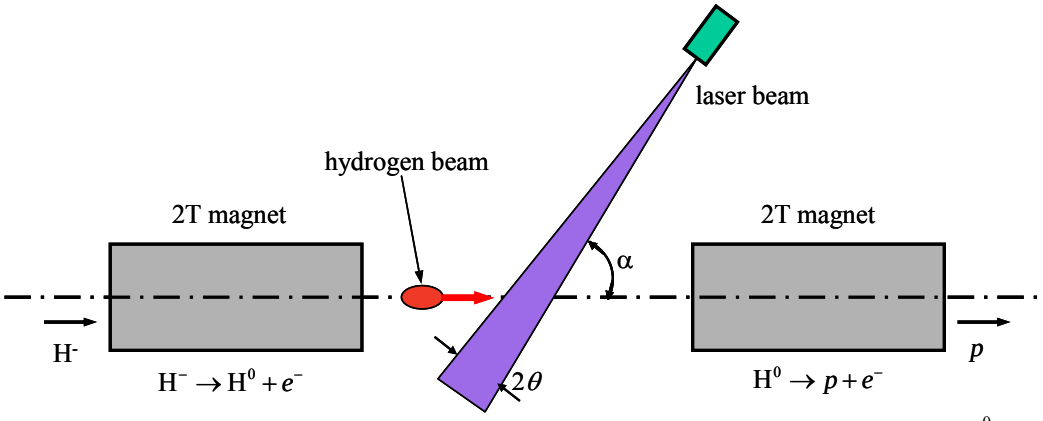

Fig. 8.1. Principle of the three-step stripping scheme. The 1.0-GeV H^- beam is stripped to H^0 by Lorentz-stripping in the first high-field magnet. The H^0 beam is excited from the n=1 to n=3 state by interaction with a laser beam arranged at the proper angle to provide the transition energy in the rest frame of the neutral hydrogen atom. Finally, the excited H^0 beam is Lorentz-stripped in a second high-field magnet, yielding a proton beam.

This project, in the third year of LDRD funding, has assembled the high-field magnets, laser transport systems, vacuum chamber, and diagnostics. The hardware is installed in the linac dump beamline, and first experimental tests have been carried out. In these tests a double-stripping efficiency of greater than 50% was achieved, proving the principle of the technique. Research and development will continue on laser stripping, with the goal of developing a scheme for the Power Upgrade.

8.3 RING FEEDBACK R&D (WBS 3.1.6)

According to simulations, coherent beam instabilities are not expected in the SNS ring up to 3.0 MW operating at 1.3 GeV. While the predictions of instability thresholds driven by conventional impedances are generally regarded as reliable at the factor-of-2 level, provided the impedance is known, those driven by the electron cloud (the "e-p instability") are extremely difficult to predict. The threshold for the e-p instability depends on many parameters, including the vacuum chamber surface geometry and material and its detailed history, the number and distribution of "seed' electrons provided by proton beam loss or stripped electrons, and the proton beam's tune spread, which is itself influenced by a number of parameters.

Given the uncertainties in the prediction of instabilities driven by the electron cloud, a transverse wideband feedback system has been included in the Power Upgrade scope. One central question has been whether a feedback system would be effective against the e-p instability at all, given the complex nature of the instability and the relative lack of understanding about it. Observations at the PSR show that the instability spans a wide bandwidth centered at about 200 MHz. These questions motivated an experimental test of active damping of the e-p instability at the LANL Proton Storage Ring (PSR). An experimental collaboration between ORNL, LANL,

Indiana University, and LBNL has been formed to design, construct, and deploy a prototype feedback system at the PSR to investigate active damping of the e-p instability.

A feedback system with 20- to 300-MHz bandwidth utilizing a 200-W power amplifier was designed, constructed, and deployed at the PSR. Experimental tests at the PSR show that the e-p instability can in fact be controlled with active feedback. Figure 8.2 shows a comparison of a vertical beam position monitor (BPM) difference signal with and without feedback. An increase in the instability threshold of 30% was achieved. The instability threshold increase was limited by amplifier power, which can be readily increased with the addition of higher power amplifiers. Continued investigation of active damping will be pursued, as well as simulations to benchmark experimental results.

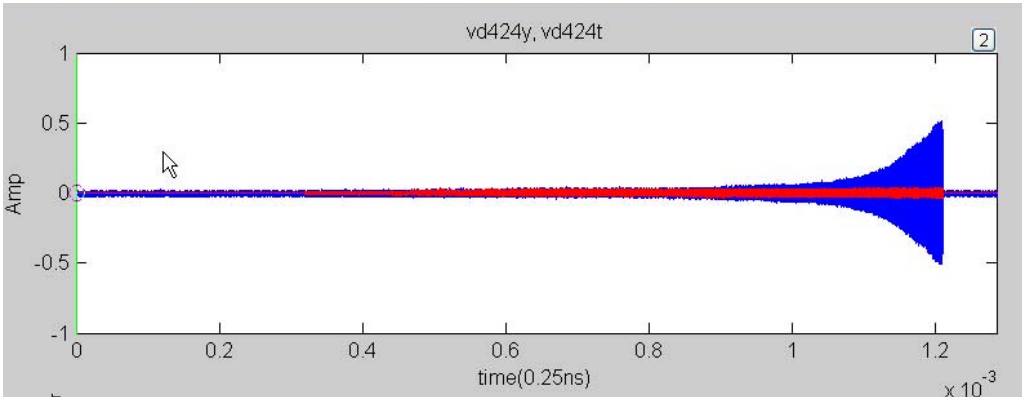

Fig. 8.2. Vertical BPM difference signal in the LANL PSR without (blue) and with (red) the wideband feedback system. The growth in amplitude at the end of beam accumulation is due to the e-p instability.

8.4 ION SOURCE AND LEBT R&D (WBS 3.1.2)

Our R&D program will develop the high-current, low-emittance ion sources and an LEBT that inflicts minimal emittance growth to meet the current requirement for producing 59-mA peak current in the MEBT. While the JAERI ion source appears to meet the Power Upgrade requirements, the source is short-lived and requires intense and time-consuming reconditioning after every run. Therefore we are interested in developing an ion source that combines the high production and low emittance of the JAERI source with the lifetime and stability typically found in rf and microwave sources. Accordingly, in addition to the JAERI source, we are considering four other ion sources.

The filament-driven, Cs-enhanced, multicusp H- source developed at JAERI [25] is shown in Fig. 8.3. It has produced the brightest H- beams with parameters that appear to meet the requirements for the SNS Power Upgrade [14, 26]. However, its extraction system does not allow the source to be operated with our baseline electrostatic LEBT, nor does it allow testing on our ion source test stand. Accordingly, we plan to collaborate with JAERI to use their source on their test stand to confirm their emittance measurements and to extend the measurements to higher and lower beam currents. After the suitability of the JAERI source is confirmed, the corresponding lifetime will be measured at the required operational parameters.

JAERI-type, filament-driven high-power discharge sources evaporate and/or sputter a significant fraction of the filaments and, therefore, require extensive reconditioning after every run. The short lifetime and the extensive reconditioning requirement constitute a significant drawback that makes us interested in longer-lived, more cost-effective sources.

A lifetime in the range of weeks has been reached with our rf-driven, Cs-enhanced, multicusp SNS-baseline ion source shown in Fig. 8.4 [27]. Its lifetime is often limited by random failures of the ten-layer Ti-free porcelain coating that insulates the antenna from the plasma. Accordingly, we can expect longer lifetimes for sources where the rf antenna is mounted outside a ceramic plasma chamber. Such a source was originally developed at DESY [28], and one SNS baseline ion source was modified to incorporate an external antenna [29].

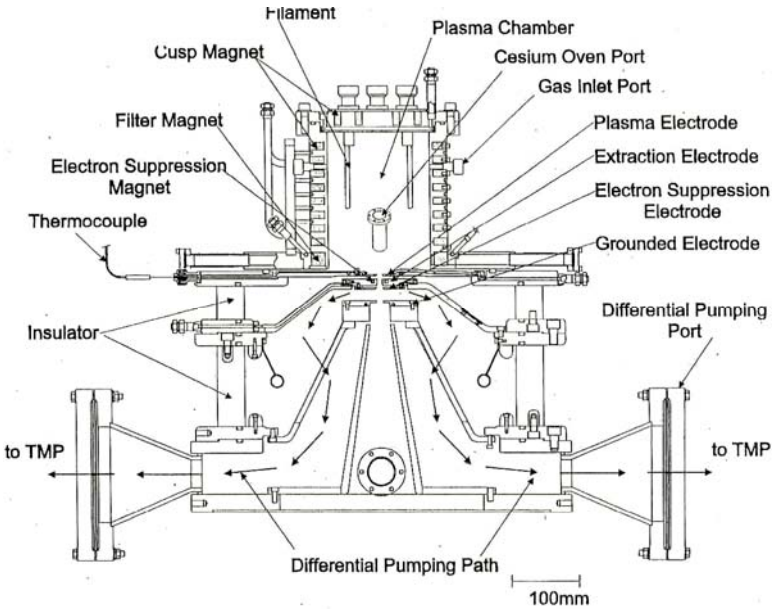

Fig. 8.3. JAERI filament-driven cesium-enhanced multicusp H⁻ source.

We suspect that the emittances of our baseline and modified rf-driven multicusp H- sources are not much different from that of the JAERI source. Therefore, we will measure the emittances of our sources at the source output on our ion source test stand when suitable scanners become available. If the measured emittances substantially exceed the emittance of the JAERI source, we will try to reduce the emittance by developing a JAERI-style extraction system.

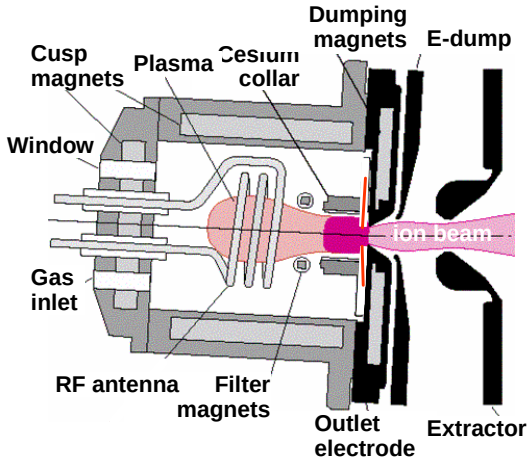

Fig. 8.4. SNS baseline rf-driven cesium-enhanced multicusp H⁻ source.

After measuring comparable emittances, the source becomes suitable for the upgrade, and we can focus on increasing the ion output. The beam current output will be increased by increasing the plasma density through increasing the absorbed rf power as well as the plasma confinement. In addition, we will increase the beam fraction produced with the cesium by improving the geometry and the cesium management.

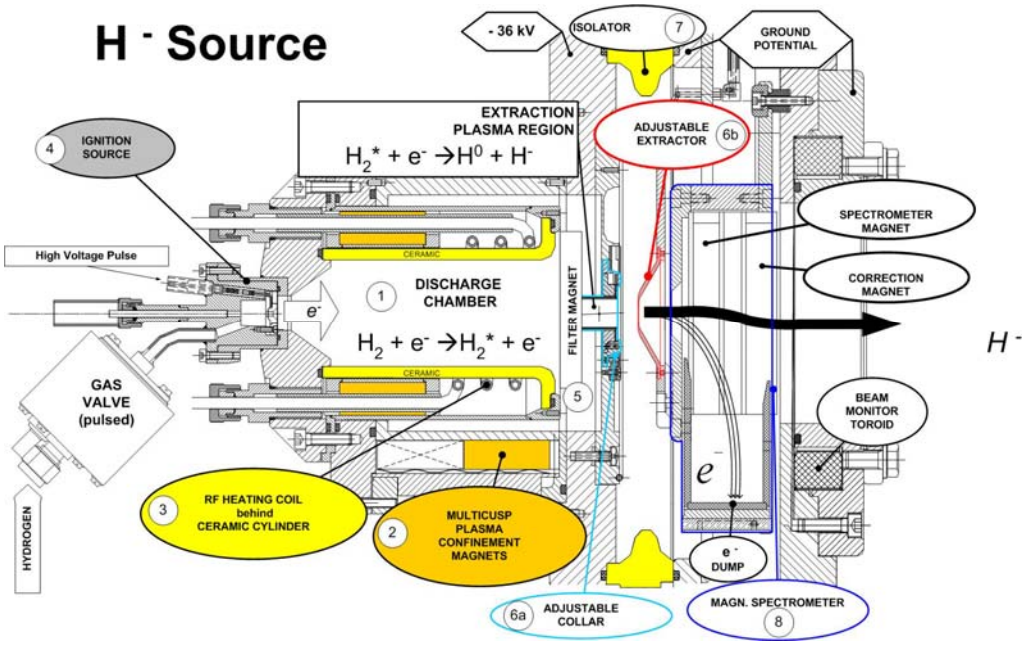

Fig. 8.5. DESY rf-driven cesium-free multicusp H^- source.

The DESY source differs from our modified source mainly through its electron dumping system and its flat diode extraction geometry, as one can see in Fig. 8.5. Without a cesium enhancement system, for short pulses and low repetition rates it produces over 50 mA H- [30], and therefore it is of interest to us. The emittances of the short pulses have a minimum around 22 mA, and they increase for higher currents [31]. However, for comparable beam currents, the DESY emittances are much larger than the emittances measured at the LEBT output with an SNS baseline source.

We are collaborating with DESY, Fermi National Accelerator Laboratory, and CERN to test the DESY source with increased ion beam pulse length using one of the SNS 2-MHz amplifiers. In addition, we plan to explore repetition rate dependencies using a burst mode. In addition, the emittances need to be remeasured, because they could be substantially smaller for longer pulses.

The DESY source has been designed for low-duty cycle, cesium-free operations and cannot meet the SNS upgrade requirements without significant modifications.

There is a risk that we may encounter technological limits with the rf/filament-driven multicusp sources before we meet the upgrade requirements. This risk is mitigated by pursuing two ion sources that are based on alternate technologies.

The Ukrainian Science Academy in Sumy has the inverted magnetron ion source shown in Fig. 8.6. It has produced ~50-mA H- beam with a 1% duty cycle without a cesium enhancement system [32]. The several-day lifetime was limited by a pulsed gas valve that would not be needed for SNS operations. The emittance exceeded our baseline requirement [33].

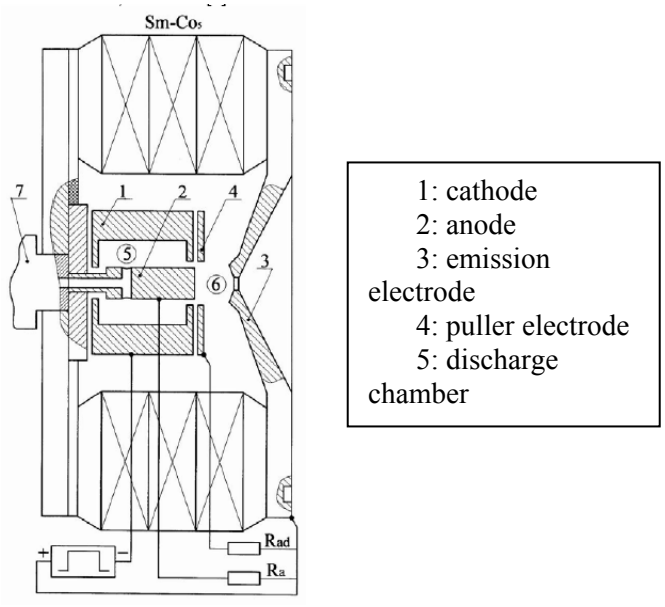

Fig. 8.6. Sumy cesium-free inverse magnetron H^- source.

We are collaborating with Sumy to equip their source with a cesium enhancement system, because the addition of cesium is expected to reduce the emittance while increasing the H- output. The source has an optimally large surface area near the outlet aperture that can be covered with Cs to enhance the temperature-dependent emission of H- from this surface. When those ions resonantly charge exchange with cold neutral atoms, the cold ions can be extracted, decreasing the emittance while increasing the current output. The goals of this collaborative effort call for first adding a cesium enhancement system and measuring the cesium-enhanced ion output and emittance. If successful, the source will be tested for repetition rate dependencies using a burst mode. If successful, a temperature control will be added to the outlet aperture, and the new performance will be measured. If all results suggest that the source can meet the upgrade requirement, it will be reengineered to handle the required 7.3% duty cycle. The reengineered source will then be tested under full requirements, and its lifetime will be determined.

Helicon is another technology that can reduce the R&D risk. Helicon plasma generators produce low-neutral-density, cool plasmas with electron densities that outperform other plasma generators by more than an order of magnitude. All these characteristics are highly desirable for an ion source, and therefore the Helicon technology is a promising alternative. So far, Helicon sources have produced modest H- and p beams with a very limited effort [34]. Figure 8.7 shows

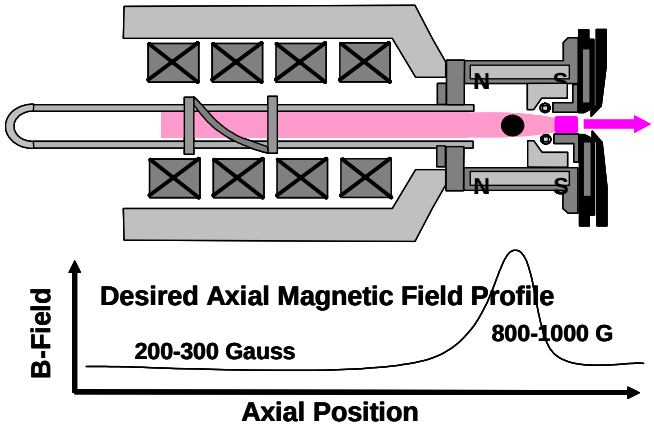

Fig. 8.7. Proof-of-principle Helicon H- source using the baseline extraction system.

the design of a magnetic configuration that should produce such electron densities near the outlet of the baseline ion source extraction aperture. We plan to collaborate with our ORNL colleagues who developed VASIMIR, a helicon plasma generator that routinely produced electron densities of 10^{13} to 10^{14} cm^{-3} in hydrogen.

As discussed in Section 5.1, it is very important to develop an LEBT that minimizes emittance growth and emittance rotation after the initial beam blanking period. We will therefore build a magnetic test LEBT (Fig. 8.8) that will allow us to measure beam emittances under the

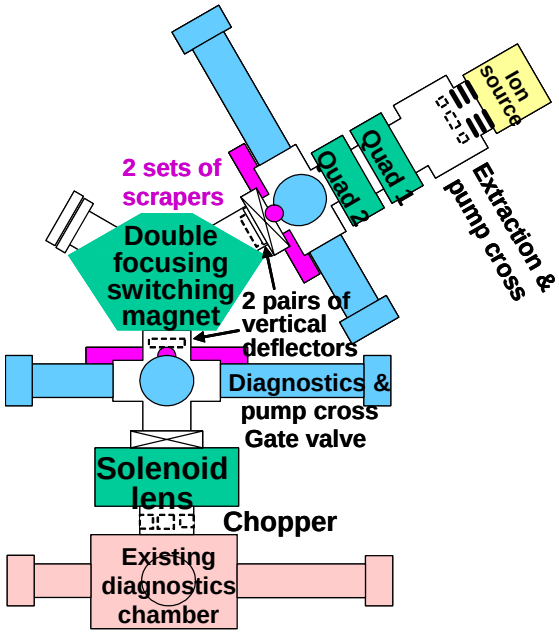

Fig. 8.8. Proposed magnetic test LEBT.

conditions we anticipate for the ion source and LEBT that are needed to meet the upgrade requirements.

This can be accomplished with a test LEBT that matches the proposed two-source magnetic Y-LEBT, except that it features only one ion source beam line. Rather than injecting the beam into the RFQ, the test LEBT injects the beam into a diagnostic chamber, which is equipped with a set of emittance scanners, a beam current monitor, and a Faraday cup. All of the proposed diagnostics can handle the full power beam required for the upgrade.

The acquisition of the magnetic test LEBT will start as soon as the funding profile allows. It is an essential part of our R&D program because it allows for refining the design of various components, such as the extraction system, the differential pumping system, and, most importantly, the magnets themselves. In addition, it will serve as a test stand for fully integrated ion source testing, including lifetime tests. It will be required for testing those sources that do no fit on the existing test stand, such as the JAERI and the DESY sources.

8.5 FUNDAMENTAL POWER COUPLER R&D (WBS 3.1.5)

The present design of the fundamental power coupler, shown in Fig. 8.9, allows for full 60-Hz 1.3-ms operation at 550-kW peak power with a margin of about 20%—that is, approximately 50 kW of average power. Although the couplers have been demonstrated to handle more than 70 kW of average power in the coupler test stand, an important consideration with a superconducting

cavity is the thermal radiation, associated with the heating of the center conductor, being absorbed by the niobium in the coupler end group. While the present conduction-cooled design was sufficient for the initial SNS power levels, enhanced cooling will be required for the Power Upgrade. Such a coupler has been developed by industry. Presently the combination of rf heating, thermal radiation, and field emission can severely decrease the field at which the cavity will quench, and even those cavities that can, in principle, reach high gradients due to the minimal field emission heating may not operate at the higher gradients due to the thermal radiation.

A number of installed medium-beta and high-beta cavities that could be operated at high gradients (15–20 MV/m) will probably be limited by these effects. For the Power Upgrade, as the beam current is increased, the maximum gradients may need to be dropped in most of the SCL in order to avoid exceeding this thermal limit. It is therefore important to design the upgrade cryomodules' fundamental power couplers with enough margin to compensate for this loss of average gradient, especially since the energy gain (and therefore the forward power) of the upgrade cryomodules is very near the maximum value anywhere in the SCL, as shown in Fig. 4.2.

With the present power coupler and a 15% control margin, only a maximum gradient of 14.5 MV/m would be attainable, lower than the 15.6-MV/m design value. An additional source of decrease of operating gradient on the present cavities is the presence of field emission, which can directly or indirectly damage cryomodule components. In some cases it has been observed that it is not possible to operate cavities at gradients much higher than the field emission threshold, which is generallly near half the maximum gradients. This implies that the upgrade cavities must compensate for those decreases in gradients. Depending on cavity position, should cavities need to be run near their maximum gradients, 20–22 MV/m, an average power of 75 kW will be required—50% higher than the initial design value.

A development study will be conducted to ascertain that the cavities can be operated at those high average power loadings. This will involve numerical studies and analyses, as well as the construction of better-cooled couplers and cavity end groups. The ideal vehicle for the experimental validation of the design and solution will be a horizontal cryostat in which appropriate power levels can be established and in which coupler and end group heating and cooling experiments can be carried out. The same cryostat will be used for cavity production purposes.

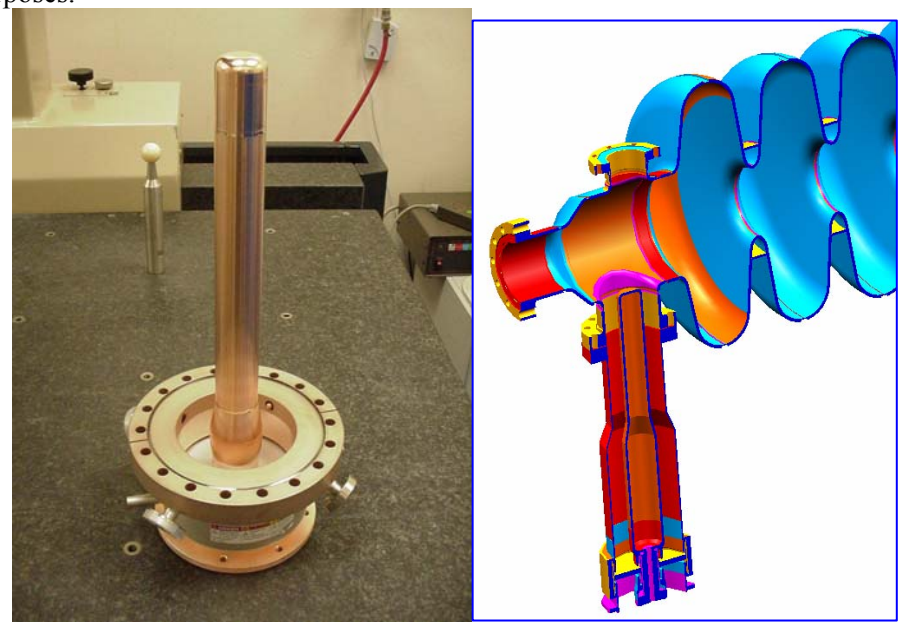

Fig. 8.9. Fundamental power coupler window and center conductor (left) and its assembly into the superconducting cavity (right).

8.6 TARGET R&D (WBS 3.1.7)

Target R&D activities have the single goal of mitigating cavitation damage erosion (CDE) of the target vessel in order to extend the life of the target while simultaneously increasing the power handling capacity. These features are directly coupled. Research conducted to date strongly suggests high sensitivity of erosion rate with beam power. Indeed, erosion rate may be proportional to beam power raised to the fourth power, so doubling beam power could increase erosion by more than an order of magnitude.

Although there are considerable uncertainties in the erosion mechanism in short pulse liquid metal targets, researchers in this area have reached a consensus that mitigation of the damaging effects is the only way to greatly extend target life and power capacity; alternate materials and surface treatments to the target vessel may have at best potential life extension of only a factor of a few times.

Mitigation approaches can be grouped into two general classes:

- Introduction of a general population of appropriately sized objects (e.g., gas bubbles) with sufficient volume fraction to absorb and/or attenuate the pressure wave that is created by the energy deposited by the proton beam in the mercury; and

- Establishment of a protective gas layer between the mercury and the most vulnerable regions of the target vessel that isolate it from the damaging pressure waves.

Achieving mitigation by either approach will be very challenging, particularly in the time frame of the Power Upgrade Project. It is not clear at this time which of these approaches is most likely to work. Nevertheless, tasks have been laid out in the critical areas.

Although there is a consensus in the field that alternate vessel materials and protective treatments have limited potential for further life extension and increasing target power capacity, a limited effort will be included.

8.6.1 Small Bubble Generation, Diagnostics, and Testing (WBS 3.1.7.1)

Theory indicates that introducing a general population of gas bubbles in total void fraction of about 0.5% and approximate size of 10 μm in diameter would be able to suppress the high initial pressure in the mercury created by the quickly deposited proton energy. Experiments where such populations were attempted demonstrated only limited damage mitigation, but difficulties in bubble generation and diagnostics were significant.

Small gas bubble generation in mercury is difficult because of mercury's high surface tension and non-wetting character. Established generating techniques for water applications may be adaptable for mercury, but development and testing will be required to achieve the desired population. Theoretical and laboratory work are required to develop devices that not only create the desired bubble population but also deliver it to the essential target regions. Present uncertainties regarding bubble lifetime and changes in population as it traverses the SNS loop will have to be resolved. Simulation techniques and test loops will be used to determine how to locate the generators in the SNS loop.

Credible diagnostics for measuring gas bubble populations in mercury are vital to making progress in developing the bubble generation technology. Due to the opacity of mercury, optical measurement of bubble populations is impossible. Acoustic techniques are the most promising means for performing these measurements, but present experience with a commercial diagnostic has shown that it does not work in the parameter space needed. Improvements to this device, alternative devices, and non-acoustic techniques to benchmark the devices are to be developed.

Development of gas-removal techniques suitable for use in the SNS loop will be required for this approach. Investigation into whether excess gas could cause loop flow problems, reduced heat removal in the heat exchanger, or faulty flow readings will be made.

These activities will draw upon university and industry expertise as well as collaboration with Japan Spallation Neutron Source (JSNS) researchers. Testing of the diagnostics can be done both at ORNL and at the JSNS.

8.6.2 Gas Wall Development, Simulation, Diagnostics, and Testing (WBS 3.1.7.2)

Development of technology for a protective gas layer in the target vessel will also be pursued. A gas layer or very high gas void fraction at the interface of the vessel and mercury would create an impedance barrier that could isolate the vessel wall from pressure pulse originating in the mercury. While this has good potential for damage mitigation, it will require the most radical changes to mercury flow in the SNS target. Free boundary flow simulation work and testing with a water loop will be used. The more promising techniques will be further developed and tested using mercury, most likely in the Target Test Facility (TTF) loop.

Diagnostics for effective gas wall coverage will require some development. Evaluating the layer coverage may involve the use of optical and electrical techniques as well as acoustic methods even for mercury testing.

Development of gas-removal techniques suitable for use in the SNS loop will also be required for this approach.

Collaboration with JSNS and assistance from universities and industry will be availed upon.

8.6.3 Damage Verification Testing, Analysis, and Simulation (WBS 3.1.7.3)

Verification testing for damage mitigation occurs both with off-line and in-beam experiments. Off-line testing of general bubble population techniques is more amenable at the JSNS test loop that will incorporate the damage-simulating device known as the Magnet Impact Testing Machine (MIMTM). However, MIMTM is a surface driving device, and the pressure pulse in a mercury spallation target is volumetric. This may be a critical difference, thus mandating testing in a proton beam facility such as the Weapons Neutron Research facility at the Los Alamos Neutron Science Center. Other verification tests for flow and bubble evolution under prototypic flow conditions will be done in the full-scale mercury loop at ORNL's TTF.

Similarly, verification of gas layer development approaches under prototypic flow conditions will be done in TTF. Verifications of damage mitigation of the gas layer approach under in-beam conditions are planned, but experiments with simultaneous prototypic flow may not be practical.

Analysis of damage has been known to be particularly lacking in specimens from in-beam experiments. Improved infrastructure and equipment for damage analysis of mercury and radiologically contaminated specimens will be procured. This will improve understanding of previous test results and enable interpretation of new experiments. As mitigation techniques improve, the ability to accurately measure (and extrapolate) test damage will become increasingly difficult without the proper tools.

Investigations of alternate target vessel materials, protective surface treatments, or armors will also be covered under this WBS element.

9. ENVIRONMENT, SAFETY, HEALTH, AND QUALITY (ESH&Q)

The Power Upgrade will comply with the SNS Environment, Safety, and Health (ES&H) Plan, the SNS Quality Manual, the SNS Operations Execution Plan, and SNS procedures. Environment, safety, health, and quality support to the Power Upgrade will be obtained from SNS and ORNL resources, coordinated through the SNS operations manager. Environment, Safety, Health, and Quality staff will participate in design reviews, vendor evaluations and selections, and facility reviews. Oversight of in-field activities will be conducted by SNS ESH&Q staff, and a dedicated staff person will provide in-field ES&H oversight of the construction and installation craft effort. Work control for the Power Upgrade will be addressed by the ORNL Standards-Based Management System for R&D activities, and job hazard analyses will be prepared to address individual tasks.

The SNS Safety Assessment Document for Proton Facilities will be modified to incorporate the changes associated with the Power Upgrade. The SNS Unreviewed Safety Issue process will be employed to address any issues that arise during Power Upgrade design, procurement, installation, commissioning, and operation.

The Power Upgrade effort will be addressed by the SNS safety committees, including the Electrical Safety Committee, the Radiation Safety Committee, and the Cryogenics Safety Committee. These committees will provide guidance and recommendations for Power Upgrade activities to the SNS operations manager.

Shielding calculations will be performed by SNS staff, using appropriate models and input provided by Power Upgrade staff. The shielding calculations will be peer-reviewed prior to submittal to the SNS Radiation Safety Committee and will guide design, commissioning, and operations.

Radiation support for the Power Upgrade activities will be provided by qualified radiation control technicians (RCTs) obtained from ORNL. The RCTs are trained in accelerator operations and activities and will interface with the SNS operations manager.

Waste associated with the construction and installation of the Power Upgrade will be addressed in the contract language. Wastes associated with Power Upgrade commissioning and operations will be subject to SNS and ORNL waste handling and disposal procedures, with guidance from the SNS waste staff. The cost of waste handling and disposal will be direct-charged to the Power Upgrade.

The Power Upgrade will be evaluated by the SNS Accelerator Safety Committee (ASC), and appropriate reviews will be conducted by the ASC prior to commissioning and operations.

10. ALTERNATIVES

The Power Upgrade will create a pulsed spallation neutron source with a beam power greater than 2.0 MW through an upgrade project of an existing neutron source. Other than the SNS, there are no existing spallation neutron sources within the United States or worldwide that can be upgraded to a beam power of greater than 2.0 MW.

Many of the decisions concerning the alternative paths for this Power Upgrade for the SNS facility were consciously made, after serious discussion, during the design phase of the initial SNS Project. For example, very early in the SNS Project, the accelerator system consisted of a 1.0-GeV warm linac and accumulator ring. The linac design and site layout did not allow an increase in the linac energy, and the upgrade path was envisaged to be an increase in linac current and the addition of a second 1.0-GeV accumulator ring and target. The change to a superconducting linac, along with several additional project change requests, enabled the upgrade path to increase the linac beam energy from 1.0 to 1.3 GeV, keeping one accumulator ring capable of operating at 1.3 GeV. In fact, the HEBT, ring and RTBT were all designed and constructed in the initial SNS Project for 1.3-GeV beam energy, allowing a doubling of the beam power. The limited site area was optimized for this upgrade path. A cost- and schedule-effective SNS Power Upgrade rests on these initial irrevocable decisions. The existing site and accelerator layout is designed for a second target station.

In the initial SCL design, space was reserved between the SCL output and the HEBT for nine additional high-beta cryomodules. At that time, two options were considered for the high-beta cavity geometry. Nine cryomodules constructed with cavities of geometric-beta equal to 0.81, as in the baseline, or new cavities of higher geometric beta, β=0.86, were considered. The latter option resulted in an increase in energy gain from 15 MV/cavity to 17 MV/cavity (when operated at full 35-MV/m peak surface field), which is not substantial enough to warrant the expense of a new cavity and cryomodule design. The warm sections for these additional cavities have been installed and operate for beam transport, so this option no longer is open, resulting in a straightforward extension of the existing linac with nine high-beta cryomodules, similar to the existing cryomodules. The tooling for these cavities and cryomodules exists.

Also, the cryogenic transfer lines exist in the tunnel for the present SNS high-beta design. This does not mean that the cryomodules cannot be further optimized, but significant change to the basic geometry of the cryomodules is not a reasonable alternative.

Although there is some margin in the linac rf systems for increasing the beam pulse length, we have chosen to maintain the SNS baseline 6% beam duty factor in the Power Upgrade. A longer beam pulse, while feasible, is a less cost-effective option that also complicates the operation of the ring; therefore, it is maintained as a backup option. Maintaining the present 60-Hz and 1.0-ms pulses allows a straightforward extension of the existing accelerator system, and in particular the linac rf system. The klystron gallery extension allows for a continuation of the existing rf system.

Another possible alternative concerns the linac beam emittance and RFQ. The beam emittance for the initial linac design is maintained in the Power Upgrade. The acceptance of the linac is limited by the DTL and CCL bore radii of 12.5 mm and 15.0 mm, respectively, which require that the front-end output beam emittance be less than 0.35 π mm-mrad (rms, normalized) for low beam loss operation. Although it may be straightforward to realize an increase in ion source current by increasing the outlet aperture of the source, the present RFQ aperture limits the accelerated beam emittance. Whereas it may be possible to design a larger-aperture RFQ to accelerate a larger emittance beam, the limited DTL and CCL apertures remain an acceptance limitation in the linac. It was therefore decided to retain the existing RFQ and to design an upgraded ion source and LEBT so that the Front End output beam emittance remains less than 0.35 π mm-mrad (rms, normalized).

11. RISKS

11.1 TECHNICAL RISKS

The Power Upgrade is specifically designed to increase the SNS beam power from 1.4 MW to greater than 2.0 MW (design goal of 3.0 MW) through the product of two factors, energy multiplied by intensity: the beam energy will be increased by 30% from 1.0 GeV to 1.3 GeV, and the time-averaged beam intensity will be increased by 10% from 1.4 mA to 1.55 mA for 2.0-MW beam power and by more than 65% from 1.4 mA to 2.3 mA for the design goal of 3.0 MW of beam power.

There is very little technical, cost, or schedule risk in increasing the SNS accelerator beam energy by 30%. The Front End, warm linac, and existing superconducting linac are not affected by this beam energy upgrade. Nine additional cryomodules will be added into the existing linac tunnel, which was designed for these additional cryomodules. These cryomodules will be built, with some improvements, following the proven and successful design of the existing high-beta cryomodules. The corresponding rf system will be a straightforward extension of the existing linac rf system. Likewise, the HEBT, ring, and RTBT tunnels and installed hardware have largely been constructed for this energy upgrade, with the exception of some ring injection-straight hardware. These hardware upgrades will be extensions of proven existing designs. The H^- beam energy cannot be significantly increased beyond 1.3 GeV because of the increased beam loss caused by Lorentz stripping of the H^- beam in the beam transport magnetic fields. Additional beam power requires additional intensity.

The accelerator technical risk is contained in the intensity side of the equation, and the two main areas are the ion source and the carbon stripping foil. These risks will be mitigated by having more than one alternative and performing R&D to determine which alternative is the optimal solution. The beam intensity in the linac will be increased without significantly increasing the beam emittance (beam size) by increasing the ion source H^- brightness. The SNS H^- ion source has produced high intensities for the Power Upgrade at low duty factor, and an aggressive R&D program will be initiated to achieve higher intensity with high duty factor, high reliability, and low emittance. An alternative to this strategy would be to use the present ion source with an increased duty factor. To achieve high reliability at this higher intensity, a magnetic, space-charge-compensated, dual-ion-source LEBT transport system will be built allowing an on-line hot spare ion source to be available at all times during operation. An alternative is to develop a very-high-reliability ion source with single transport engineered for minimum replacement time.

In addition to the H^- ion source, the beam heating of the carbon stripping foil that converts H^- ions to protons in the injection straight contains some technical risk. As discussed earlier, there are two immediate solutions to mitigate this risk. Research and development is under way to produce and test diamond foils that can accommodate this increased beam intensity. This R&D has been successful thus far and will be intensified for the Power Upgrade. The other alternative is the design of a multi-foil stripping region.

The target technical risk is mostly from cavitation damage erosion from the beam pressure wave; target R&D activities have the single goal of mitigating cavitation damage erosion of the target vessel in order to extend the life of the target and allow an increase in the power-handling capacity. Researchers in this area have reached a consensus that mitigation of the damaging effects is the only way to greatly extend target life and power capacity. Alternate materials and surface treatments to the target vessel may have a potential life extension of only a factor of a few times. Mitigation approaches can be grouped into two general classes: the introduction of

appropriate gas bubbles with sufficient volume fraction to absorb the pressure wave, or the establishment of a protective gas layer between the mercury and the most vulnerable regions of the target vessel that isolate it from the pressure wave. Mitigation may be achieved by either approach. It is not clear at this time which approach is most likely to work; therefore, aggressive R&D is required.

The maximum achievable intensity in the accumulator ring will be limited ultimately by collective effects. Very detailed and thorough studies of collective effects have been performed for the baseline SNS ring. These studies include full treatment of space-charge forces in three dimensions; estimates of instability thresholds from the measured and estimated ring impedance; and estimates of electron-cloud production and electron-proton instability effects. Calculations indicate that the threshold for these instabilities occurs at intensities above 3.0 MW. These studies have made use of the existing simulation tools that have been utilized for design of the baseline SNS and that have been tested and benchmarked to a variety of experiments. These studies will continue. To mitigate the potential risk of transverse instabilities, a wideband active feedback system will be installed as part of the upgrade.

11.2 OTHER RISKS

These technical risks provide the largest components to the cost and schedule risks. The early phases of the Power Upgrade are structured to more clearly identify and mitigate these technical risks. In particular, the early phases of the project will concentrate on the detailed design and procurement of hardware for the energy-increase factor of the Power Upgrade and simultaneously performing R&D on the intensity-increase target aspects of the upgrade, increasing the overall time for R&D on the technical risk areas. These risks will be addressed through design improvements, prototypes, schedule contingency, and cost contingency. There is very little cost and schedule risk to energy extension of the SCL.

The cryogenics system for the SRF Facility to support component testing and R&D in the facility will also reduce cost and schedule risks. To reduce serious SNS downtime and financial risks by the loss of cooling and helium, this cryogenics system could be designed to be capable of maintaining the linac at 4 K during CHL maintenance or major system breakdowns.

The injection beam dump is a schedule risk and an even more substantial cost risk. The need to upgrade this dump remains an open question, and a final determination can only be made after experience is gained from high-power operation. If necessary, the beam dump could be modified or replaced.

Other risks are summarized below:

Stakeholder risks: The SNS Facility downtime required for some of the installation and subsequent beam commissioning represents a significant stakeholder risk. The present schedule allows 9 months for these activities, starting in September 2011 and ending in June 2012. During this period, the SNS Facility will not be available to support user operations. Every attempt will be made to minimize this downtime.

ES&H, legal, and regulatory risks: The approved Safety Assessment Documentation for the initial SNS Project included provisions for this Power Upgrade; consequently, there is little risk in these areas.

Location, site, safeguards, and security risks: The Power Upgrade will occur on the SNS site on the ORNL campus. The site was optimized for this Power Upgrade. The new equipment will be installed in existing buildings. These risks are minimal.

Engineering, interfaces, and integration risks: The Power Upgrade will be performed almost entirely within the SNS Facility Directorate of ORNL, minimizing interface and integration issues. The existing SNS staff is deeply experienced in the engineering, interface, and integration skills required for successful project completion. These risks are minimal.

Technical risks, along with schedule, cost, and scope risk will be listed, tracked, and updated by project technical leaders and management as a living document in order to avoid overlooking important risks and to ensure that the risk mitigation effort has adequate management oversight. The responsibility for risk management rests with the Power Upgrade line management. The technical leaders and project management staff will identify risk areas, develop risk mitigation plans, and monitor performance against those plans. The design engineers will establish the specific approaches to addressing the individual risk elements. An important factor in this risk management effort is the existing experience of the Power Upgrade technical and management personnel resulting from the successful risk management of the initial SNS Project.

12. COST AND SCHEDULE

The Power Upgrade cost and schedule have been organized to capture and implement the technical scope required for the high-level parameters listed in Table 4.1. This technical scope has been discussed in Chapters 5–8 and is summarized in Table 12.1. It is based on the mission, physics objectives, and configuration features defined in the Critical Decision (CD-0) document signed by the director, DOE Office of Science, in November 2004.

At CD-0, the preliminary range for the TPC was set at $120M to $160M, and CD-4 was projected in FY 2011. Since the time that those estimates were made, Basic Energy Sciences has provided less-aggressive funding guidance that has extended the project's schedule to FY 2012, with a corresponding impact on the cost range due to escalation. With the delay in completion, the TPC is $160M and the cost range is $150M to $173M.

To organize the project cost estimate, a Level 4 Work Breakdown Structure has been developed to identify all scope elements, implementation responsibilities, and integrated supporting activities. A Level 4 WBS dictionary has been also completed to further define the Level 4 WBS elements and provide scope control. The WBS has 56 Level 3 and Level 4 elements where costs are rolled up for reporting purposes.

The project schedule has been developed to meet the DOE Office of Science direction provided in the director's mission need decision. In general, activities are scheduled at Level 5 and are phase-based. Presently the resource loaded schedule contains more than 750 activities.

12.1 COST ESTIMATE BASIS

The SNS Power Upgrade Project is in a unique position to establish an accurate construction-ready cost estimate in a short period of time. The start of conceptual design on the Power Upgrade overlaps with the end of the initial SNS construction project. Because of that timing, the Power Upgrade is utilizing design and procurement data that are currently being implemented on the base program. This ability to utilize actual current experience with the personnel involved in its initial development adds significant validity and accuracy to the Power Upgrade conceptual design report (CDR) estimate. Only a few areas principally represented by the R&D activities required conceptual or engineering estimates. These areas are the upgraded target, ion source and stripper foil configurations.

In the critical area of cryomodule procurement estimates, study contracts were placed with three potential industrial suppliers who were tasked to develop conceptual cost estimates and schedules for the nine additional cryomodules based on the existing SNS design. These studies were evaluated against a conceptual estimate for the same scope provided by TJNAF, the partner laboratory responsible for designing and building the original SNS cryomodules. The rf system for the 36 cavities is a straightforward extension of the existing SCL rf system with similar costs.

The largest major procurements are shown in Table 12.2. These costs sum to $40M and are dominated by the SCL cryomodules and associated rf system. The construction and procurement timespans are also shown. These estimates are based directly on recent SNS experience.

The Power Upgrade cost estimate directly contains 221 full-time-equivalent (FTE) years of project staff, including the Project Office with ES&H, quality assurance, procurement, physicists, engineers, designers, and technicians. Over the life of the project, this averages about 42 FTEs per year. The planned incremental operating budget allows an increase in the SNS staff of 23 FTEs per year. Project management and senior physics and engineering support will be provided by a small fraction of the existing experienced SNS staff. The remainder of the Power Upgrade staff will be temporary hires with ORNL temporary positions, ORNL matrixed staff, subcontractors, and some staff from other DOE laboratories. The cost of this staff is from projected ORNL staff rates.

Table 12.1 Summary of Scope for the SNS Power Upgrade

WARM LINAC SCOPE
- Four high-reliability, 80 mA, 6% duty factor, H^- Ion Source
- Dual ion source magnetic space-charge compensated beam transport with PS
- HVCM upgrade for higher beam power
- Faraday cup and SCL BPM beam diagnostics upgrades

COLD LINAC SCOPE
- Nine high-beta cryomodules and related equipment
  - 36 high-beta cavities with mechanical and piezo tuners
  - 36 improved HOM couplers with improved feedthroughs and cooling
  - 36 FPC with higher power and improved vacuum and cooling
  - 9 sets of transfer line U Tubes
- Equip SRF facility
- Rf system for nine high-beta cryomodules
  - 36 klystrons
  - 3 HVCM systems with upgrades for higher average power capabilities
  - 6 transmitters, 36 WG sets, loads, circulators and LLRF modules
  - 33 piezo tuner drivers and controls.

HEBT-RING-RTBT SCOPE
- HEBT energy corrector and spreader cavities with HP and LLRF systems
- Ring injection straight
  - New Chicane #2 and #3 dipole magnets with rad hard coils and PS
  - New injection region vacuum chambers, including e- collection
  - Injection region quick disconnects and remote handling capability
  - Upgrade 2 injection kicker PS for 1500 A
- Upgrade primary stripper foil mechanism, including current readout
- Two additional extraction kicker modules with PS, PFN, and modified tanks
- Upgrade ring rf system charging supplies
- Install e-p solenoid and clearing electrode PS
- New rad hard coils and PS for RTBT DH13 dipole
- Build ring wideband feedback system for instability control
- Improve ring halo and target profile beam diagnostics

TARGET SCOPE
- Design, fabricate, and install improved target module with bubble injection
- Design, fabricate, and install improved inner reflector plug for > 2 MW
- Upgrade target utilities for high-power bubble-injection Hg target
- Design, fabricate, and install high-power aluminum proton beam window

FACILITIES MODIFICATIONS SCOPE
- Procure and install 2 K refrigerator for SRF facility
- Complete ac power and water distribution for 1.0-1.3 GeV
- Add additional linac and ring ac power distribution

Table 12.2. Major procurement costs with timespans for the SNS Power Upgrade Project

9 high-beta cryomodules	$17,139K	25 months
6 HPRF transmitters	$6,859K	20 months
36 klystrons	$5,189K	24 months
3 high-voltage converter modulators	$4,390K	18 months
Inner reflector plug	$3,107K	12 months
Site electrical modifications	$2,249K	9 months
Target module	$1,093K	12 months

The cost estimate also directly contains 51,600 hours of construction Davis-Bacon labor costed at the present Oak Ridge Construction Labor Agreement rates, escalated forward as needed with both a contractor markup and 15% foreman factor.

12.2 COST

12.2.1 R&D Cost

The Power Upgrade Project R&D cost sums to $8.3M. Those costs are broken down into five major tasks in Table 12.3 below. The largest R&D costs are for the development of the bubble injection target design. This target research has an estimated cost of $5.3M.

Table 12.3. SNS Power Upgrade Project R&D costs

($K, escalated, burdened)

Ion source R&D	1346
Superconducting linac R&D	154
Accelerator physics R&D	1065
Ring R&D	417
Target R&D	5281
TOTAL	8264

12.2.2 Non R&D Cost

In escalated dollars, the Power Upgrade TPC is estimated to be $160M. Its associated cost for facilities modifications is $4.1M. The cost range has been refined and confirmed to be between $150M and $173M, which is consistent with DOE Office of Science direction. The cost summary breakdown for the Power Upgrade construction cost is shown in Table 12.4. Table 12.5 shows a projected funding profile for the Power Upgrade based on DOE guidance provided in March 2006 with a preliminary TPC of $160M. Details of the TPC cost range are listed in Table 12.6.

12.2.3 Operating Costs

The incremental increase in the SNS annual operating cost from the Power Upgrade Project is estimated to be between $10M and $13M per year. This cost divides into funding for 23 additional staff personnel for about $5M, with the remainder for materials, services, and additional electrical power costs.

12.3 SCHEDULE

12.3.1 Schedule Estimate Basis

The Power Upgrade Summary Schedule is shown in Fig. 12.1. Due to differences in R&D required for the accelerator and target, these two prongs of the project have separate critical decision milestones for performance baseline approval, construction start, and approval for

Table 12.4 Total project cost estimate for the SNS Power Upgrade Project ($K, escalated, burdened)

	Cost	Subtotal
Warm Linac (3.3.1)		**7,141**
Ion Source / LEBT	3,926	
HVCM upgrade and Ion Source electrical upgrade	1,370	
Warm Linac diagnostics	1,845	
Cold Linac (3.3.2)		**51,229**
Nine high-beta cryomodules, 24 new cavities, 12 supplied by SNS	17,205	
Installation and testing of 9 HB cryomodules	3,505	
RF system for 9 high-beta cryomodules	21,333	
Electrical systems upgrade	8,151	
Nine additional U-Tubes	310	
Dignostics upgrade	725	
SRF Facility (3.3.3)		**6,656**
Cavity facility	1,921	
Cryo facility assembly area	302	
Cryo system	4,433	
Ring (3.3.4)		**13,167**
Ring injection system	3,984	
Ring & HEBT RF systems upgrade	1,618	
Electrical systems upgrade	3,683	
Diagnostics upgrade	2,752	
Ring injection dump	1,130	
Integrated Controls (3.3.5)	6,292	**6,292**
Target (3.4)		**20,788**
Hg Target	7,932	
Reflector / Moderator Plug	7,331	
Proton Beam Window & Halo Monitor	1,204	
Target support and subsystems	4,322	
Total cost for technical components		**105,273**
Facilities Modifications (3.5)		**3,315**
Site Substations & Electrical Power	2,628	
CHL (Pit) Modifications	573	
Site Communications & Controls	113	
Total cost for facilities modifications		**3,315**
R&D (3.1)		**8,264**
R&D for higher power Hg target module with bubble injection	5,281	
SCL input power coupler R&D for higher power with improved cooling	154	
Injection stripper foil R&D	417	
Ion source R&D	1,346	
Accelerator physics R&D for high power operation	1,065	
Total cost for R&D		**8,264**
FY05 Proposal Development (3.1.1)		**500**
Project Management (3.2)		**8,599**
Systems testing and commissioning (3.6)		**780**
Contingency		**33,270**
Total cost for SNS Power Upgrade Project		**160,000**

Table 12.5 SNS Power Upgrade proposed FY funding profile ($M)

	Prior	FY 2008	FY 2009	FY 2010	FY 2011	FY 2012	Total
TPC	7.0	25	50	50	25	3	160

Table 12.6 SNS Power Upgrade cost range

($k,Escalated, Burdened, with Contingency)

WBS	Title	Minimum TPC	Estimated TPC	Maximum TPC
3.1	**Research & Development**	8,764	8,764	8,764
3.2	**Project Support**	9,802	9,802	9,802
3.3.1	**Warm Linac**	6,804	9,073	9,073
	Select Simple LEBT	(2,268)		
3.3.2	**Cold Linac**	64,677	65,182	65,182
	Delete 33 Piezo Tuners controls	(505)		
3.3.3	**SRF Facility Equipment**	6,349	8,259	8,259
	Alternative refrigerator concept	(1,910)		
3.3.4	**Ring Systems**	15,192	16,887	23,338
	Add Ring Injection Dump complexity			5,000
	Delete HEBT Cavities	(1,695)		
	Add dynamic tuning supplies			471
	Add primary scraper			344
	Add Ring/RTBT collimation shielding			212
	Add closed loop water cooling			424
3.3.5	**Integrated Control Systems**	7,157	7,860	8,360
	Add Ring Injection Dump			500
	Select Simple LEBT	(260)		
	Delete chipmunks required	(153)		
	Delete HEBT Cavities	(160)		
	Delete Piezo Tuners controls	(130)		
3.4	**Target Systems**	26,991	29,316	33,648
	New diagnostic in PBW			660
	Installation cost will be double			1,672
	Power Handling upgrade not required	(2,326)		
	Additional Power Handling upgrade			2,000
3.5	**Facilities Modifications**	3,504	4,077	6,287
	Additional cooling tower			2,210
	Delete CHL Pit	(573)		
3.6	**Commissioning**	780	780	780
		150,020	160,000	173,493

operations. Similar to the cost estimate basis, the schedule has been developed from direct firsthand experience with the initial SNS Project. The exception to that is the possible cryomodule production from industry. An analysis of the three industrial supplier reports for nine additional cryomodules resulted in the selection of a 42-month schedule for these cryomodules from the start of design until the last unit is delivered at SNS for acceptance testing and installation. This time span constitutes the central piece of the Power Upgrade critical path for the accelerator. Table 12.7 lists the preliminary major milestones for the Power Upgrade.

The critical component of the SNS Power Upgrade critical path schedule is the installation period during which the neutron science program will be interrupted by accelerator and target modifications. This impact must be minimized. Minimizing the length of the shutdown and SNS's ability to achieve the required modifications within it are more important than the exact start and finish dates of the shutdown. To highlight the importance of creating a reliable plan on which a firm commitment can be made to the user community, the SNS Power Upgrade team has created a specific milestone in FY 2009 when the Outage Plan must be finalized. The Power

Upgrade schedule calls for a 9-month installation shutdown beginning in October 2011. Every effort will be made to minimize this downtime.

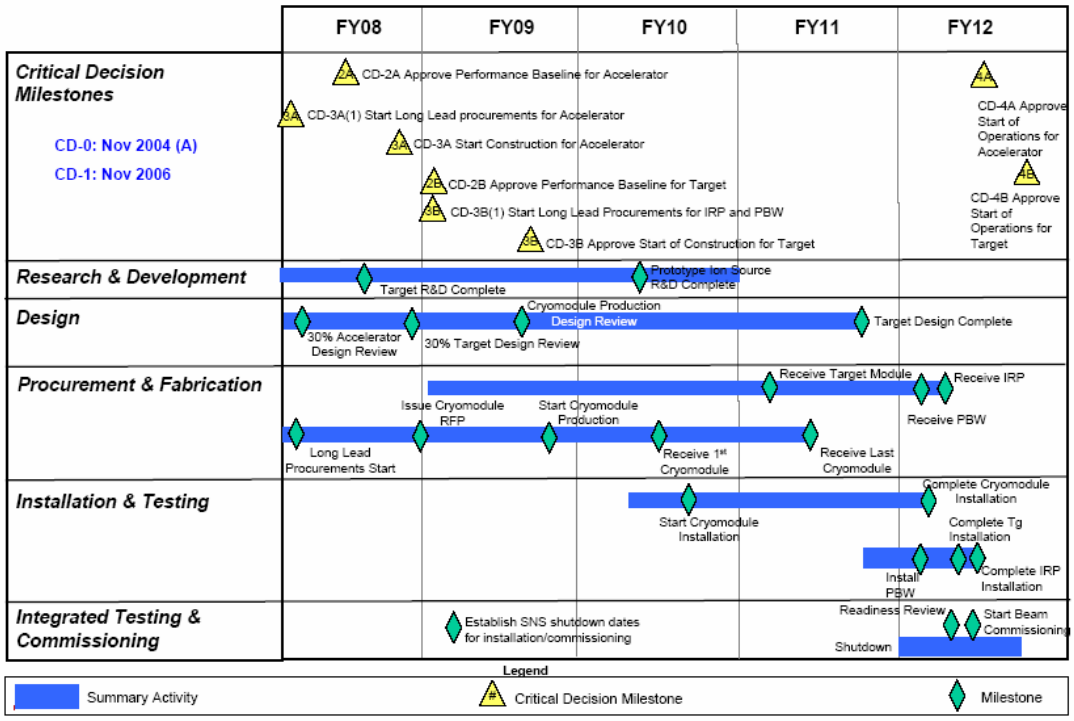

Fig. 12.1. Summary schedule for the SNS Power Upgrade Project.

12.3.2 Project Critical Path

The critical path for CD-4A is through the high-beta cryomodules activities. The critical path for CD-4B is through the mercury target. The sequence and spans associated with these critical paths are:

Accelerator Critical Path	
Cavity Improvement Program	October 2007–June 2009
HB CM preproduction preparation	June 2009–August 2009
HB CM production	August 2009–March 2011
Cryomodule Test Facility operational	May 2010
HB CM testing	May 2010–April 2011
HB CM installation	July 2010–November 2011
Linac commissioning	February 2012–March 2012

Target Critical Path	
Target R&D	Feb 2005–May 2008
Target design	May 2008–Mar 2010
Finalize Installation Outage Plan	January 2009
Target procurements	August 2009–January 2011
Target installation	October 2011–February 2012
Target testing	February 2012–April 2012
Target commissioning	May 2012–June 2012

Table 12.7. Preliminary milestones for the SNS Power Upgrade Project

Milestone/ WBS	Definition	Schedule Date
CD – 0	Approve mission need	November 2004A
3.2.1	CDR Review	May 2006
CD – 1	Approve alternative selection and cost range	November 2006
CD - 2A	Approve performance baseline for accelerator	February 2008
3.2.1	Complete preliminary safety assessment document	June 2008
CD – 3A(1)	Approve start of long-lead procurements for accelerator	October 2007
CD – 3A	Approve start of construction for accelerator	August 2008
3.3.2.3	Klystron procurements start	December 2007
3.3.2.1	Issue cryomodule purchase order	September 2008
CD - 2B	Approve performance baseline for target	October 2008
3.3.2.1	Cryomodule production final design review	June 2009
3.1.7	R&D for target complete	May 2008
3.4	Establish SNS shutdown dates for PUP installation/commissioning	January 2009
CD-3B(1)	Approve long-lead procurement authority for IRP and proton beam window	October 2008
3.3.2.1	Cryomodule production start	August 2009
CD-3B	Approve start of construction for target	July 2009
3.5.1.2	SRF lab complete	January 2010
3.3.2.1	Receive first cryomodule	April 2010
3.3.2.1	Receive last cryomodule	March 2011
3.3.2.1	Start cryomodule installation	July 2010
3.4.1.2	IRP replacement start installation	February 2012
3.4.1.2	IRP testing complete	June 2012
3.4.2.1	Target utilities upgrade complete	March 2012
3.3.2..1	Complete cryomodule installation	November 2011
3.4.1.1	Upgraded target installed	February 2012
3.2.1	Complete FSAD	July 2010
3.6.2.1	Readiness Review	February 2012
3.6.2.1	Start beam commissioning	Mar 2012
CD - 4A	Approve start of operations for accelerator (early finish)	Mar 2012
3.6.2.2	Start target commissioning	May 2012
CD - 4B	Approve start of operations for target (early finish)	June 2012
CD – 4	Project complete	September 2012

Activities that are in the SNS Power Upgrade scope of work and must be initiated prior to the first year of major project funding in FY 2008 are:

- SRF Cavity Testing Capability
- SRF Cryomodule Testing Facility (Cave)

Among these activities, the SRF cavity testing capability using a horizontal test apparatus (HTA) must be operational by September 2007. Completion of the HTA by this date will allow testing of incremental cavity improvements necessary to support the cavity procurement process. The Power Upgrade cavity procurement bid package preparation is scheduled to start in September 2008.

12.4 COST AND SCHEDULE SUMMARY

The SNS Power Upgrade Total Project Cost of $160M is well defined for the conceptual phase of the project. The TPC cost range is between $150M and $173M and depends mostly on scope risks to the project that will be resolved with facility operating experience. As noted earlier, this is the direct result of starting the Power Upgrade immediately after the initial SNS Project is completed. It is valuable for the upgrade project to have the direct benefit of the original construction project to initiate conceptual design, cost estimation, and scheduling.

The Power Upgrade contingency is 28.4% on the TEC.

The 47-month span for the SNS Power Upgrade (from CD-3A to CD-4B) is adequate. The planned CD-4A accelerator project completion date of March 2012 provides six months' float against the Office of Science schedule guidance of completion in FY 2012, while the target CD-4B completion date of June 2012 provides three months' float.

13. REFERENCES

1. National Research Council, *Major Facilities for Materials Research and Related Disciplines* (the Seitz-Eastman Report), 1984.

2. U.S. Department of Energy (DOE) Basic Energy Sciences Advisory Committee (BESAC), *Neutron Sources for America's Future* (the Kohn Panel Report), 1993.

3. BESAC Report (the Russell Panel Report), 1996.

4. DOE Office of Science, *Facilities for the Future of Science, A Twenty Year Outlook*, November 2003.

5. N. Takeda and J. H. Billen, *PARMILA Code*, LA-UR-98-4478, Los Alamos National Laboratory, Los Alamos, New Mexico.

6. J. Wei et al., "Collective Effects and Their Control at the Spallation Neutron Source Ring," EPAC2002; J. Holmes et al., "Space Charge Dynamics in High Intensity Rings," PRST-AB 2, 114202, 1999; A. Fedotov and I. Hofmann, "Half-Integer Resonance Crossing in High-Intensity Rings," PRST-AB 5, 024202, 2002; A. Fedotov et al., "Excitation of Resonances Due to the Space Charge and Magnet Errors in the SNS Ring," PAC2001; A. Fedotov et al., "Effect of Space Charge on Stability of Beam Distribution in the SNS Ring," PAC2001; J. Beebe-Wang et al., "Space Charge and Magnet Error Simulations for the SNS Accumulator Ring," EPAC2000; A. Fedotov et al., "Halo and Space-Charge Issues in the SNS Ring," EPAC2000; D. Jeon and J. Holmes, "Effects of Resonances on Halo Formation in High Intensity Rings," EPAC2000; S. Cousineau et al., "Studies of the Coherent Half-Integer Resonance," EPAC2002; A. Fedotov and I. Hofmann, "Half-Integer Resonance Crossing and Space-Charge Limit," EPAC2002.

7. V. Danilov et al., "Transverse Impedance Implementation in ORBIT," PAC2001; K. Woody et al., "Longitudinal Impedance Simulations in ORBIT: Benchmarking and Application to the SNS Extraction Kicker," PAC2001; D. Davino et al., "Reducing Beam Coupling Impedances in SNS Ring Extraction Kickers," PAC2001; A. Fedotov et al., "Exploring Transverse Beam Stability in the SNS in the Presence of Space Charge," EPAC2002; D. Davino et al., "Measurements of the Coupling Impedance of the SNS Extraction Kickers," EPAC2002.

8. V. Danilov et al., "Calculations of the Electron Accumulation in the SNS Storage Ring," PAC2001; M. Blaskiewicz, "Implications of the PSR Instability for the SNS," EPAC2000; M. Pivi and M. Furman, "Electron Cloud Updated Simulation Results for the PSR, and Recent Results for the SNS," *Proceedings of ECLOUD2002*; M. Blaskiewicz, et al., *Physics Review Special Topics: Accelerators and Beams* **6**, 014203 (2003).

9. J. A. Holmes et al., *ICFA Beam Dynamics Newsletter* **30**, April 2003.

10. J. D. Galambos et al., P*hysical Review Special Topics: Accelerators and Beams* **3**, 034201 (2000); S. Cousineau et al., *Physical Review Special Topics: Accelerators and Beams* **7**, 094201 (2004); S. Cousineau et al., *Physical Review Special Topics: Accelerators and Beams* **6**, 074202 (2003); S. Cousineau, J. Holmes, and E. Metral, *Proceedings of EPAC2004*, 2221; S. Cousineau et al., *Proceedings of EPAC2004*, 2224; I. Hofmann et al., *Proceedings of PAC2005*.

11. S. Cousineau, *Understanding Space Charge and Controlling Beam Loss in High Intensity Synchrotrons*, Ph.D. thesis, Indiana University, 2003.

12. W. Weng et al., *Proceedings of EPAC2002*, p. 1070.

13. M. P. Stockli et al., *Review of Scientific Instruments* **77** (2006).

14. H. Oguri, Y. Okumura, and K. Hasegawa, *Review of Scientific Instruments* **73** (2002), p. 1021.

15. M. P. Stockli and R. F. Welton, *Review of Scientific Instruments* **75** (2004), p. 1646.

16. J. Sherman et al., *Review of Scientific Instruments* **69** (1998), p. 1003.

17. R. Becker et al., *Proceedings of EPAC2004*, p. 1192.

18. AccelSoft, Trace 3-D, PBO Lab 2.0 Platform.

19. Spallation Neutron Source, *Final Safety Assessment Document for Proton Facilities*, SNS-102030103-ES0018-R00, Oak Ridge, Tennessee.

20. A. Shishlo et al., "Self-Consistent Electron Cloud Simulations for Long Proton Bunches," *Proceedings of PAC2005*.

21. V. Danilov et al., "Self-Consistent Time Dependent Two Dimensional and Three Dimensional Space Charge Distributions with Linear Force," *Physical Review Special Topics: Accelerators and Beams* **6**, 094202.

22. C. J. Liaw et al., "Lifetime of Carbon Stripping Foils for the Spallation Neutron Source," *Proceedings of PAC2001*, p. 1538. (See also I. Yamane, *American Institute of Physics Conference Proceedings* **642** (2002), p. 335.

23. R. Shaw et al., "Corrugated Thin Diamond Foils for SNS H^- Injection Stripping," *Proceedings of PAC2005*.

24. V. Danilov et al., "Three Step H^- Charge Exchange Injection with a Narrowband Laser," *Physical Review Special Topics: Accelerators and Beams* **6**, 053501.

25. H. Oguri et al, *Review of Scientific Instruments* **71** (2000), p. 975.

26. M. P. Stockli and R. F. Welton, *Review of Scientific Instruments* **75** (2004), p. 1646.

27. R. F. Welton, M. P. Stockli, and S. N. Murray, *Review of Scientific Instruments* **77** (2006).

28. J. Peters, *Review of Scientific Instruments* **69** (1998), p. 992.

29. R. F. Welton et al., *Review of Scientific Instruments* **77** (2006).

30. J. Peters, *Review of Scientific Instruments* **77** (2006).

31. J. Peters, *Review of Scientific Instruments* **75** (2004), p. 1709.

32. Y. V. Kursanov, P. A. Litvinov, and V. A. Baturin, *American Institute of Physics Conference Proceedings* **763** (2005), p. 229.

33. V. Baturin, Ukrainian Science Academy, Sumy, Ukraine, personal communication, 2004.

34. S. Mordyk et al., *Review of Scientific Instruments* **77** (2006); G. S. Eom et al., *Plasma Sources Science and Technology* **10** (2001), p. 417.